

**DEMONSTRATION OF A FULL-SCALE RETROFIT OF THE
ADVANCED HYBRID PARTICULATE COLLECTOR
TECHNOLOGY**

TECHNICAL PROGRESS REPORT

July 2003 – September 2003

Prepared by:

Tom Hrdlicka
Otter Tail Power Company
Plant Engineer

William Swanson
Otter Tail Power Company
Principal Engineer

Prepared for:

United States Department of Energy
National Energy Technology Laboratory
DOE Award No. DE-FC26-02NT41420

Submitting Organization:

Otter Tail Power Company
Big Stone Plant
PO Box 218
Big Stone City, SD 57216-0218

DISCLAIMER

This report was prepared as an account of work sponsored by an agency of the United States Government. Neither the United States Government nor any agency thereof, nor any of their employees, makes any warranty, express or implied, or assumes any legal liability or responsibility for the accuracy, completeness, or usefulness of any information, apparatus, product, or process disclosed, or represents that its use would not infringe privately owned rights. Reference herein to any specific commercial product, process, or service by trade name, trademark, manufacturer, or otherwise does not necessarily constitute or imply its endorsement, recommendation, or favoring by the United States Government or any agency thereof. The views and opinions of authors expressed herein do not necessarily state or reflect those of the United States Government or any agency thereof.

ABSTRACT

The Advanced Hybrid Particulate Collector (AHPC), developed in cooperation between W.L. Gore & Associates and the Energy & Environmental Research Center (EERC), is an innovative approach to removing particulates from power plant flue gas. The AHPC combines the elements of a traditional baghouse and electrostatic precipitator (ESP) into one device to achieve increased particulate collection efficiency. As part of the Power Plant Improvement Initiative (PPII), this project is being demonstrated under joint sponsorship from the U.S. Department of Energy and Otter Tail Power Company. The EERC is the patent holder for the technology, and W.L. Gore & Associates is the exclusive licensee.

The project objective is to demonstrate the improved particulate collection efficiency obtained by a full-scale retrofit of the AHPC to an existing electrostatic precipitator. The full-scale retrofit is installed on an electric power plant burning Powder River Basin (PRB) coal, Otter Tail Power Company's Big Stone Plant, in Big Stone City, South Dakota. The \$13.4 million project was installed in October 2002. Project related testing will conclude in November 2004.

The following Technical Progress Report has been prepared for the project entitled "Demonstration of a Full-Scale Retrofit of the Advanced Hybrid Particulate Collector Technology" as described in DOE Award No. DE-FC26-02NT41420. The report presents the operation and performance results of the system.

POINT OF CONTACT

For further information on the “Demonstration of a Full-Scale Retrofit of the Advanced Hybrid Particulate Collector Technology”, please contact:

William Swanson
Otter Tail Power Company
Big Stone Plant
PO Box 218
Big Stone City, SD 57216-0218

TABLE OF CONTENTS

Section	Page
TABLE OF CONTENTS	V
LIST OF ACRONYMS	VII
EXECUTIVE SUMMARY	1
PROJECT NOMENCLATURE DISCUSSION	3
1.0 INTRODUCTION	4
1.1 HISTORY OF DEVELOPMENT	6
1.2 DESIGN OF THE PERFORATED PLATE <i>ADVANCED HYBRID</i> [™] FILTER CONFIGURATION	6
1.3 PRESSURE DROP THEORY AND PERFORMANCE EVALUATION CRITERIA.....	10
1.4 9000-ACFM PILOT-SCALE RESULTS	14
1.5 FULL-SCALE DESIGN AND DIFFERENCES BETWEEN FULL AND PILOT SCALE.....	18
2.0 EXPERIMENTAL	21
2.1 INDEPENDENT CHARACTERISTICS.....	21
2.1.1 Independent Characteristic Chart	21
2.1.2 Bag Layout	22
2.2.1 Dependent Data.....	23
2.2.2 Instrument Location Diagram.....	25
2.2.3 Data Retrieval	26
2.2.4 Data Reduction.....	26
3.0 RESULTS AND DISCUSSION	27
3.1 GENERAL RESULTS AND DISCUSSION	27
4.0 CONCLUSIONS	31
5.0 APPENDICES	33
APPENDIX A – COMMENTS ON ANOMALIES OF GRAPHICAL DATA	34
APPENDIX B- GRAPHICAL & TABULAR PERFORMANCE DATA	35
B1 GROSS PLANT LOAD.....	35
B2 FLUE GAS FLOW (KSCFM).....	36
B3 FLUE GAS FLOW (KACFM)	37
B4 INLET GAS TEMPERATURE.....	38
B5 TUBESHEET DP.....	39
B6 FLANGE-TO-FLANGE DP	40
B7 AIR-TO-CLOTH RATIO	41
B8 OPACITY.....	42
B9 NO _x EMISSIONS	43
B10 SO ₂ EMISSIONS.....	44
B11 OUTLET GAS TEMPERATURE	45
B12 OUTLET PRESSURE	45

B12 OUTLET PRESSURE	46
B13 TEMPERATURE PER CHAMBER	47
B14 FUEL BURN RECORD	51
B15 FUEL ANALYSIS RECORD	54
B16 ASH ANALYSIS RECORD	57
B17 ULTIMATE COAL ANALYSIS	58
B18 PHOTOGRAPHS	59
B19 ESP POWER BY CHAMBER	60
B20 ESP TABULAR DATA.....	64
B21 PULSE COUNTER READINGS	65
B22 COMPRESSED AIR FLOW.....	66
B23 BAG LAYOUT DIAGRAM	67
B24 POPR TEST RESULTS.....	68
B25 HUMIDIFICATION TEST RESULTS	69
B26 FLUENT STUDY.....	70

LIST OF ACRONYMS

A/C	air-to-cloth ratio
AG	(Swiss, translation roughly is Incorporation or consolidation)
AHPC	advanced hybrid particulate collector
APS	aerodynamic particle sizer
COHPAC	compact hybrid particulate collector
CPC	condensation particle counter
DOE	U.S. Department of Energy
EERC	Energy & Environmental Research Center
EPA	U.S. Environmental Protection Agency
ePTFE	expanded polytetrafluoroethylene
ESP	electrostatic precipitator
FF	fabric filter
HEPA	high-efficiency particulate air
HiPPS	high-performance power system
MWh	megawatt hours
µm	micrometer
NSPS	New Source Performance Standards
O&M	operating and maintenance
OEMs	original equipment manufacturers
OTP	Otter Tail Power Company
P&ID	Piping and Instrumentation Diagram
PID	Proportional-Integral-Derivative
PJBH	pulse-jet baghouse
PM	particulate matter
PPS	polyphenylene sulfide
PRB	Powder River Basin
PJFF	pulse-jet fabric filter
P-84	aromatic polyimide fiber
QAPP	quality assurance project plan
RGFF	reverse-gas fabric filter
SCA	specific collection area
SMPS	scanning mobility particle sizer
TR	transformer-rectifier
UND	University of North Dakota
W.C.	water column

EXECUTIVE SUMMARY

This document summarizes the operational results of a project titled “Demonstration of a Full-Scale Retrofit of the Advanced Hybrid Particulate Collector Technology”. The Department of Energy’s National Energy Technology Laboratory awarded this project under the Power Plant Improvement Initiative.

The advanced hybrid particulate collector (AHPC) was developed with funding from the U.S. Department of Energy (DOE). The AHPC combines the best features of electrostatic precipitators (ESPs) and baghouses in novel manner. The AHPC combines fabric filtration and electrostatic precipitation in the same housing, providing major synergism between the two methods, both in particulate collection and in transfer of dust to the hopper. The AHPC provides ultrahigh collection efficiency, overcoming the problem of excessive fine-particle emissions with conventional ESPs, and solves the problem of reentrainment and recollection of dust in conventional baghouses.

Big Stone Power Plant operated a 2.5 MWe slipstream AHPC (9000 scfm) for 1½ years. The AHPC demonstrated ultrahigh particulate collection efficiency for submicron particles and total particulate mass. Collection efficiency was proven to exceed 99.99% by one to two orders of magnitude over the entire range of particles from 0.01 to 50 µm. This level of control is well below any current particulate emission standards. These results were achieved while operating at significantly higher air-to-cloth ratios (12 ft/min compared to 4 ft/min) than standard pulse-jet baghouses. To meet a possible stricter fine-particle standard or 99.99% control of total particulate, the AHPC is the possible economic choice over either ESPs or baghouses by a wide margin.

Otter Tail Power Company and its partners, Montana-Dakota Utilities and NorthWestern Energy, installed the AHPC technology into an existing ESP structure at the Big Stone Power Plant. The overall goal of the project is to demonstrate the AHPC concept in a full-scale application. Specific objectives are to demonstrate 99.99% collection of all particles in the 0.01 to 50 µm size range, low pressure drop, overall reliability of the technology and long-term bag life.

The results demonstrated in this quarter are much improved compared to the previous quarters. There are signs that this improvement may not be sustainable as the residual drag of the bags is increasing steadily during the quarter.

The Big Stone Plant has been returned to full load, however the system is rather marginal. There are still

efforts to improve performance, focused on system gas flow dynamics. This knowledge is being sought through the use of CFD modeling by Fluent Inc.

The team is hopeful that trouble free, full load operation of the plant is maintained so the focus can remain on proactive performance enhancements rather than reactive changes.

The largest and most successful change made to the system remains the complete bag change accomplished during the wash outage in June. However, this is also the largest unknown as there is very little operating history in our process of this bag type. If the bag change is viewed as successful, it could also have a dramatic effect on the overall cost of the system. The installed bags are approximately 1/4th the cost of the original bags. More operating history is needed to completely evaluate this change.

PROJECT NOMENCLATURE DISCUSSION

When this technology was originally developed, the device was referred to as the “Advanced Hybrid Particulate Collector”. Since the original development, from concept to an attempt at a commercial demonstration, the name of the technology has changed to “Advanced HybridTM”. This name was trademarked by W.L. Gore and Associates, Inc. to aid in the commercialization effort and tries to maintain the continuity of the successful history to date. Either “Advanced Hybrid Particulate Collector” (AHPC) or “Advanced HybridTM” refers to the same process and equipment.

1.0 INTRODUCTION

The *Advanced Hybrid*[™] filter combines the best features of ESPs and baghouses in a unique approach to develop a compact but highly efficient system. Filtration and electrostatics are employed in the same housing, providing major synergism between the two collection methods, both in the particulate collection step and in the transfer of dust to the hopper. The *Advanced Hybrid*[™] filter provides ultrahigh collection efficiency, overcoming the problem of excessive fine-particle emissions with conventional ESPs, and solves the problem of reentrainment and re-collection of dust in conventional baghouses.

The goals for the *Advanced Hybrid*[™] filter are as follows: > 99.99% particulate collection efficiency for particle sizes ranging from 0.01 to 50 μm , applicable for use with all U.S. coals, and cost savings compared to existing technologies.

The electrostatic and filtration zones are oriented to maximize fine-particle collection and minimize pressure drop. Ultrahigh fine-particle collection is achieved by removing over 90% of the dust before it reaches the fabric and using a GORE-TEX[®] membrane fabric to collect the particles that reach the filtration surface. Charge on the particles also enhances collection and minimizes pressure drop, since charged particles tend to form a more porous dust cake. The goal is to employ only enough ESP plate area to precollect approximately 90% of the dust. ESP models predict that 90%–95% collection efficiency can be achieved with full-scale precipitators with a specific collection area (SCA) of less than 100 ft^2/kacfm (1, 2). FF models predict that face velocities greater than 12 ft/min are possible if some of the dust is precollected and the bags can be adequately cleaned. The challenge is to operate at high A/C ratios (8–14 ft/min) for economic benefits while achieving ultrahigh collection efficiency and controlling pressure drop. The combination of GORE-TEX[®] membrane filter media (or similar membrane filters from other manufacturers), small SCA, high A/C ratio, and unique geometry meets this challenge.

Studies have shown that FF collection efficiency is likely to deteriorate significantly when the face velocity is increased (3, 4). For high collection efficiency, the pores in the filter media must be effectively bridged (assuming they are larger than the average particle size). With conventional fabrics at low A/C ratios, the residual dust cake serves as part of the collection media, but at high A/C ratios, only a very light residual dust cake is acceptable, so the cake cannot be relied on to achieve high collection efficiency. The solution is to employ a sophisticated fabric that can ensure ultrahigh collection efficiency and endure frequent high-energy cleaning. In addition, the fabric should be reliable under the most severe chemical environment likely to be encountered (such as high SO_3).

Assuming that low particulate emissions can be maintained through the use of advanced filter materials and that 90% of the dust is precollected, operation at face velocities in the range of 8–14 ft/min should be possible, as long as the dust can be effectively removed from the bags and transferred to the hopper without significant redispersion and re-collection. With pulse-jet cleaning, heavy residual dust cakes are not typically a problem because of the fairly high cleaning energy that can be employed. However, the high cleaning energy can lead to significant redispersion of the dust and subsequent re-collection on the bags. The combination of a very high-energy pulse and a very light dust cake tends to make the problem of redispersion much worse. The barrier that limits operation at high A/C ratios is not so much the dislodging of dust from the bags as it is the transferring of the dislodged dust to the hopper. The *Advanced Hybrid*[™] filter achieves enhanced bag cleaning by employing electrostatic effects to precollect a significant portion of the dust and by trapping in the electrostatic zone the redispersed dust that comes off the bags following pulsing.

1.1 History of Development

The *Advanced Hybrid*[™] filter concept was first proposed to DOE in September 1994 in response to a major solicitation addressing air toxics. DOE has been the primary funder of the *Advanced Hybrid*[™] filter development since that time, along with significant cost-sharing from industrial cosponsors. Details of all of the results have been reported in DOE quarterly technical reports, final technical reports for completed phases, and numerous conference papers. A chronology of the significant development steps for the *Advanced Hybrid*[™] filter is shown below.

- September 1994 - *Advanced Hybrid*[™] filter concept proposed to DOE
- October 1995 - September 1997 - Phase I - *Advanced Hybrid*[™] filter successfully demonstrated at 0.06-MW (200-acfm) scale
- March 1998 - February 2000 - Phase II - *Advanced Hybrid*[™] filter successfully demonstrated at 2.5-MW (9000-acfm) scale at Big Stone Plant
- September 1999 - August 2001 - Phase III - *Advanced Hybrid*[™] filter commercial components tested and proven at 2.5-MW scale at Big Stone Plant
- Summer 2000 – Minor electrical damage on bags first observed
- January–June 2001 – To prevent electrical damage, the *Advanced Hybrid*[™] filter perforated plate configuration was developed, tested, and proven to be superior to the original design
- July 2001 - December 2004 - Mercury Control with the *Advanced Hybrid*[™] Filter - Extensive additional testing of the perforated plate concept was conducted with the 2.5-MW pilot unit

1.2 Design of the Perforated Plate *Advanced Hybrid*[™] Filter Configuration

After bag damage was observed in summer 2000, extensive experiments were carried out at an Energy & Environmental Research Center (EERC) laboratory to investigate the interactions between electrostatics and bags under different operating conditions. The 200-acfm *Advanced Hybrid*[™] filter was first operated without fly ash under cold-flow conditions with air. The effects of electrode type, bag type, plate-to-plate spacing, the relative distance from the electrodes to plates compared to the distance from the electrodes to the bags (spacing ratio), and various grounded grids placed between the electrodes and bags were all evaluated. Several of the conditions from the cold-flow tests were selected and further evaluated in hot-flow coal combustion tests. While all of these tests resulted in very low current to the bags, there appeared to be a compromise in overall *Advanced Hybrid*[™] filter performance for some configurations.

A configuration that appeared to have promise was a perforated plate design in which a grounded

perforated plate was installed between the discharge electrodes and the bags to protect the bags. On the opposite side of the electrodes, another perforated plate was installed to simulate the geometric arrangement where each row of bags would have perforated plates on both sides, and no solid plates were used. The discharge electrodes were then centered between perforated plates located directly in front of the bags. With this arrangement, the perforated plates function both as the primary collection surface and as a protective grid for the bags. With the 200-acfm *Advanced Hybrid*[™] filter, the perforated plate configuration produced results far better than in any previous *Advanced Hybrid*[™] filter tests and provided adequate protection of the bags.

Based on the 200-acfm results, a perforated plate configuration was designed and installed on the 9000-acfm slipstream pilot unit at the Big Stone Power Plant. The differences between the new perforated plate design and the previous *Advanced Hybrid*[™] filter can be seen by comparing Figure 1 with Figure 2. Figure 1 is a simplified top view of the 9000-acfm *Advanced Hybrid*[™] filter configuration at the start of Phase III, which had a plate-to-plate spacing of 23.6 in. For the perforated plate configuration (Figure 2), the bag spacing was not changed, allowing use of the same tube sheet as in the previous configuration (Figure 1). However, the distance from the discharge electrodes to the perforated plates as well as the distance from the bags to the perforated plates can be reduced without compromising performance. Therefore, one of the obvious advantages of the perforated plate configuration is the potential to make the *Advanced Hybrid*[™] filter significantly more compact than the earlier design.

Another difference is that directional electrodes are not required with the perforated plate design. With the previous design, directional electrodes (toward the plate) were needed to prevent possible sparking to the bags. This means that conventional electrodes can be used with the *Advanced Hybrid*[™] filter. Electrode alignment is also less critical because an out-of-alignment electrode would simply result in potential sparking to the nearest grounded perforated plate, whereas with the old design, an out-of-alignment electrode could result in sparking to a bag and possible bag damage.

While the perforated plate configuration did not change the overall *Advanced Hybrid*[™] filter concept (precollection of > 90% of the dust and enhanced bag cleaning), the purpose of the plates did change. The perforated plates serve two very important functions: as the primary collection surface and as a protective grid for the bags. With approximately 45% open area, there is adequate collection area on the plates to collect the precipitated dust while not restricting the flow of flue gas toward the bags during normal filtration. During pulse cleaning of the bags, most of the reentrained dust from the bags is forced back through the perforated plates into the ESP zone. The 9000-acfm results as well as the 200-acfm results showed better ESP collection than the previous design while maintaining good bag cleanability. The better

ESP collection efficiency is likely the result of forcing all of the flue gas through the perforated plate holes before reaching the bags. This ensures that all of the charged dust particles pass within a maximum of one-half of the hole diameter distance of a grounded surface. In the presence of the electric field, the particles then have a greater chance of being collected. In the old *Advanced Hybrid*[™] filter design, once the gas reached the area between the electrodes and bags, it would be driven toward the bags rather than the plates, and a larger fraction of the dust was likely to bypass the ESP zone.

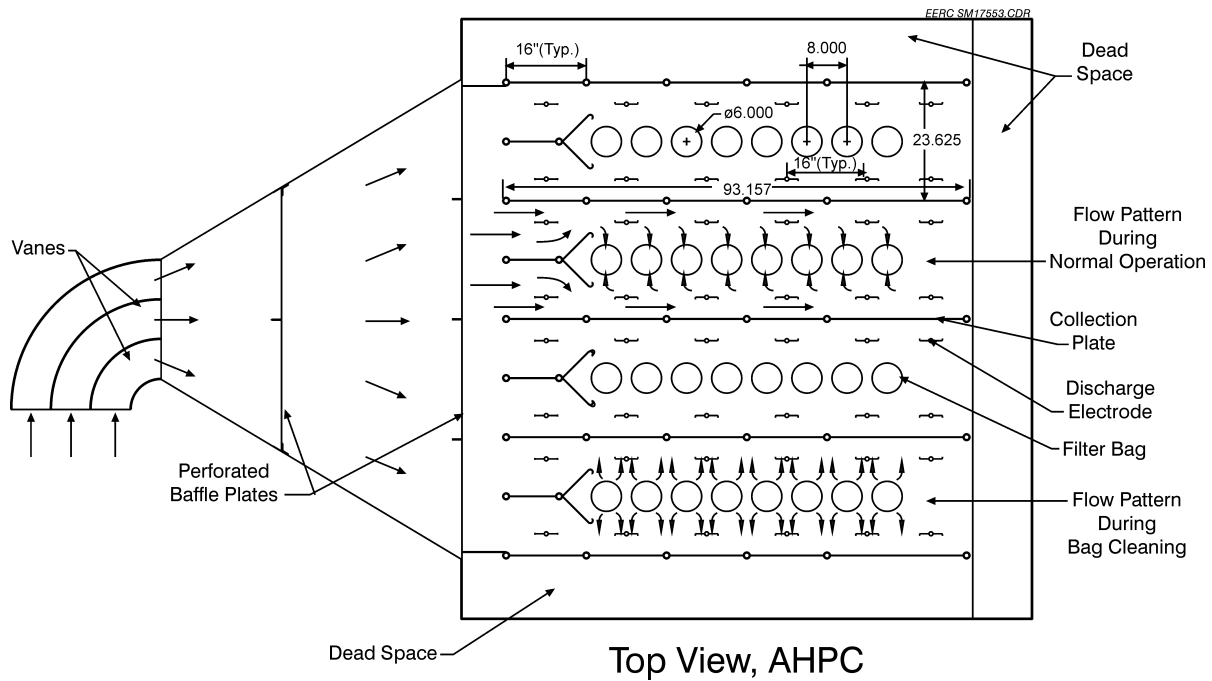


Figure 1. Top view of the old configuration for the 9000-acfm *Advanced Hybrid™* filter at Big Stone.

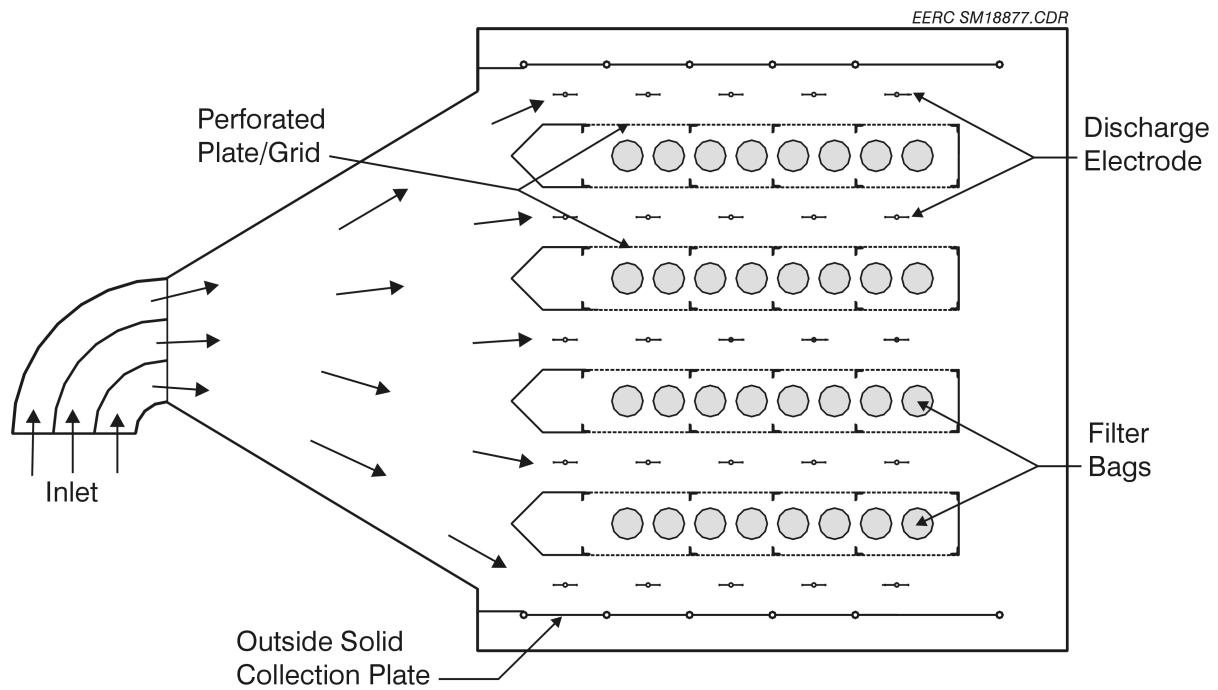


Figure 2. Top view of the perforated plate configuration for the 9000-acfm *Advanced Hybrid™* filter.

1.3 Pressure Drop Theory and Performance Evaluation Criteria

Pressure drop across the bags is one of the main operational parameters that defines overall performance. It must be within capacity limits of the boiler fans at the maximum system flow rate. Since acceptable pressure drop is so critical to successful operation, a detailed discussion of the theory and factors that control pressure drop follows.

For viscous flow, pressure drop across a FF is dependent on three components:

$$dP = K_f V + K_2 W_R V + \frac{K_2 C_i V^2 t}{7000} \quad [\text{Eq. 1}]$$

where:

dP = differential pressure across baghouse tube sheet (in. W.C.)

K_f = fabric resistance coefficient (in. W.C.-min/ft)

V = face velocity or A/C ratio (ft/min)

K₂ = specific dust cake resistance coefficient (in. W.C.-ft-min/lb)

W_R = residual dust cake weight (lb/ft²)

C_i = inlet dust loading (grains/acf)

t = filtration time between bag cleaning (min)

The first term in Eq. 1 accounts for the pressure drop across the fabric. For conventional fabrics, the pore size is quite large, and the corresponding fabric permeability is high, so the pressure drop across the fabric alone is negligible. To achieve better collection efficiency, the pore size can be significantly reduced, without making fabric resistance a significant contributor to pressure drop. The GORE-TEX[®] membrane filter media allows for this optimization by providing a microfine pore structure while maintaining sufficient fabric permeability to permit operation at high A/C ratios. A measure of the new fabric permeability is the Frazier number which is the volume of gas that will pass through a square foot of fabric sample at a pressure drop of 0.5 in. W.C. The Frazier number for new GORE-TEX[®] bags is in the range from 4 to 8 ft/min. Through the filter, viscous (laminar) flow conditions exist, so the pressure drop varies directly with flow velocity. Assuming a new fabric Frazier number of 6 ft/min, the pressure drop across the fabric alone would be 1.0 in. W.C. at an A/C ratio (filtration velocity) of 12 ft/min.

The second term in Eq. 1 accounts for the pressure drop contribution from the permanent residual dust cake that exists on the surface of the fabric. For operation at high A/C ratios, the bag cleaning must be sufficient to maintain a very light residual dust cake and ensure that the pressure drop contribution from this term is reasonable. The contribution to pressure drop from this term is one of the most important indicators of longer-term bag cleanability.

The third term in Eq. 1 accounts for the pressure drop contribution from the dust accumulated on the bags since the last bag cleaning. K_2 is determined primarily by the fly ash particle-size distribution and the porosity of the dust cake. Typical K_2 values for a full dust loading of pulverized coal (pc)-fired fly ash range from about 4 to 20 in. W.C.-ft-min/lb but may, in extreme cases, cover a wider range. Within this term, the bag-cleaning interval, t , is the key performance indicator. The goal is to operate with as long of a bag-cleaning interval as possible, since more frequent bag pulsing can lead to premature bag failure and require more energy consumption from compressed air usage. An earlier goal for the pilot-scale tests was to operate with a pulse interval of at least 10 min while operating at an A/C ratio of 12 ft/min. While this goal was exceeded in the pilot-scale tests, a pulse interval of only 10 min is now considered too short to demonstrate good *Advanced Hybrid*[™] filter performance over a longer period. With a shorter pulse interval, the *Advanced Hybrid*[™] filter does not appear to make the best use of the electric field, because of the reentrainment that occurs just after pulsing. Current thought is that a pulse interval of at least 60 min is needed to demonstrate the best long-term performance.

Total tube sheet pressure drop is another key indicator of overall performance of the *Advanced Hybrid*[™] filter. Here, the goal was to operate with a tube sheet pressure drop of 8 in. W.C. at an A/C ratio of 12 ft/min. Note that the average pressure drop is not the same as the pulse-cleaning trigger point. For many of the previous and current tests, the pulse trigger point was set at 8 in. W.C., but the average pressure drop was significantly lower.

To help analyze filter performance, the terms in Eq. 1 can be normalized to the more general case by dividing by velocity. The dP/V term is commonly referred to as drag or total tube sheet drag, D_T :

$$\frac{dP}{V} = D_T = K_f + K_2 W_R + \frac{K_2 C_i V t}{7000} \quad [\text{Eq. 2}]$$

The new fabric drag and the residual dust cake drag are typically combined into a single term called residual drag, D_R :

$$D_T = D_R + \frac{K_2 C_i V t}{7000} \quad [\text{Eq. 3}]$$

The residual drag term then is the key indicator of how well the bags are cleaning over a range of A/C ratios, but may still be somewhat dependent on A/C ratio. For example, it may be more difficult to overcome a dP of 10 in. W.C. to clean the bags than cleaning at a dP of 5 in. W.C. For most baghouses, the residual drag typically climbs somewhat over time and must be monitored carefully to evaluate the longer-

term performance. Current thought is that excellent *Advanced Hybrid*TM filter performance can be demonstrated with a residual drag value of 0.6 or lower.

Between bag cleanings, from the second term in Eq. 3, the drag increases linearly with K_2 (dust cake resistance coefficient), C_i (inlet dust concentration), V (filtration velocity), and t (filtration time). For conventional baghouses, the C_i term is easily determined from an inlet dust loading measurement, and approximate K_2 values can be determined from the literature or by direct measurement. However, for the *Advanced Hybrid*TM filter, the concentration of the dust that reaches the bags is generally not known and would be very difficult to measure experimentally. From the Phase I laboratory tests, results indicated approximately 90% of the dust was precollected and did not reach the fabric. However, this amount is likely to fluctuate significantly with changes to the electrical field and with the dust resistivity. Since C_i is not known, for evaluation of *Advanced Hybrid*TM filter performance, the K_2 and C_i can be considered together:

$$K_2 C_i = \frac{(D_T - D_R)7000}{Vt} \quad [\text{Eq. 4}]$$

Evaluation of $K_2 C_i$ can help in assessing how well the ESP portion of the *Advanced Hybrid*TM filter is functioning, especially by comparing with the $K_2 C_i$ during short test periods in which the ESP power was shut off. For the Big Stone ash, the $K_2 C_i$ value has typically been about 20 without the ESP field. For the 9000-acfm pilot *Advanced Hybrid*TM filter, longer-term $K_2 C_i$ values of 1.0 have been demonstrated with the ESP field on, which is equivalent to 95% precollection of the dust by the ESP. Again, the goal is to achieve as low of a $K_2 C_i$ value as possible; however, good *Advanced Hybrid*TM filter performance can be demonstrated with $K_2 C_i$ values up to 4, but this is interdependent on the residual drag and filtration velocity.

Eq. 4 can be solved for the bag-cleaning interval, t , as shown in Eq. 5. The bag-cleaning interval is inversely proportional to the face velocity, V , and the $K_2 C_i$ term and directly proportional to the change in drag before and after cleaning (delta drag). The delta drag term is dependent on the cleaning set point or maximum pressure drop as well as the residual drag. The face velocity, delta drag, and $K_2 C_i$ terms are relatively independent of each other and should all be considered when the bag-cleaning interval is evaluated. However, as mentioned above, the drag may be somewhat dependent on velocity if the dust does not clean off the bags as well at high velocity as at low velocity. Similarly, the $K_2 C_i$ is somewhat dependent on velocity for a constant plate collection area. At the greater flow rates, the SCA of the precipitator is reduced, which will result in a greater dust concentration, C_i , reaching the bags.

$$t = \frac{(D_T - D_R)7000}{VK_2C_i} \quad [\text{Eq. 5}]$$

By evaluating these performance indicators, the range in possible A/C ratios can be calculated by using Eq. 1. For example, using the acceptable performance values of a 60-min pulse interval and a residual drag of 0.6, Eq. 1 predicts that a K_2C_i value of 2.33 would be needed when operating at an A/C ratio of 10 ft/min and a pulse trigger of 8 in. W.C. Obviously, deterioration in the performance of one indicator can be offset by improvement in another. Results to date show that performance is highly sensitive to the A/C ratio and that excellent *Advanced Hybrid*[™] filter performance can be achieved as long as a critical A/C ratio is not exceeded. If the A/C ratio is pushed too high, system response is to more rapidly pulse the bags. However, too rapid of pulsing tends to make the residual drag increase faster and causes the K_2C_i to also increase, both of which lead to poorer performance. The design challenge is to operate the *Advanced Hybrid*[™] filter at the appropriate A/C ratio for a given set of conditions.

1.4 9000-acfm Pilot-Scale Results

During the summer of 2002 the 9000-acfm *Advanced Hybrid*[™] filter was operated from June 28 through early September with minimal changes to the operating parameters. This is the longest time the pilot unit was operated without interruption and is the best example of the excellent performance demonstrated with the 9000-acfm *Advanced Hybrid*[™] filter. One of the main objectives of the summer 2002 tests was to assess the effect of carbon injection for mercury control on longer-term *Advanced Hybrid*[™] filter performance. In order to achieve steady-state *Advanced Hybrid*[™] filter operation prior to starting carbon injection, the *Advanced Hybrid*[™] filter was started with new bags on June 28 and operated continuously until the start of the carbon injection for mercury control in August. Operational parameters are given in Table 1, and the bag-cleaning interval, pressure drop, and K_2C_i data from June 28 to September 3 are shown in Figures 3-5. The daily average pressure drop data increased slightly with time as would be expected after starting with new bags. When the carbon was started on August 7, there was no perceptible change in pressure drop. The bag-cleaning interval was somewhat variable as a result of temperature and load swings, but, again there was no increase when the carbon feed was started. The K_2C_i values are an indication of the amount of dust that reaches the bags and subsequently relate to how well the ESP portion of the *Advanced Hybrid*[™] filter is working. Again, there was no perceptible change when the carbon was started. These data show that the *Advanced Hybrid*[™] filter can be expected to provide good mercury removal with upstream injection of carbon without any adverse effect on performance.

From August 21 to August 26, the *Advanced Hybrid*[™] filter current was deliberately reduced to 25 mA compared to the normal 55 mA setting (see Figures 3-5) to see if good mercury removal could be maintained. The bag-cleaning interval dropped to about one-half, and the K_2C_i value approximately doubled, which would be expected. Both of these indicate that about twice as much dust reached the bags at 25 mA compared to 55 mA. However, almost no effect on pressure drop was seen. This implies that it should be possible to optimize *Advanced Hybrid*[™] filter operational parameters to get the best overall mercury removal while maintaining good *Advanced Hybrid*[™] filter performance.

Table 1. 2.5-MW Advanced Hybrid™ Filter Test Parameters and Operational Summary, June 28 - September 2, 2002

A/C Ratio	10 ft/min
Pulse Pressure	70 psi
Pulse Duration	200 ms
Pulse Sequence	87654321 (multibank)
Pulse Trigger	8.0 in. W.C.
Pulse Interval	260 - 400 min
Temperature	260° - 320°F
Rapping Interval	15 - 20 min
Voltage	58 - 62 kV
Current	55 mA

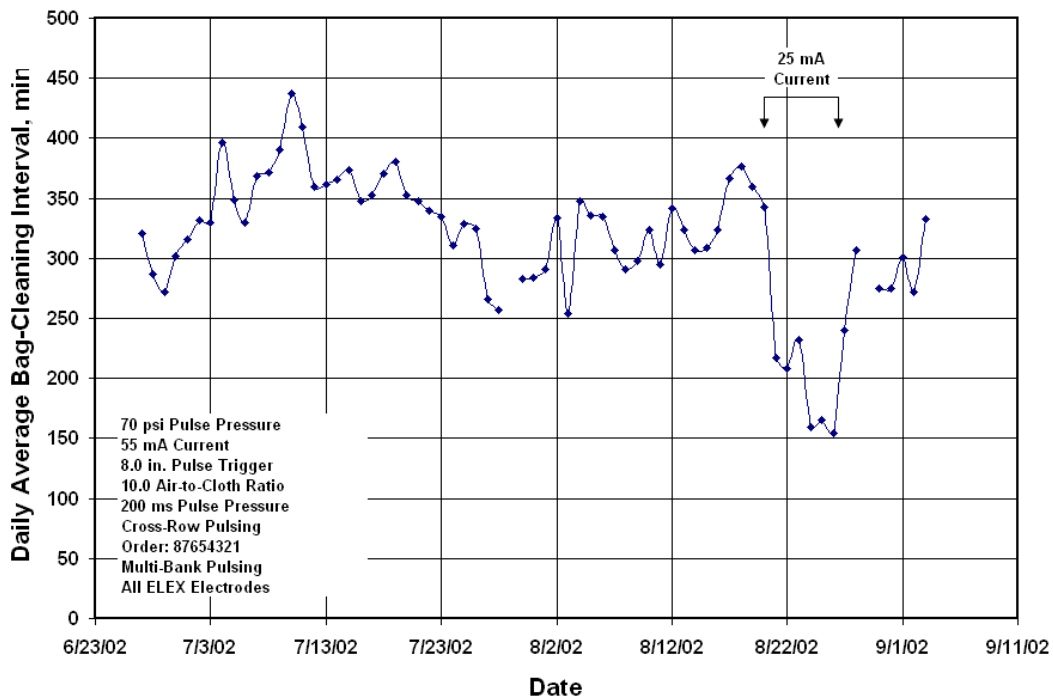


Figure 3. Daily average bag-cleaning interval for summer 2002 tests with the 9000-acfm Advanced Hybrid™ filter.

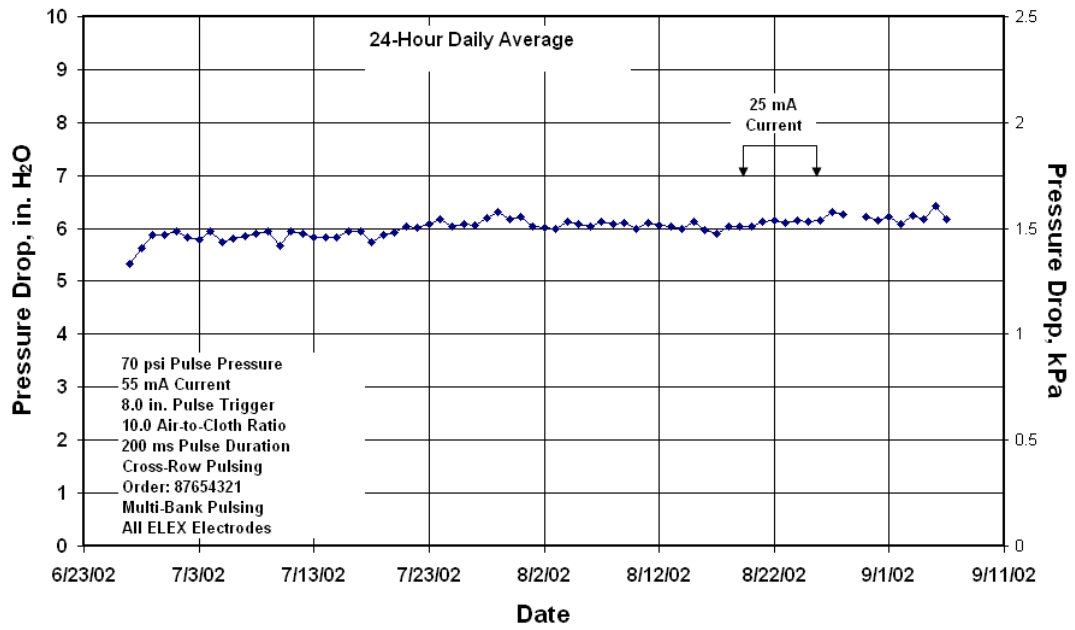


Figure 4. Daily average pressure drop for summer 2002 tests with the 9000-acfm *Advanced Hybrid*TM filter.

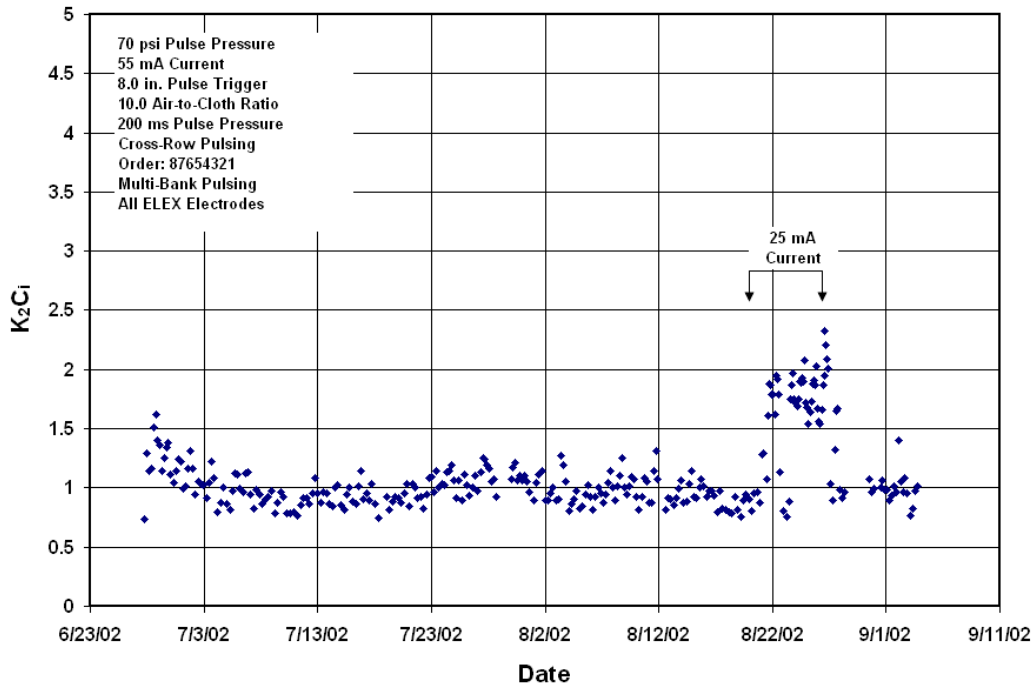


Figure 5. K_2C_i for summer 2002 tests with the 9000-acfm *Advanced Hybrid*TM filter.

A summary of the results in Table 2 shows the excellent operational performance achieved with the 9000-acfm at an A/C ratio of 10 ft/min.

Table 2. Summary of 9000-acfm Pilot-Scale Results from Summer 2002

A/C Ratio	10 ft/min
Average dP	~6 in. W.C.
Bag-Cleaning Interval	2–5 hr
Residual Drag	0.4–0.5
K_2C_i	0.9–1.5

The 9000-acfm pilot *Advanced Hybrid*TM filter was also used to vary the operational parameters to assess the most critical effects. One of the most important findings was the observed significant effect of the pulse interval on the K_2C_i value, as shown in Figure 6. The large increase in K_2C_i at the lowest pulse intervals indicates that the benefit of the electric field is diminished at lower pulse intervals. This indicates that for good *Advanced Hybrid*TM filter performance, a minimum allowable pulse interval should be established. Based on Figure 6, a 60 min pulse interval would be a good minimum performance goal.

**K_2C_i Versus Bag-Cleaning Cycle Time for the 2.5-MW (9000-acfm)
Advanced Hybrid™ Filter**

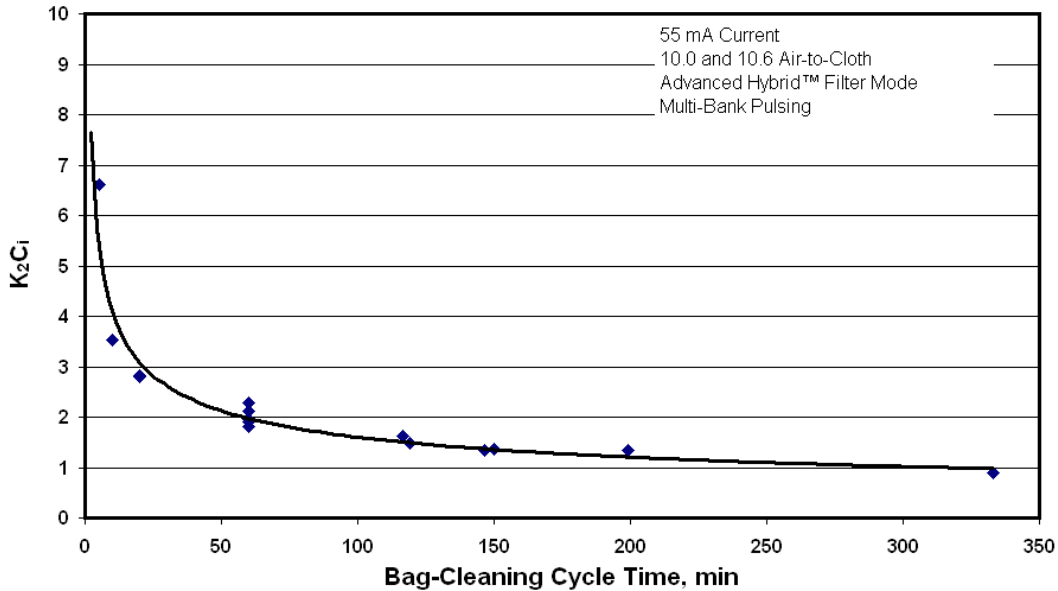


Figure 6. Effect of pulse interval on K_2C_i for 9000-acfm pilot *Advanced Hybrid™* filter.

1.5 Full-Scale Design and Differences Between Full and Pilot Scale

The original ESP at Big Stone consisted of a Lurgi-Wheelabrator design with four main chambers and four collecting fields in series within each chamber. Only the last three fields in each chamber were converted into an *Advanced Hybrid™* filter while the first field was unchanged (Figure 7). Since the ESP plates are 40 ft high, but the *Advanced Hybrid™* filter bags are only 23 ft long, there is a large open space between the bottom of the bags and the hoppers (Figure 8). The outer six compartments (Figure 7) are arranged with 20 rows and 21 bags per row, while the six inner compartments have 19 rows with 21 bags per row. The total number of planned bags for the 12 compartments was 4914. However, because of a spacing limitation from the electrode rapping mechanism, a total of 81 bags had to be removed, so the total number of bags in service is 4834.

The main differences between the 2.5-MW pilot *Advanced Hybrid™* filter and the full-scale Big Stone *Advanced Hybrid™* filter are as follows:

- The pilot unit has a small precollection zone consisting of one discharge electrode, while the full-scale unit has no precollection zone (without the first field on). The effect would be better ESP collection (lower K_2C_i) in the pilot unit. The pilot unit has shorter bags, 15 ft versus 23 ft for the

full-scale *Advanced Hybrid*[™] filter. The expected result would be better bag cleaning with the pilot unit (lower residual drag).

- The full-scale *Advanced Hybrid*[™] filter has an ESP plate spacing of 12 in. compared to 13.5 in. for the pilot-scale unit. The expected result is somewhat better ESP collection efficiency.
- The entrance velocity of the flue gas is 4–8 ft/s for the full-scale unit versus 2 ft/s in the pilot-scale unit. The expected effect is better ESP collection efficiency with the pilot unit.
- The pilot unit has very uniform side inlet flow distribution while the full-scale *Advanced Hybrid*[™] filter has flow from the side for the first *Advanced Hybrid*[™] filter compartment and from the bottom in the back 2 compartments.

In the pilot unit all of the flow is uniformly distributed from the side and none of the flow comes from the bottom. In the full-scale *Advanced Hybrid*[™] filter, flow entering the first *Advanced Hybrid*[™] filter chamber comes from the side (similar to the pilot unit). The flow to the back two compartments must first travel below the first *Advanced Hybrid*[™] filter compartment and then either directly up from the bottom into the compartment or up from the bottom into the areas between compartments and then horizontally into the compartments (Figure 9).

Big Stone Layout

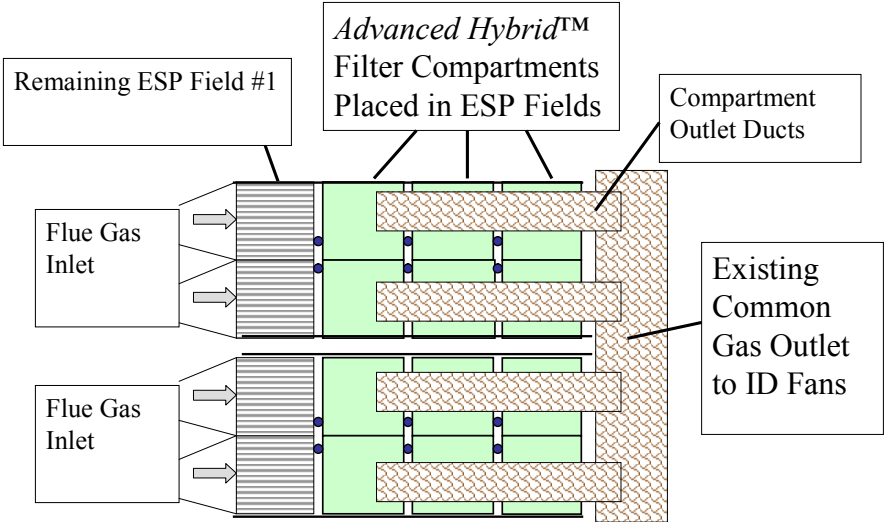


Figure 7. Top view of the *Advanced Hybrid™* filter full-scale retrofit configuration at Big Stone.

Advanced Hybrid™ Filter Retrofit

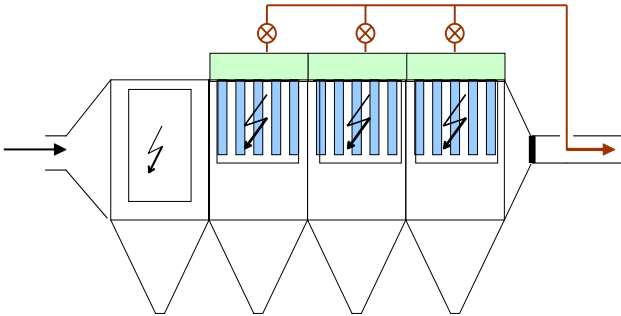


Figure 8. Side view of the *Advanced Hybrid™* filter full-scale retrofit configuration at Big Stone.

2.0 EXPERIMENTAL

2.1 Independent Characteristics

2.1.1 Independent Characteristic Chart

The following chart lists the specific independent characteristics of the Advanced Hybrid System. If changes are made to the independent data, they will be described in the section listed under the “Notes” column.

Table 3.

Data	Status	Notes
ESP Collecting Surface	170,500 ft ²	Unchanged
# of Discharge Electrodes	2,706	Unchanged
# of Filter Bags	4834	Unchanged
Filter Bag Dimensions	7 Meters Long, 6 Inches Diameter	Unchanged
Filter Bag Surface Area	36.07 ft ²	Unchanged
Filter Bag Material	See 2.1.2	Unchanged
Pulse Pressure	80 psi	Unchanged
Cleaning Mode	Threshold Control	Unchanged
TR Rating of AH Field	1500 ma, 55 kV	Unchanged
TR Rating of Inlet ESP Field	2000 ma, 55 kV	Unchanged
Inlet ESP Field Data		
Inlet Field Dimensions ¹	45 gas passages, 40 feet high, 14 feet deep/chamber	Unchanged
Inlet Field Plate Area ¹	50,400 ft ²	Unchanged
Inlet Field Electrodes ¹	Wheelabrator bed frame “Star” Electrodes	Unchanged

¹The inlet ESP field was left in place. The design is the original configuration as installed in 1975. It is not the intentions to operate the inlet field, however it was left in place as an added benefit of the system.

2.1.2 Bag Layout

The following is a description of the number and type of bags in the system. Some plugging of bags may occur, but in general, this should be an accurate description of the system with regards to filtration distribution. A diagram of the bag layout is included in Appendix B22.

Table 4 Bag Layout and Type Description

Compartment	Number of Bags	Bag Type
Chamber 1A Field 2	100/313	GORE-TEX™ Felt/GORE-TEX™ Membrane /Cond. PPS Felt/ GORE-TEX™ Membrane
Chamber 1A Field 3	413	PPS Felt/GORE-TEX™ Membrane
Chamber 1A Field 4	413	PPS Felt/GORE-TEX™ Membrane
Chamber 1B Field 2	392	GORE-TEX™ Felt/GORE-TEX™ Membrane
Chamber 1B Field 3	392	PPS Felt/GORE-TEX™ Membrane ¹
Chamber 1B Field 4	393	PPS Felt/GORE-TEX™ Membrane
Chamber 2A Field 2	81/312	GORE-TEX™ Felt/GORE-TEX™ Membrane /Cond. PPS Felt/ GORE-TEX™ Membrane
Chamber 2A Field 3	393	GORE-TEX™ Felt/GORE-TEX™ Membrane
Chamber 2A Field 4	393	PPS Felt/GORE-TEX™ Membrane
Chamber 2B Field 2	413	GORE-TEX™ Felt/GORE-TEX™ Membrane
Chamber 2B Field 3	413	Cond. PPS Felt/ GORE-TEX™ Membrane
Chamber 2B Field 4	413	PPS Felt/GORE-TEX™ Membrane

2.2 Dependent Characteristics

2.2.1 Dependent Data

The dependent data is largely presented in graphical format in the Appendix. The specific data points that are instrumented and presented are as follows;

Plant Gross Load: Continuously monitored TDC-3000 calculated value based on the generator output voltage and current. When the plant trips offline or shuts down for maintenance, the plant gross load will be zero

Total Flue Gas Flow: Continuously monitored using United Science Inc.'s Ultra Flow 100 ultrasonic flow monitor. The flow monitor is located at the stack midlevel (see position #6 on Diagram 1). The readout of the flow monitor is in kscfm using 68°F and 29.92 in HG as standard conditions. The flow is converted to kacfm using the following equation:

$$\text{Gas Flow (kacfm)} = \frac{(\text{Gas Flow(kscfm)} * (460 + \text{Inlet Gas Temp}^\circ \text{F}))}{(460 + 68^\circ \text{F})} * \frac{29.92 \text{ in HG}}{(28.56 \text{ in HG} + \text{AHPC outlet Pressure})}$$

Inlet Flue Gas Temperature: Continuously monitored using a grid of Type E thermocouples. The thermocouples are located at the AHPC inlet (see position #1 on Diagram 1). There are eight thermocouples at the inlet of each of the four AHPC chambers for a total of 32 thermocouples.

Tubesheet Differential Pressure: Continuously monitored on two of the twelve compartments. Pressure taps above and below the tubesheet (see positions #3 and #4 on Diagram 1) are equipped with Honeywell 3000 Smart DP Transmitters.

Flange–Flange Differential Pressure: Continuously monitored using two Honeywell 3000 Smart DP Transmitters at the AHPC inlet (see position # 2 on Diagram 1) and two Honeywell 3000 Smart DP Transmitters at the AHPC outlet (see position #5 on Diagram 1). Continuously calculated by the TDC- 3000 by taking the difference between the flue gas pressure at the AHPC inlet and outlet.

Air-to-Cloth Ratio: Calculated by dividing the Gas Flow (acfm) by the total surface area of the bags.

Opacity: Continuously measured by the plant opacity monitor, Monitor Labs Model #LS541

Flue Gas Outlet Pressure: Continuously monitored using two Honeywell 3000 Smart DP Transmitters at the AHPC outlet (see position #5 on Diagram 1). The inlet pressure can be determined by the difference between the outlet pressure, and the flange-to-flange pressure drop.

Temperature per Chamber: See Inlet Temperature above.

ESP Power Consumption: Continuously monitored with a watt-hour meter to each chamber.

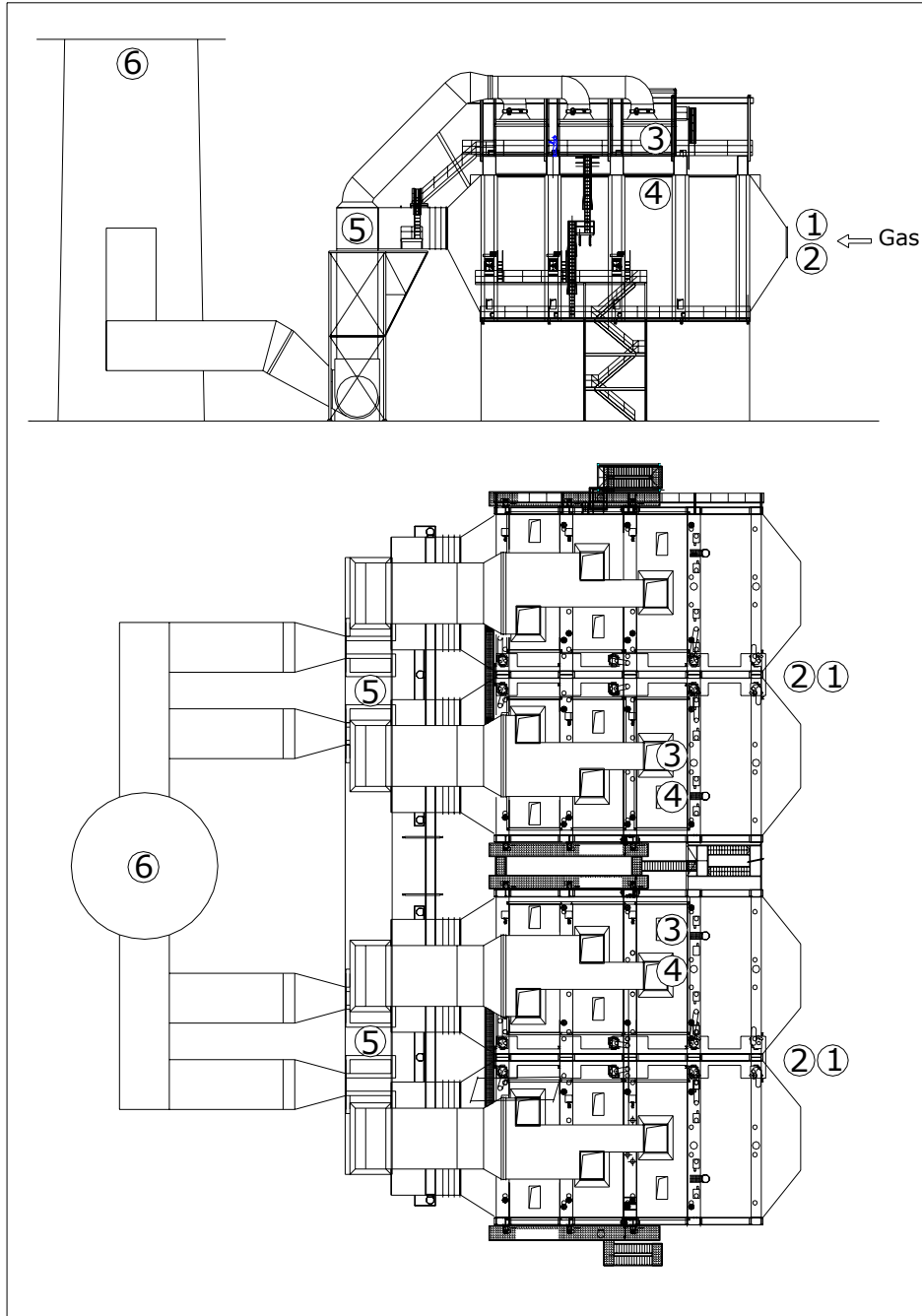
Compressed Air Flow: Continuously monitored using a Diamond II Annubar flow sensor equipped with a Honeywell 3000 Smart DP Transmitter. This ANNUBAR instrument is in the compressed air supply line after the compressors but before the desiccant dryer.

The non-instrumented data that can be found in the appendix is as follows

- Coal Analysis
- Operating Hours
- Flyash Analysis
- Coal and Alternative fuel Burned

2.2.2 Instrument Location Diagram

- 1 & 2: Advanced Hybrid Inlet
- 3 & 4: Above and Below Tubesheet
- 5: Advanced Hybrid Outlet
- 6: Plant Stack



2.2.3 Data Retrieval

Big Stone Plant's Honeywell TDC-3000 process control system monitors and controls a large number of actuators, sensors, and processes using PID controllers, programmable logic controllers, and special-purpose programs. Data gathered by the TDC-3000 is retrieved using an existing plant historian database. The dependent characteristic data presented in this report is calculated using 60-minute averages of the TDC-3000 readings, which are recorded every minute.

2.2.4 Data Reduction

Reported NO_x and SO₂ emissions have had 5% of data removed due to erroneous spikes occurring during daily calibration of CEMS instrumentation. No other assumptions or restrictions were used to transform the raw measured data into a form usable for interpretation.

3.0 RESULTS AND DISCUSSION

3.1 General Results and Discussion

3.1.1 Chronological History of Significant Accomplishments

Quarter 1 (October 2002 – December 2002)

System Startup	October 2002
Rapper Problems Realized	November 2002
Pulse Valve Problems Realized	November 2002
EERC Testing Completed	November 2002
Inlet Field Energized	December 2002

Quarter 2 (January 2003 – March 2003)

Soybeans burned at Big Stone as Alternative Fuels	January 2003
Derates due to high dP across the AH system begin	January 2003
Comparative Testing of Pilot unit to full-scale unit	February 2003
Plant shut down to wash boiler	February 2003

Quarter 3 (April 2003 – June 2003)

Meeting to discuss improvement options	April 2003
Bags washed in two chambers	April/May 2003
Pitot data used for evaluation and decision	May 2003
Decision to replace filter bags	May 2003
Complete bag changeout	June 2003
Inlet field evaluated	June 2003
Plant restored to full load	June 2003

Quarter 4 (July 2003 – September 2003)

Big Stone limited to 440 – 445 MW not due to AH	July/Sept 2003
Performance Tests	July/Sept 2003
Fluent Analysis Plan	Sept 2003
Preliminary baffle design submitted	Sept 2003

3.1.2 Discussion of Results of Significant Accomplishments

General Comments

In general the Advanced Hybrid system has performed significantly better this quarter than in previous quarters. The system is still not performing as is required to demonstrate it commercially. The excellent performance seen immediately after the outage in June has not been maintained, as the differential pressure has risen from 7 to 8.5 INH₂O at the highest A/C ratios seen so far. The inlet ESP field remains charged to reduce the ash loading to the Advanced Hybrid system.

The focus of this quarter is to maintain stable operation of the power plant and delve further into the available data and instrumentation tools to understand the root causes of the performance differences between the pilot unit and the full-scale unit demonstrations.

Performance Testing

A series of performance tests were conducted to measure current performance. These tests are:

- A/C ratio range testing with the inlet field not energized
- Power Off /Plate Rapper Testing (POPR)
- Humidification Testing
- Further pitot testing as a basis for Computational Fluid Dynamic Modeling

The A/C ratio range testing is documentation of existing performance with the inlet field on and off to determine performance over an A/C ratio range. These results are summarized in the following two tables;

Table 5 - Advanced Hybrid Performance with inlet field OFF

Date	A/C ft/min	Inlet Temp deg F	K ₂ C _i	Drag Residual	Pulse Interval min
8/5/03	9.67	294.29	4.22	0.61	36.81
8/3/03	9.66	288.21	3.66	0.59	47.17
7/15/03	9.49	287.83	4.01	0.53	56.87
7/19/03	9.48	306.32	3.80	0.61	45.77
8/24/03	9.15	309.42	3.99	0.67	38.55
7/14/03	8.79	289.11	3.25	0.52	94.75
7/13/03	8.66	279.42	2.45	0.50	140.64
8/2/03	8.36	270.88	2.64	0.56	124.63
9/17/03	8.05	286.92	3.06	0.63	103.27
9/2/03	8.00	269.94	2.44	0.61	138.64
9/1/03	7.98	268.47	2.74	0.60	127.58

Table 6 - Advanced Hybrid performance with inlet field ON

Date	A/C ft/min	Inlet Temp deg F	K ₂ C _i	Drag Residual	Pulse Interval min
8/6/03	10.17	296.20	1.81	0.61	68.76
9/28/03	10.15	289.03	1.91	0.63	57.00
10/22/03	9.77	295.33	2.06	0.62	69.23
8/7/03	9.60	287.57	0.82	0.57	234.36
8/12/03	9.49	288.73	0.76	0.58	252.96
9/12/03	8.84	282.05	1.11	0.61	211.54
9/10/03	8.69	290.25	0.66	0.66	322.00
10/5/03	8.57	274.37	0.82	0.64	288.75
9/16/03	8.17	280.08	0.35	0.64	839.79
9/4/03	7.71	270.58	0.38	0.67	869.04

The test periods were limited to times of reduced plant load in the evenings. During these periods either the inlet field was de-energized (Table 5) or the conditions were noted if the inlet field was left on (Table 6). The results are similar to those obtained in the second quarter of the demonstration period. When referring to the results from Table 5, there is a considerable difference in the K₂C_i values of the system when compared to the pilot unit. It is estimated that the K₂C_i valued for the pilot unit would be less than 1 at an A/C ratio of 9.0 fpm. The full-scale unit K₂C_i at 9.0 fpm appears to be about 4.0. This is an ash loading rate to the bags of four times the rate when compared to the pilot unit. These results lead us to focus on performance improvement effort in the Advanced Hybrid ESP section. Contrarily, the residual drag portion of the system is now comparable with the results of the pilot unit at approximately 0.5 – 0.6 INH₂O/ft/min.

The Power Off Plate Rap tests were performed by turning off the power to the individual compartments and rapping the ESP components to try to improve the ash collection of the ESP section. A graph of these results is included in Appendix B24. In this specific test, as in almost all the power off rapping tests, the ESP power increased slightly, but had no significant effect in the K₂C_i, Residual Drag, or differential pressure. This may indicate there is a portion of flue gas bypassing the ESP zones or another problem with flow distribution.

The humidification test was another short-term improvement test to determine if the existing plant flue gas conditioning system could be used to improve ESP performance. The humidification system was used to inject a minimum amount of water and proprietary chemical to determine if an improvement could be made. As can be seen in the graph in Appendix B25, very little improvement was seen during this test.

The last significant testing was the analysis of the existing pitot tube data. As was described by W.L. Gore and Associates, there appears to be a fairly significant K2Ci performance difference between the first, second, and third section of some individual compartments. Pitot testing indicated the K2Ci value of the bags in the middle section of Chamber 2A Field 3 was about 2.0, while the back section of Chamber 2A Field 3 was about 5.0. In another interesting comparison, the front section of Chamber 2A Field 4 was about 4.5, while the middle section of Chamber 2A Field 4 was about 1.5. This is described by the graph in Appendix B26. All of these test results point towards a gas flow distribution issue that may help explain the difference in loading rate between the pilot and full-scale unit.

Performance Improvement Effort

Now that the Big Stone Plant has returned to full load capability, an effort towards a long-term improvement is being made. This effort is focused on the gas flow dynamics of the system and how an understanding of these dynamics may aid us in improving the system. Fluent Inc. was brought on board to evaluate the system through Computational Fluid Dynamic (CFD) modeling of the existing system. A description of the effort by Fluent Inc. is included in Appendix B27. The most reasonable approach to improvement of the ESP portion of the system is the addition of baffles below the bag rows in each section. A proposal in the form of a presentation is included in Appendix B28 with further details on the principal theory of the baffles.

The results of the Fluent Inc. modeling should be completed in the next quarter of demonstration.

4.0 CONCLUSIONS

System Performance

Some of the dramatic improvements in system performance demonstrated at the end of the previous quarter have continued in this quarter. The primary indices for performance are as follows;

- Opacity (Appendix B8)
- Air-to-cloth ratio (Appendix B7)
- Tubesheet dP (Appendix B5)
- Compressed air flow (Appendix B22)

Opacity remained at nearly constant levels of around 5-6 % during the quarter. This is still higher than was measured during the initial phases of the demonstration but are within the reasonable accuracy of the meter. The stack exhaust remains very clean, with no particulate emissions visible to the naked eye.

The A/C ratio has risen to approximately 11.5 during the warmest days of the summer. This level of gas flow is likely to continue into the early fall months unless the ambient temperature decreases dramatically before the next boiler wash outage (scheduled for early December).

The tubesheet dP remained at a relatively controllable level through the summer months. Only during the period of warmest gas inlet temperatures did the differential pressure increase above 8.0 INH₂O. This is a dramatic improvement from the first three quarters of operation as can be seen from the graphical data in the Appendix.

The compressed air flow of the system has gradually increased from approximately 700 acfm, to nearly constant pulsing at 2000 acfm. This indicates a gradual increase in residual drag. It is likely that the ash cake forming on the bag surface is becoming harder to remove and maintaining this differential pressure in the future is unlikely.

Performance Improvement

The performance improvement options that are currently underway focus on the gas dynamics of the system. The basis of this has been the testing performed as described in section 3.1.2. Fluent Inc. was

contracted to develop a detailed CFD model to aid this effort. The most likely change discussed is the addition of flow baffles beneath the individual bag rows to divert the flue gas into the ESP zone. The results of this modeling should be completed in the next quarter of demonstration.

5.0 APPENDICES

APPENDIX A – COMMENTS ON ANOMALIES OF GRAPHICAL DATA

Appendix B5 & B6. The initial dP data was not historized correctly, so the first couple of days of dP history do not exist in the Plant Historian.

Appendix B19. Significant increases in Chamber Power typically indicate periods where the initial inlet field was energized, although spikes also occur during periods of reduced loading on the unit.

Appendix B8. Opacity Graph shows two spikes in the opacity reading that were not real (1/15/2003 & 3/1/2003). These spikes were instrumentation failures and/or calibrations.

Appendix B8. Opacity graph shows spikes around 6/10/2003. These are instrument difficulties, and not representative of actual opacity.

Appendix B15. bam, ebm, etc. are Powder River Basin mine codes

Appendix B14 & 15. The “adjustment” refers to an end of the month correction based on a comparison between visual levels and bookkeeping levels.

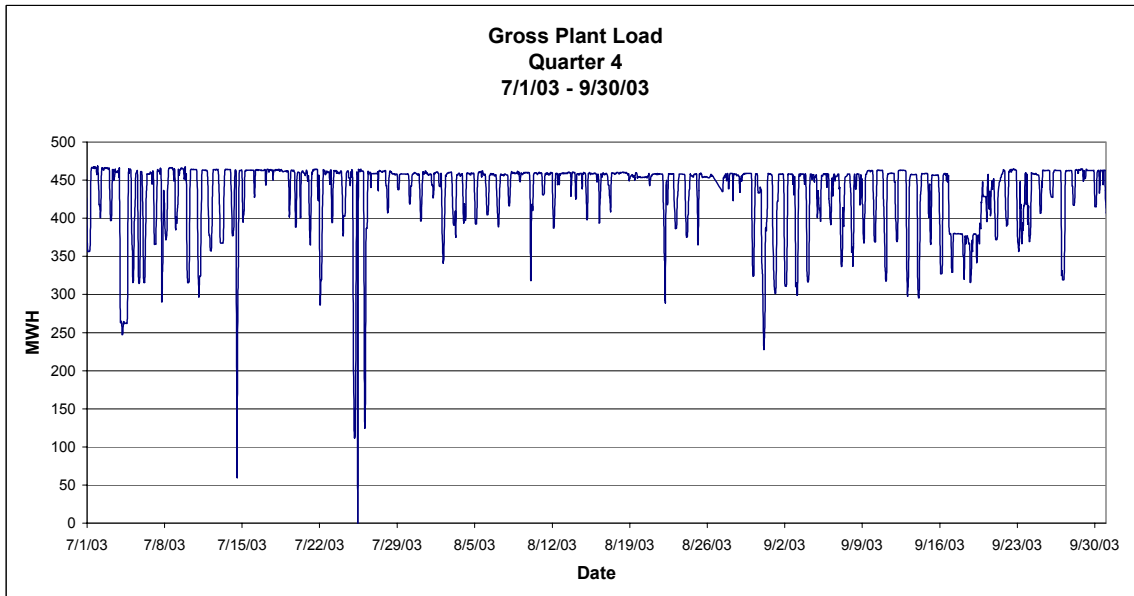
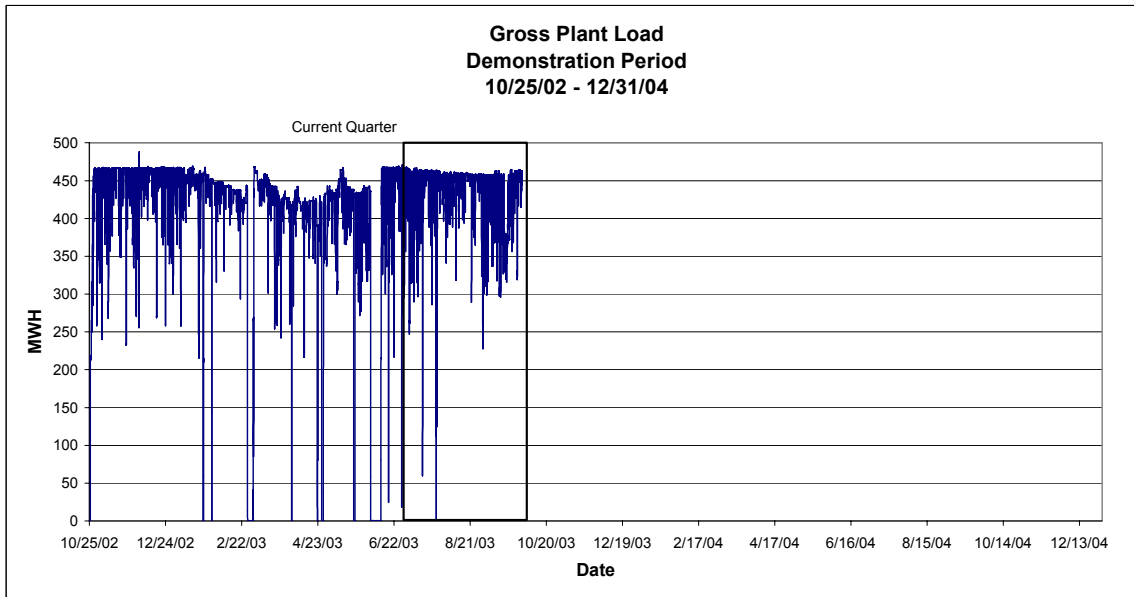
Appendix B21. Pulse counter graph seems to indicate no pulsing after the June 12, 2003 startup until the end of June. However, the scale is so large and the pulse cycle frequency was so insignificant, that it cannot be seen as a clear increase until the next quarter. The number of pulse cycles by June 30,2003 was 284.

Appendix B2, B3 & B7. Low stack flow readings around 7/21/2003 are instrument problems and not real readings. As can be seen in B1, the plant was on-line and operating during the indicated period of no flow.

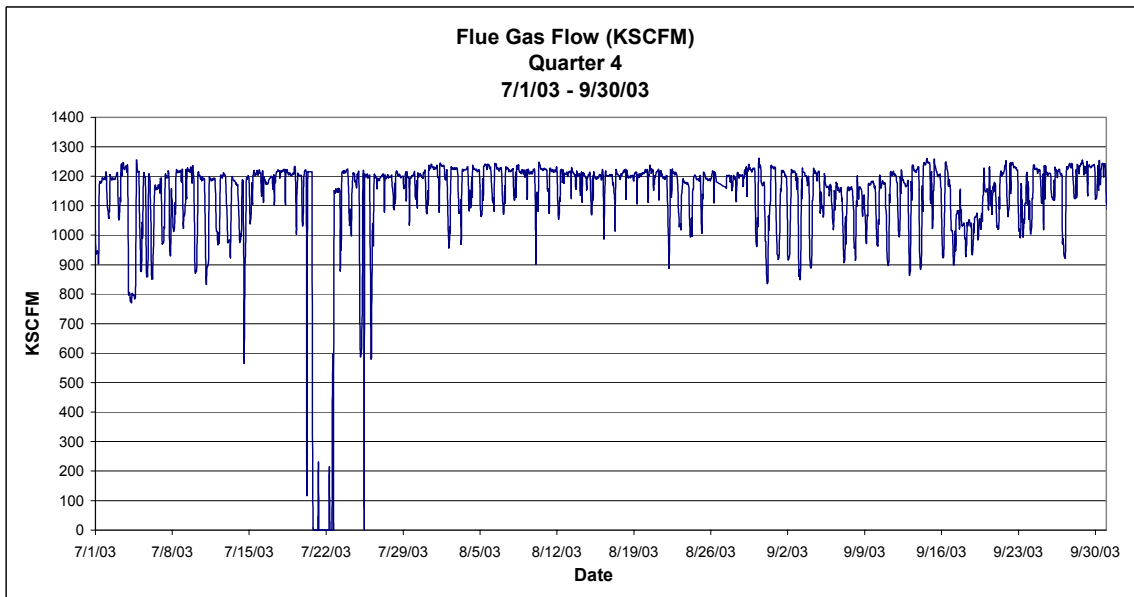
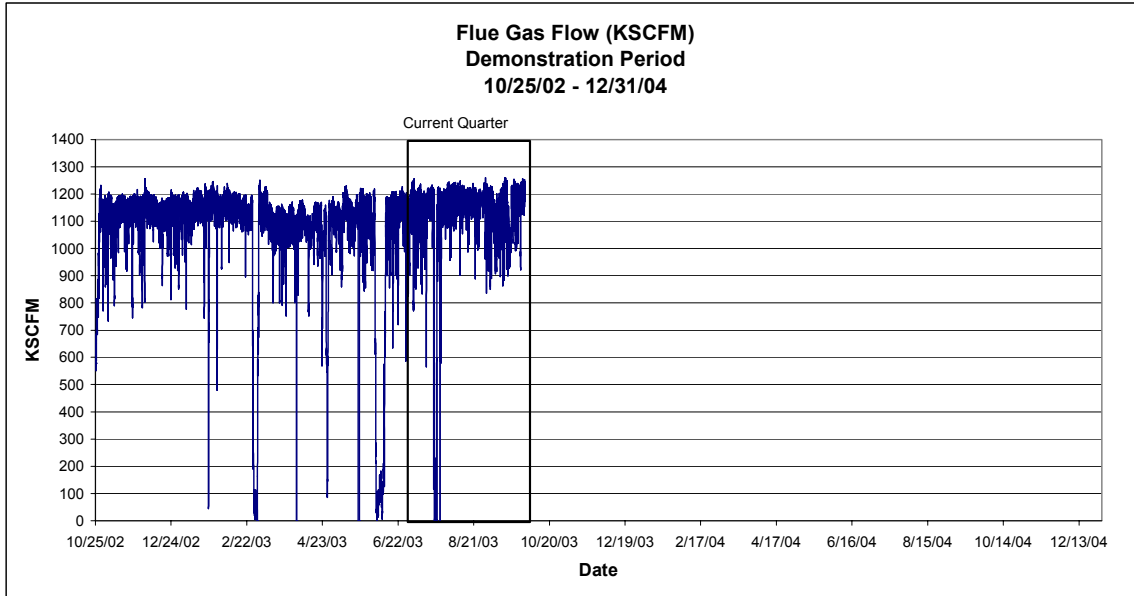
Appendix B8. Opacity spikes around 7/21/2003 and 9/23/2003 are instrument problems and not representative of actual high opacity.

APPENDIX B- GRAPHICAL & TABULAR PERFORMANCE DATA

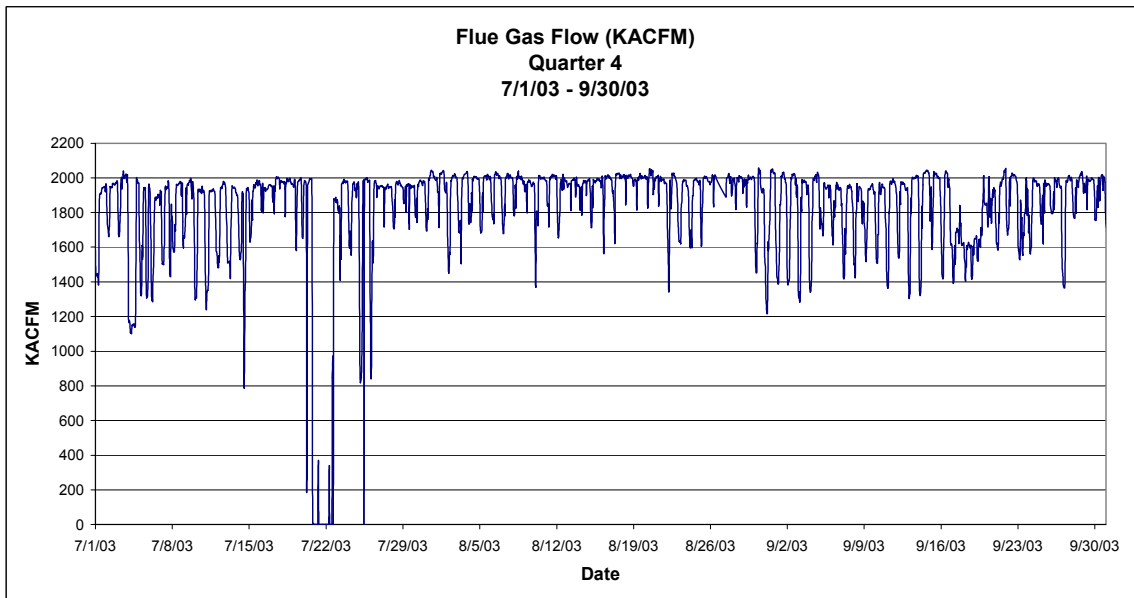
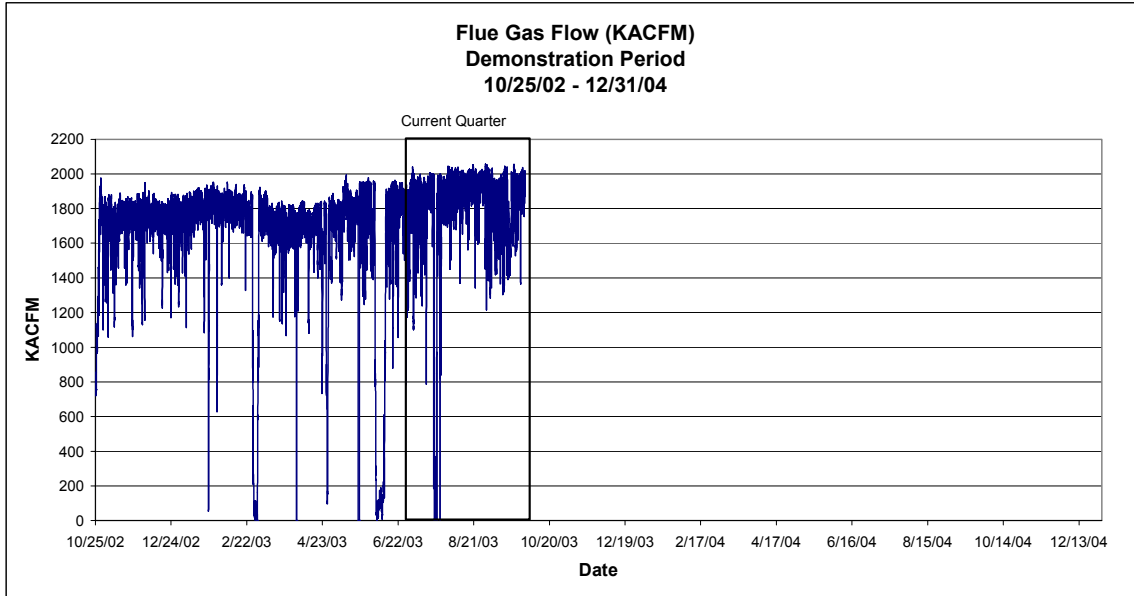
B1 Gross Plant Load



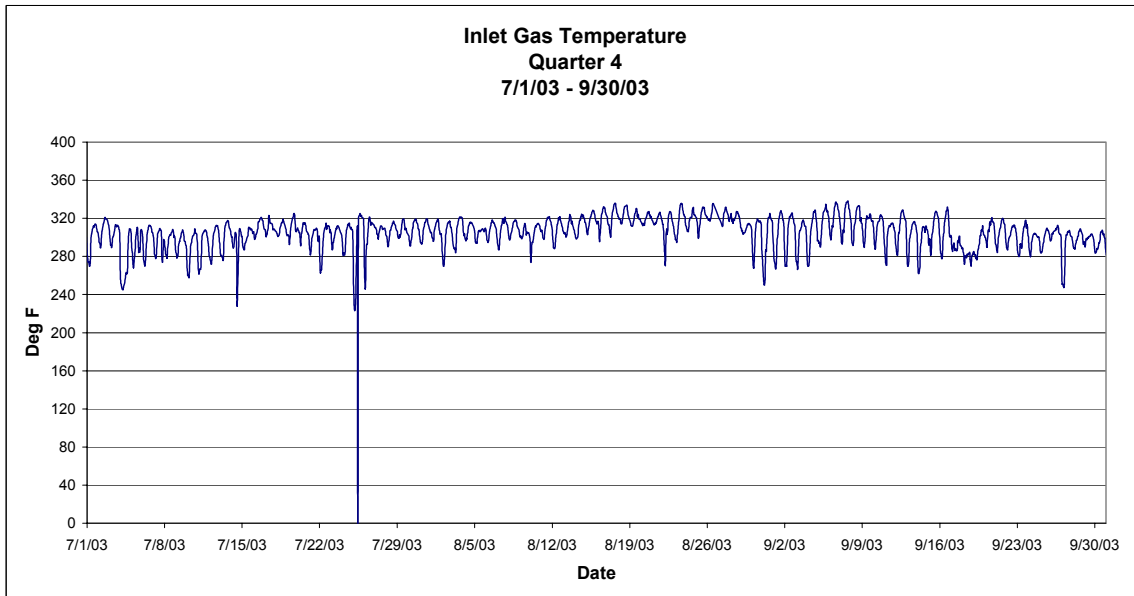
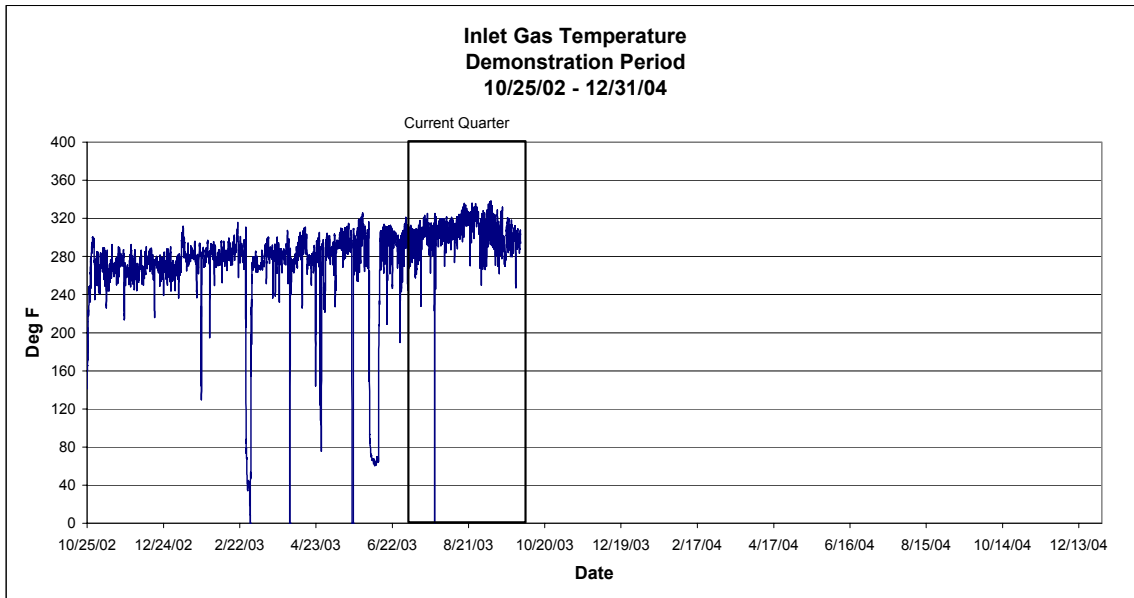
B2 Flue Gas Flow (KSCFM)



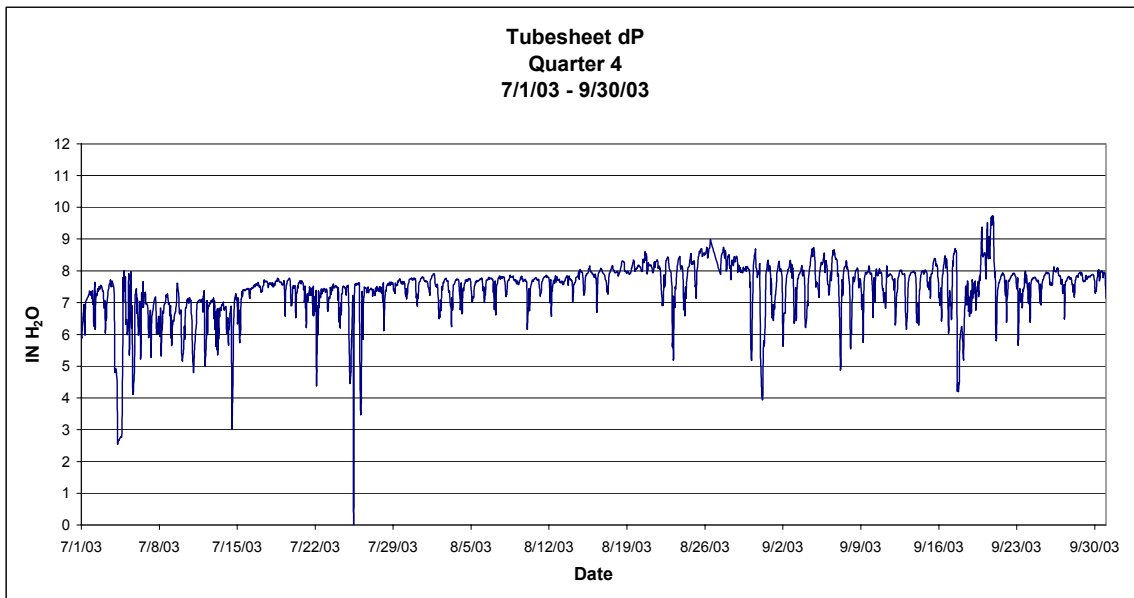
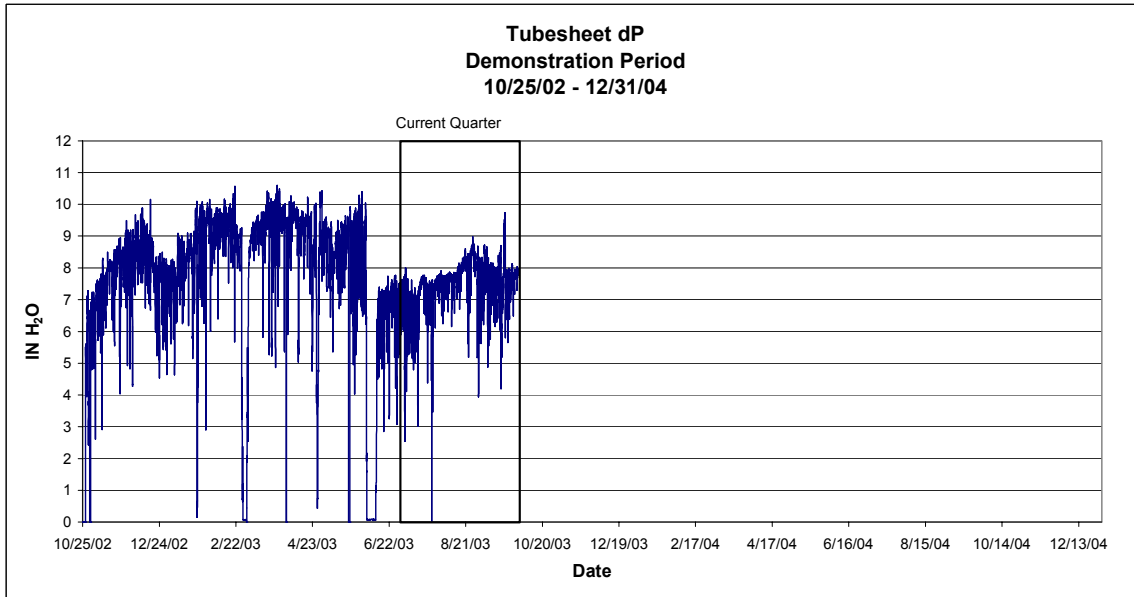
B3 Flue Gas Flow (KACFM)



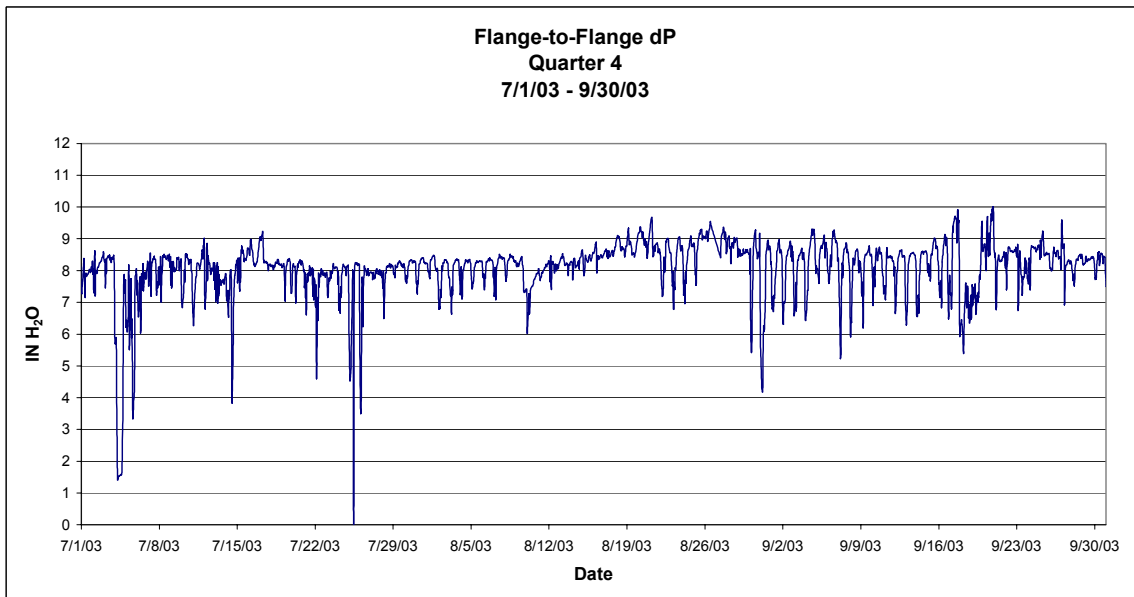
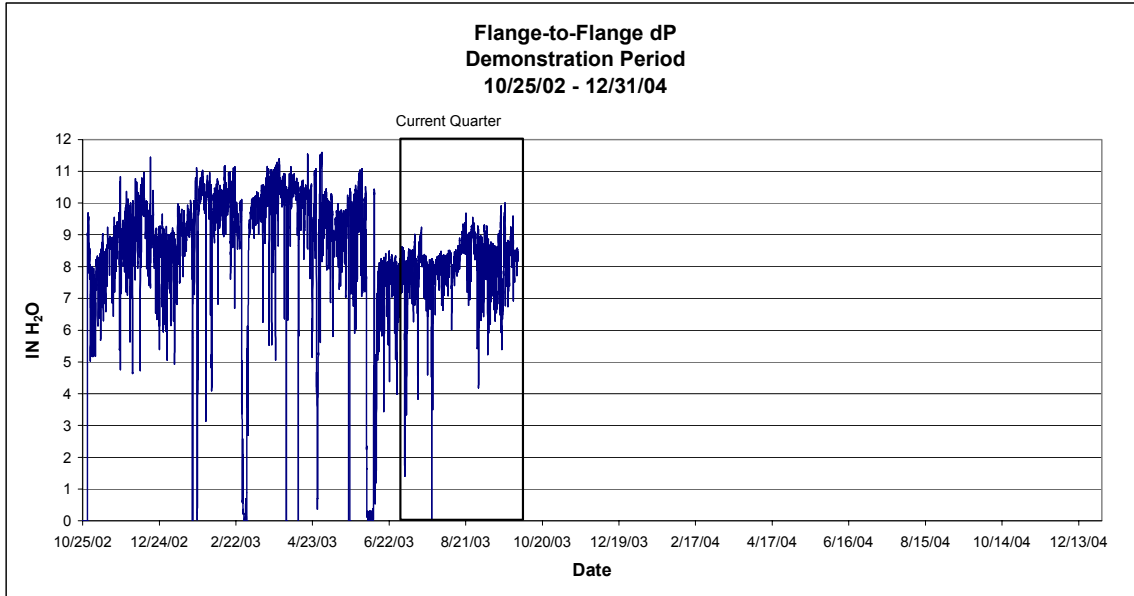
B4 Inlet Gas Temperature



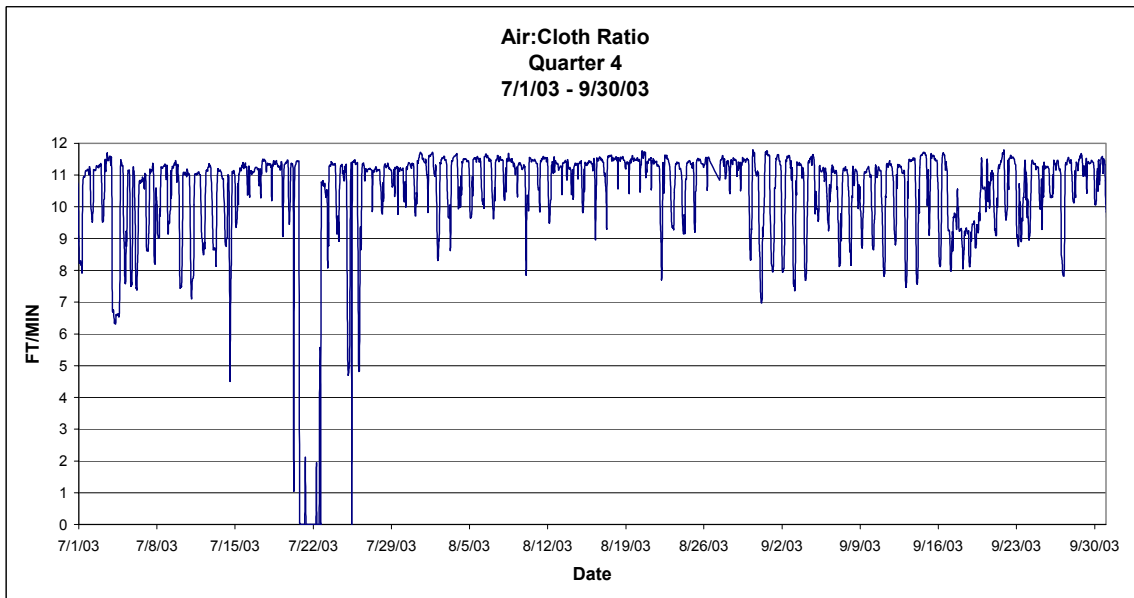
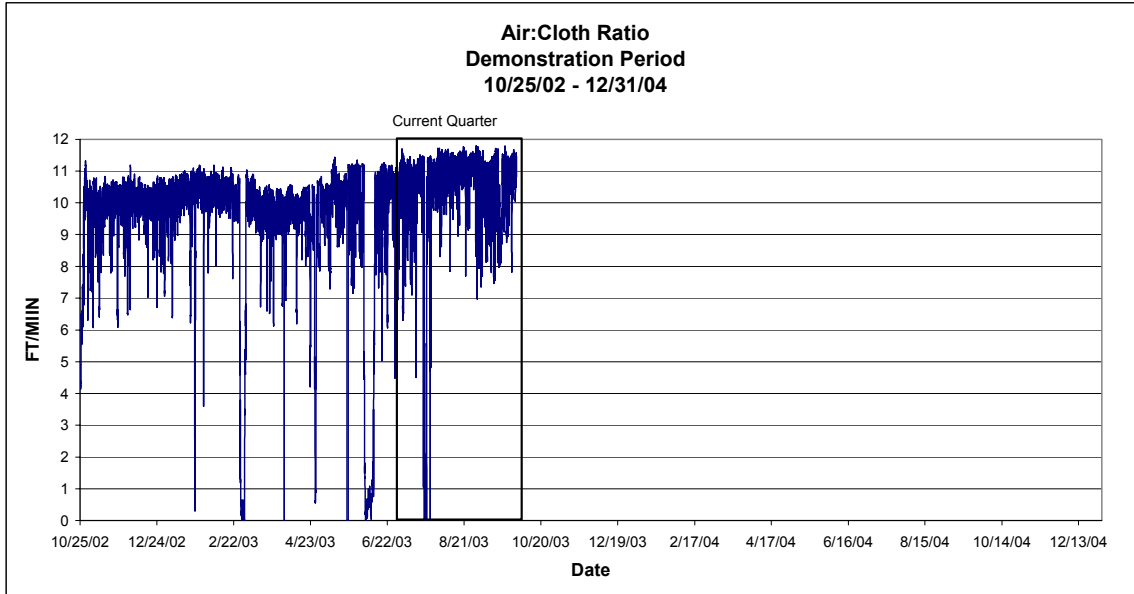
B5 Tubesheet dP



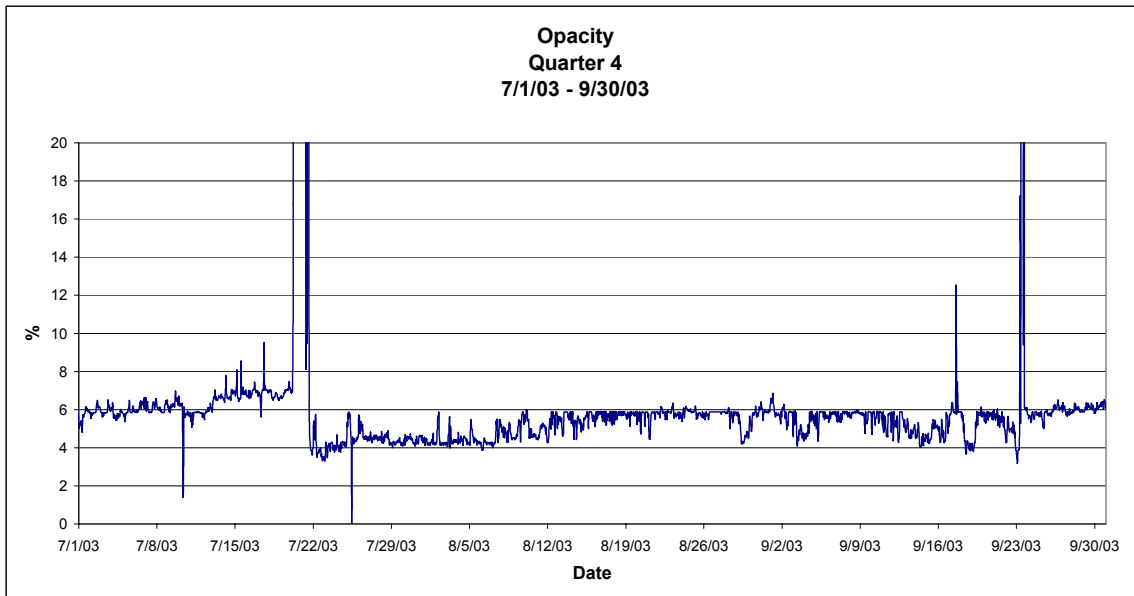
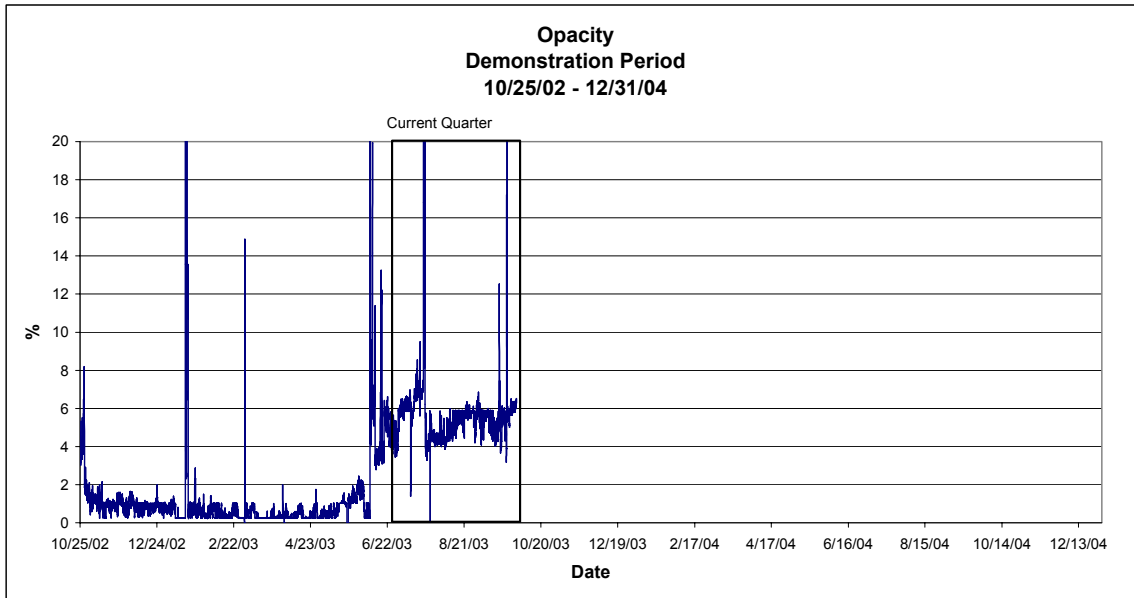
B6 Flange-to-Flange dP



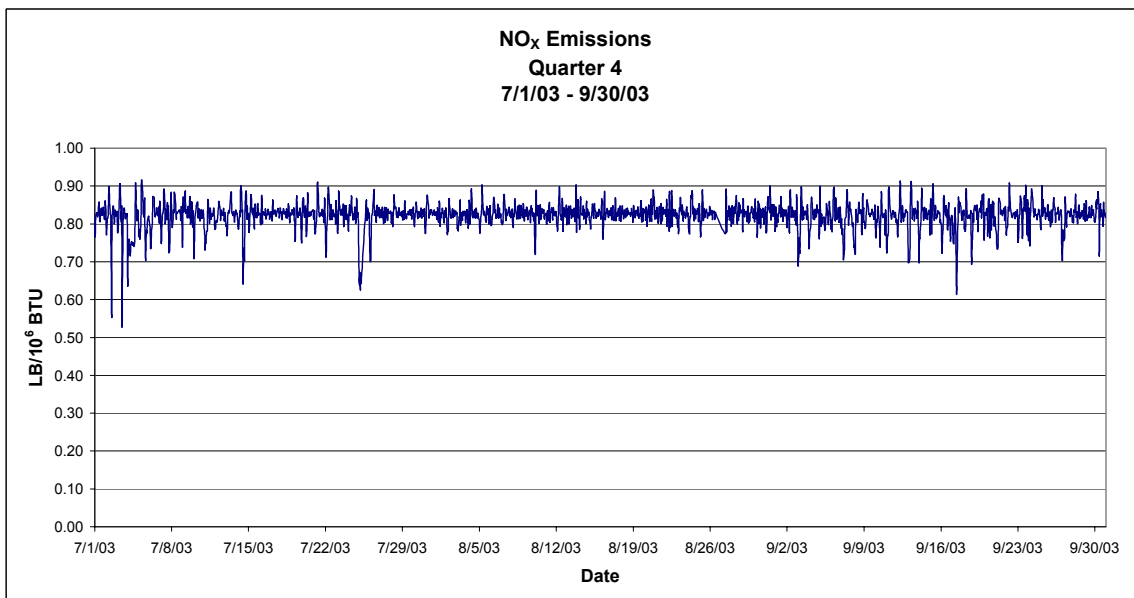
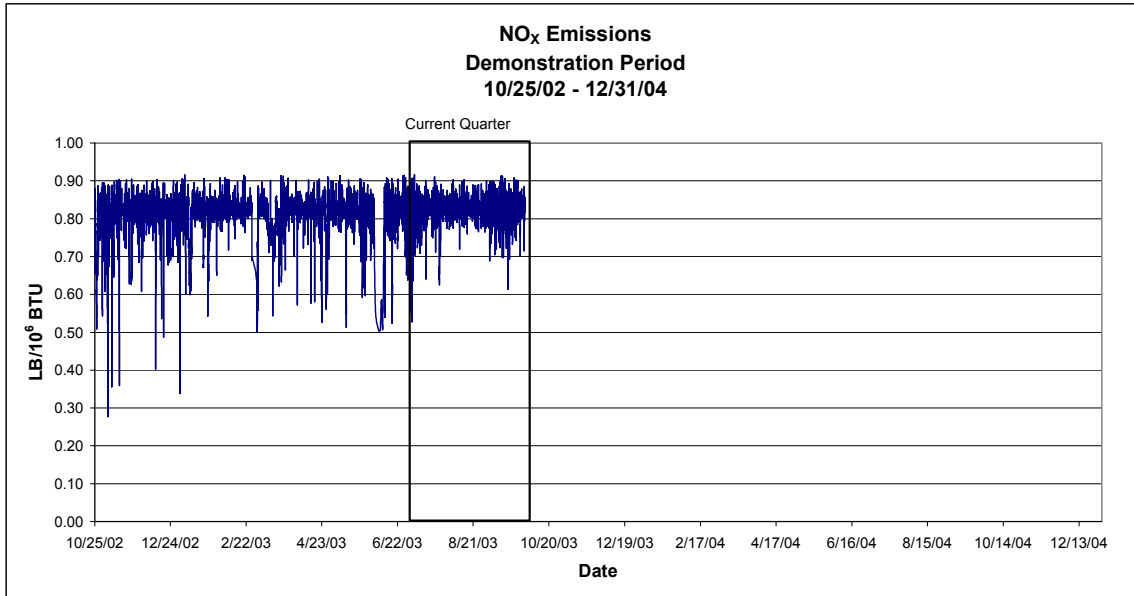
B7 Air-to-Cloth Ratio



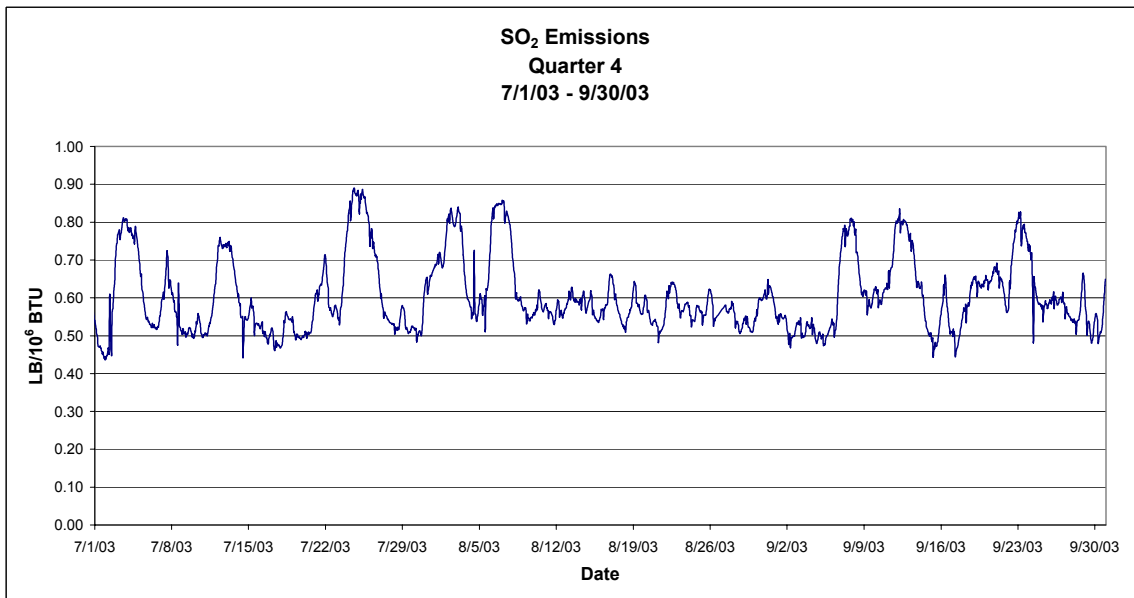
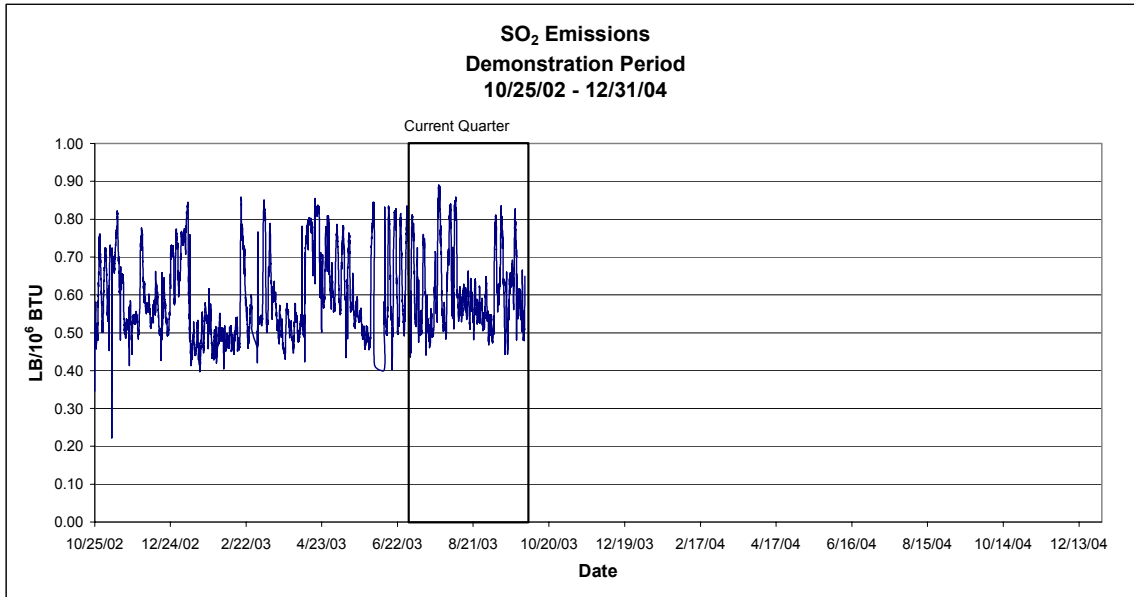
B8 Opacity



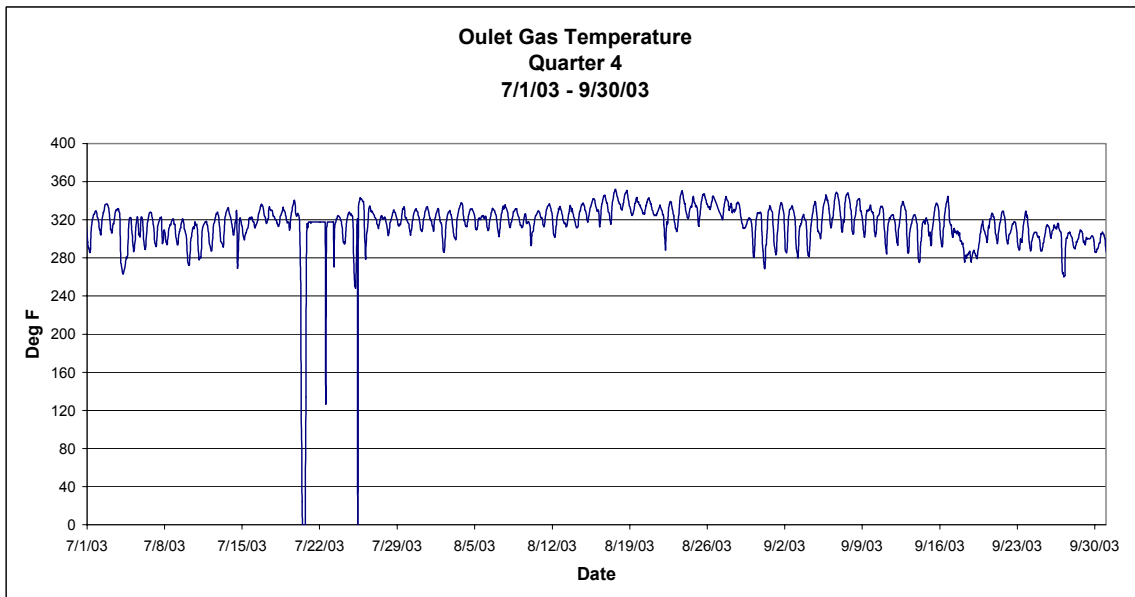
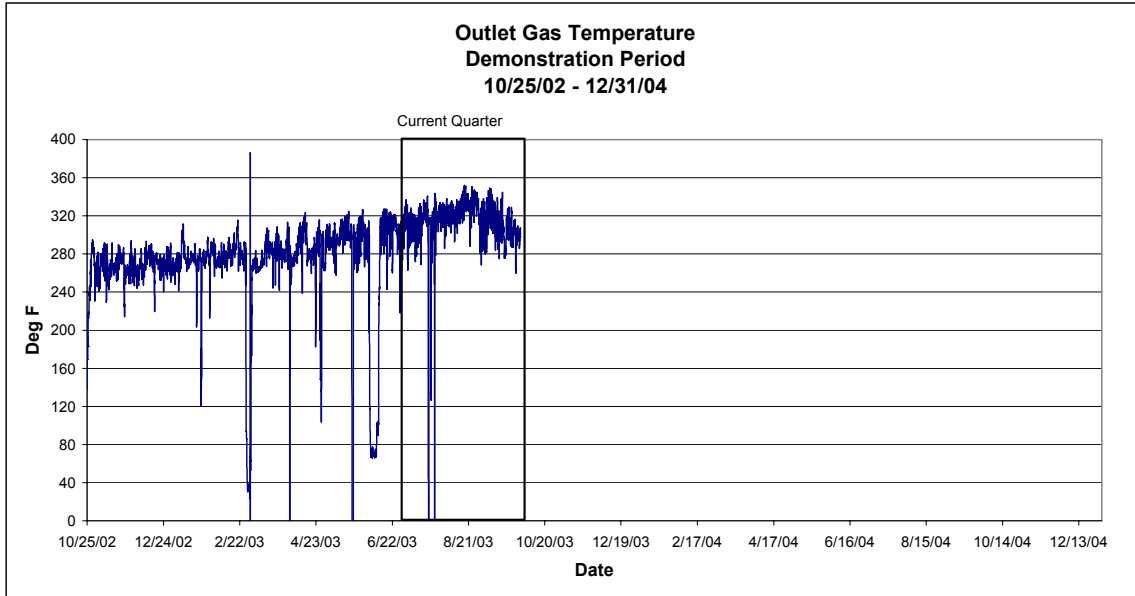
B9 NO_x Emissions



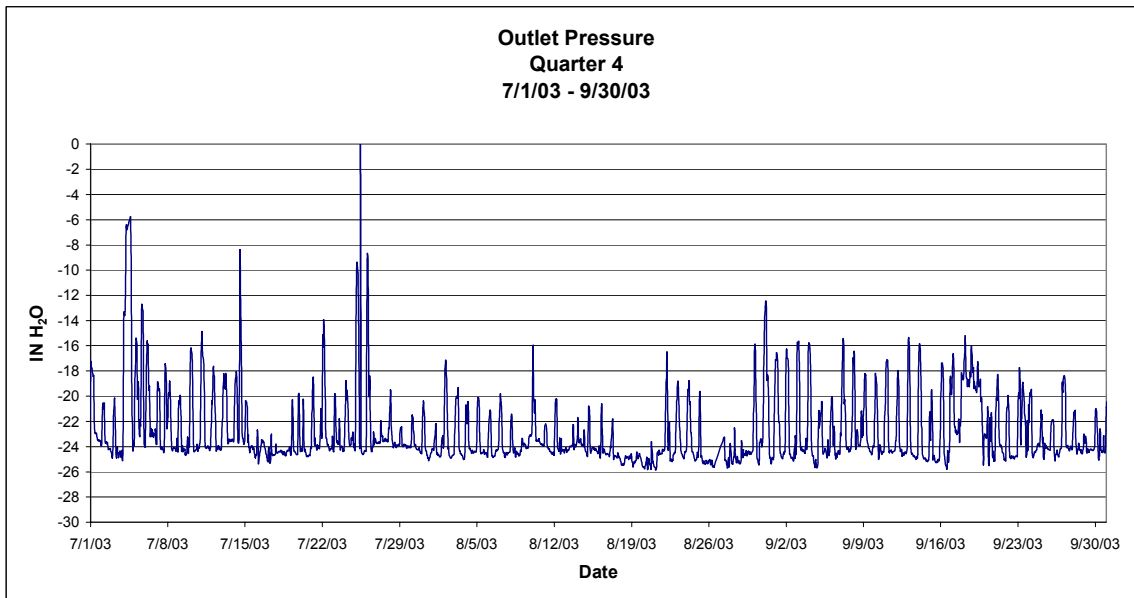
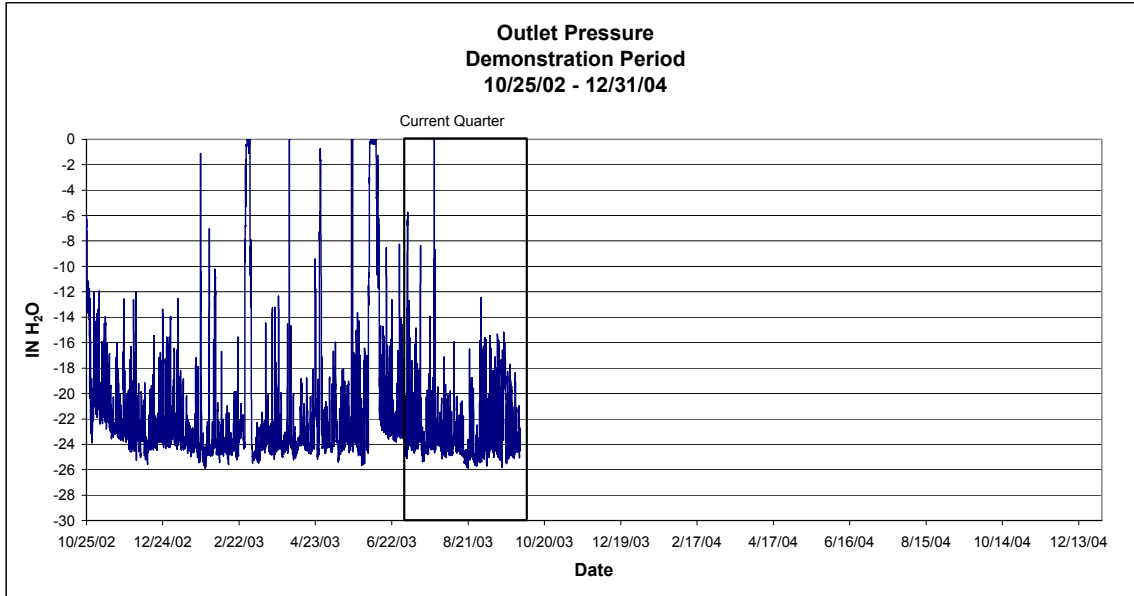
B10 SO₂ Emissions



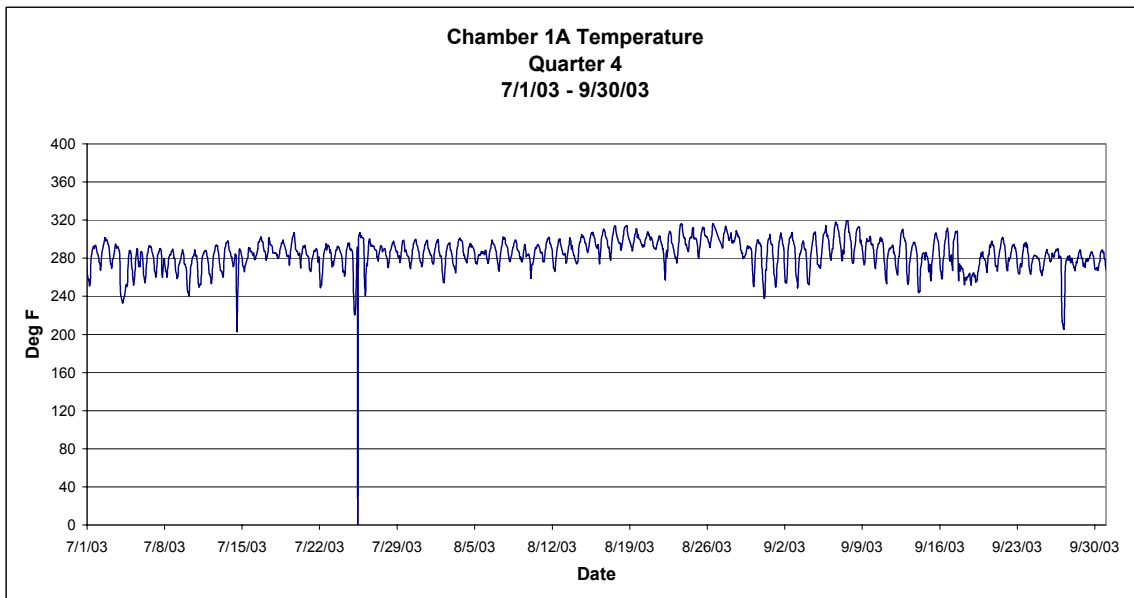
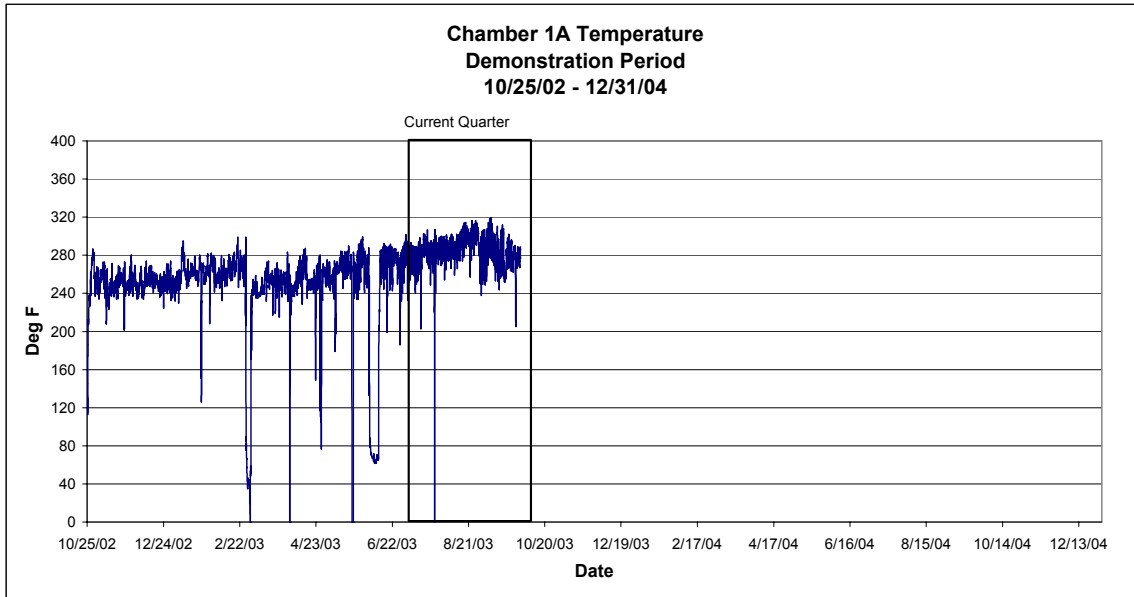
B11 Outlet Gas Temperature

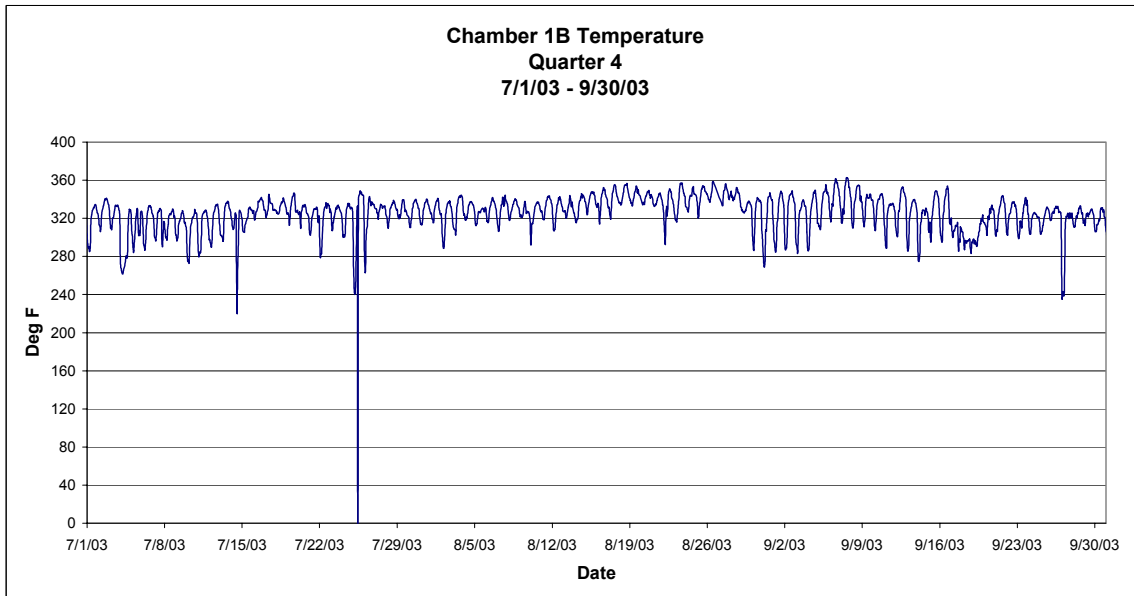
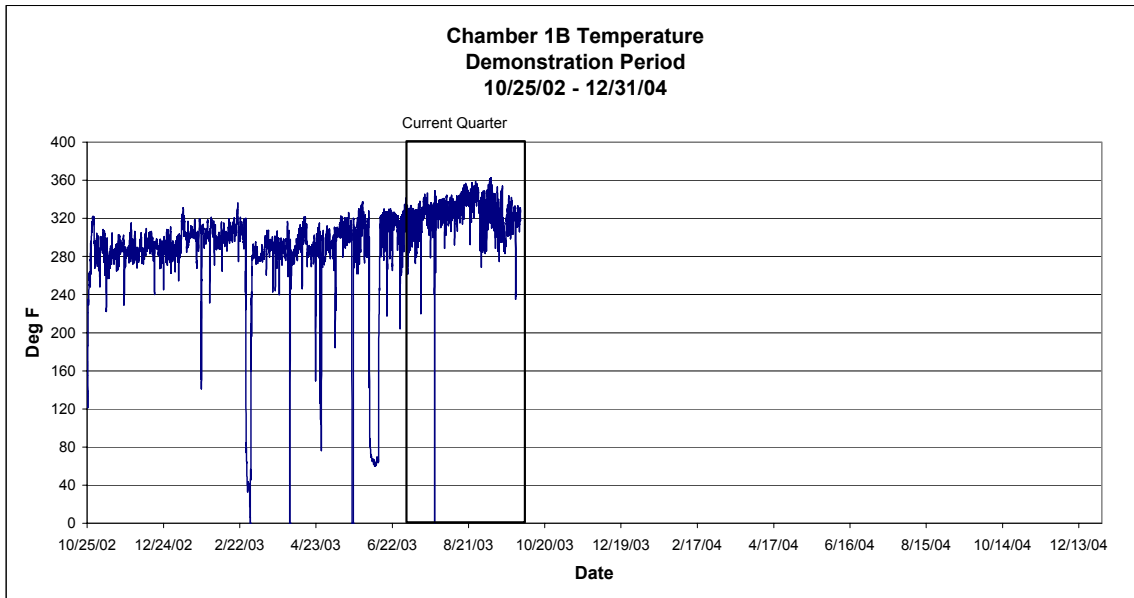


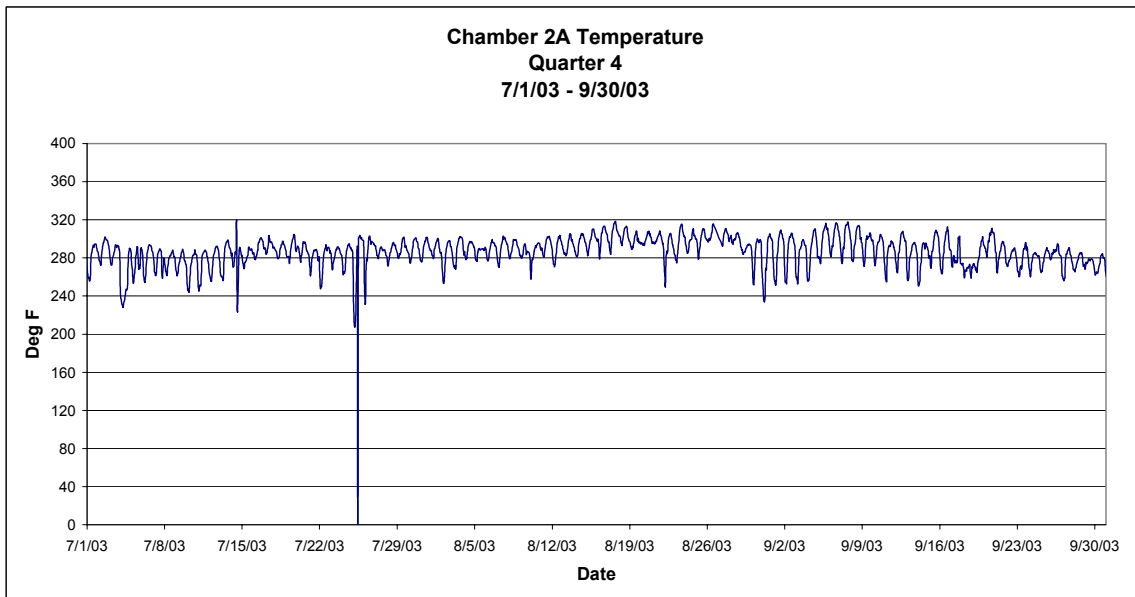
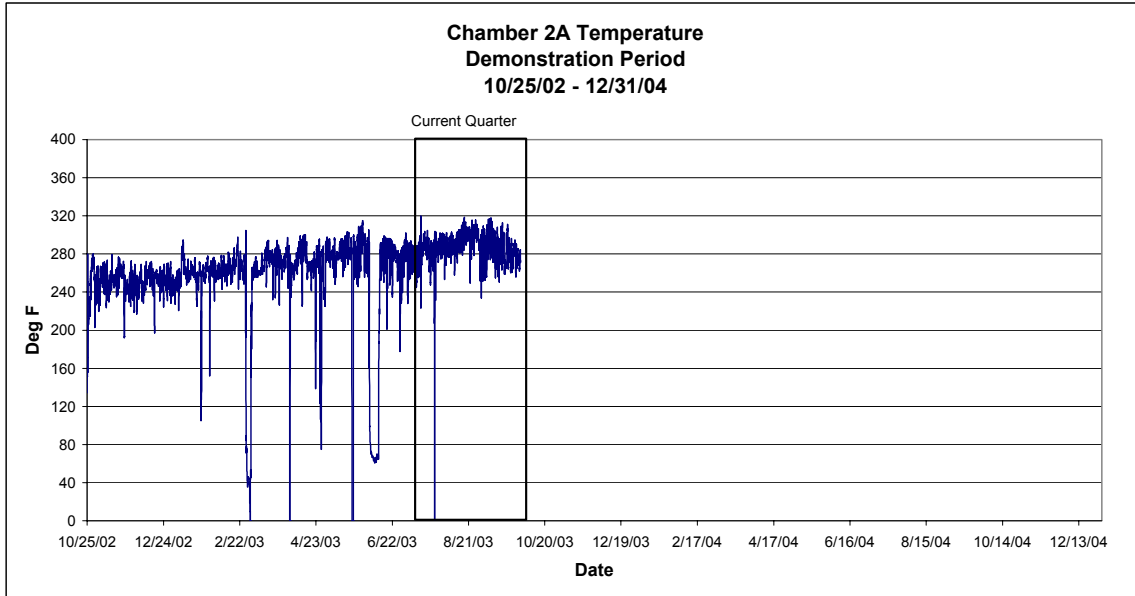
B12 Outlet Pressure

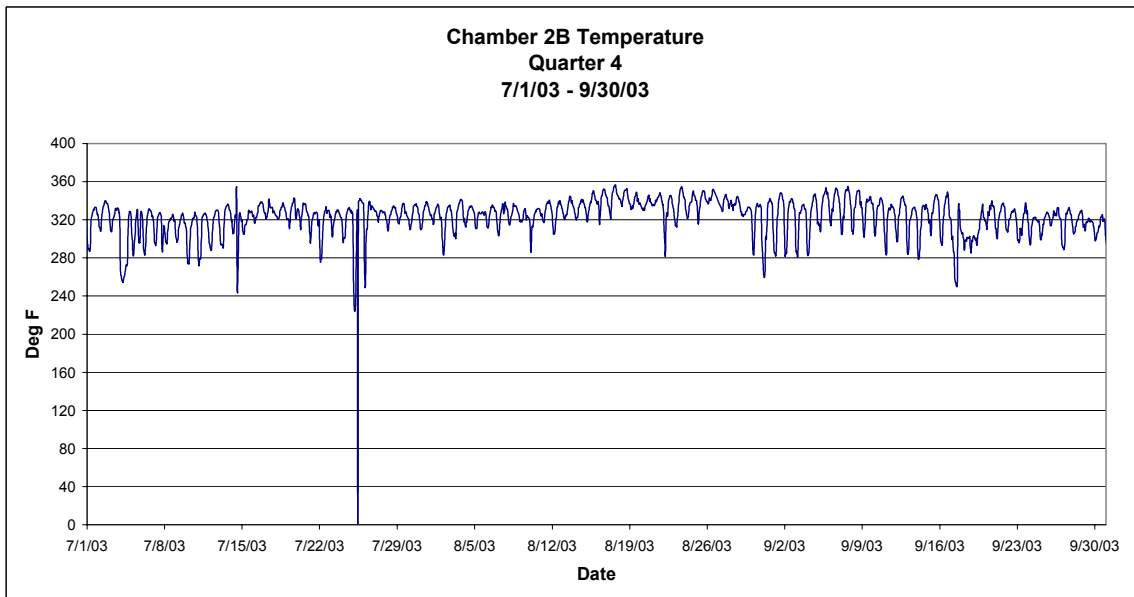
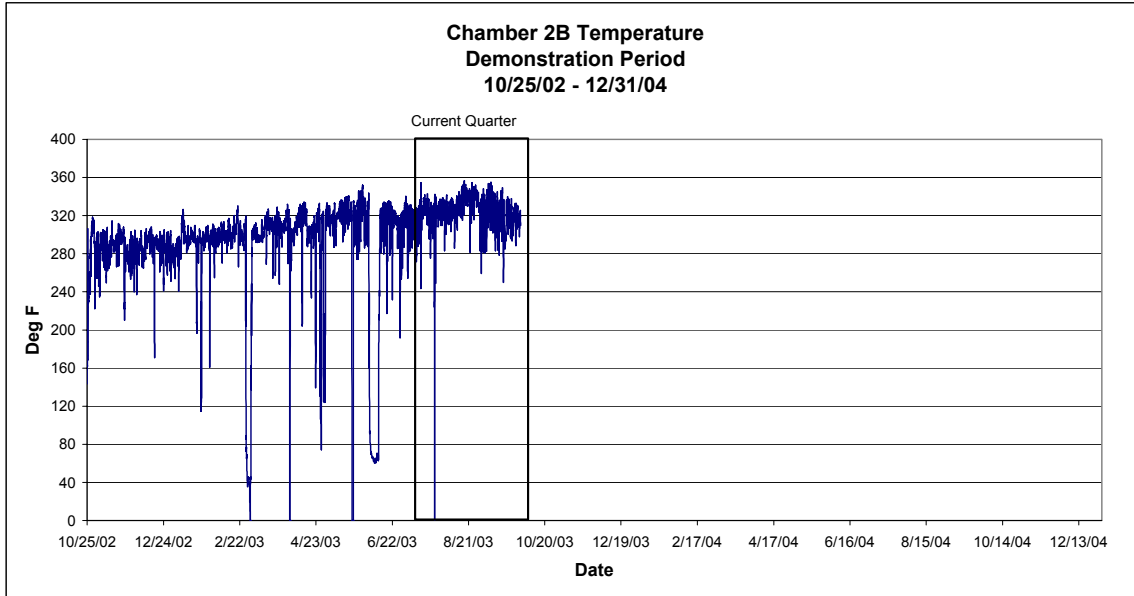


B13 Temperature per Chamber









B14 Fuel Burn Record

BIG STONE PLANT FUEL BURN RECORD - page 1 Jul-03
--

DATE	Coal (Tons)	P. Coke (Tons)	TDF (Tons)	Waste Seeds (Tons)	Toner (Tons)	Gran. Insul. (Tons)	Canvas Belting (Tons)	Plastic Chips (Tons)
1-Jul-03	5,608.91	0.00	92.25	380.44	0.00	0.00	0.00	0.00
2-Jul-03	6,015.40	0.00	27.52	474.68	0.00	0.00	0.00	0.00
3-Jul-03	6,544.89	0.00	73.64	23.87	0.00	0.00	0.00	0.00
4-Jul-03	4,873.10	0.00	0.00	0.00	0.00	0.00	0.00	0.00
5-Jul-03	5,833.60	0.00	0.00	0.00	0.00	0.00	0.00	0.00
6-Jul-03	6,044.60	0.00	0.00	0.00	0.00	0.00	0.00	0.00
7-Jul-03	5,899.67	0.00	71.91	71.12	0.00	0.00	0.00	0.00
8-Jul-03	6,241.19	0.00	25.32	94.59	0.00	0.00	0.00	0.00
9-Jul-03	6,305.42	0.00	96.76	91.92	0.00	0.00	0.00	0.00
10-Jul-03	5,807.50	0.00	100.00	75.00	0.00	0.00	0.00	0.00
11-Jul-03	5,939.50	0.00	0.00	0.00	0.00	0.00	0.00	0.00
12-Jul-03	6,269.10	0.00	0.00	0.00	0.00	0.00	0.00	0.00
13-Jul-03	6,282.60	0.00	0.00	0.00	0.00	0.00	0.00	0.00
14-Jul-03	5,493.97	0.00	70.85	39.18	0.00	0.00	0.00	0.00
15-Jul-03	6,311.10	0.00	24.00	117.93	26.47	0.00	0.00	0.00
16-Jul-03	6,525.20	0.00	0.00	0.00	0.00	0.00	0.00	0.00
17-Jul-03	6,477.53	0.00	74.24	113.33	0.00	0.00	0.00	0.00
18-Jul-03	6,706.77	0.00	22.62	48.41	0.00	0.00	0.00	0.00
19-Jul-03	6,507.10	0.00	0.00	0.00	0.00	0.00	0.00	0.00
20-Jul-03	6,703.70	0.00	0.00	0.00	0.00	0.00	0.00	0.00
21-Jul-03	6,560.20	0.00	0.00	0.00	0.00	0.00	0.00	0.00
22-Jul-03	6,099.20	0.00	0.00	0.00	0.00	0.00	0.00	0.00
23-Jul-03	6,304.46	0.00	162.95	95.89	0.00	0.00	0.00	0.00
24-Jul-03	6,202.95	0.00	72.30	141.55	0.00	0.00	0.00	0.00
25-Jul-03	5,521.04	0.00	46.39	92.57	0.00	0.00	0.00	0.00
26-Jul-03	5,869.10	0.00	0.00	0.00	0.00	0.00	0.00	0.00
27-Jul-03	6,624.50	0.00	0.00	0.00	0.00	0.00	0.00	0.00
28-Jul-03	6,418.90	0.00	93.00	72.50	0.00	0.00	0.00	0.00
29-Jul-03	6,652.26	0.00	24.17	48.67	0.00	0.00	0.00	0.00
30-Jul-03	6,493.44	0.00	70.91	94.55	0.00	0.00	0.00	0.00
31-Jul-03	6,868.90	0.00	0.00	0.00	0.00	0.00	0.00	0.00
Adjustment	0.00							
Total Burned	192,005.80	0.00	1,148.83	2,076.20	26.47	0.00	0.00	0.00
Total Delivered	154,635.98	0.00	1,271.15	1,974.87	26.47	0.00	0.00	0.00
HHV	8561	0	15000	7187	16932	0	0	0
% Ash	4.61%	0.00%	7.04%	1.10%	0.00%	0.00%	0.00%	0.00%
Tons Ash	8,860.09	0.00	80.88	22.84	0.00	0.00	0.00	0.00

BIG STONE PLANT
FUEL BURN RECORD - page 1
Aug-03

DATE	Coal (Tons)	P. Coke (Tons)	TDF (Tons)	Waste Seeds (Tons)	Toner (Tons)	Gran. Insul. (Tons)	Canvas Belting (Tons)	Plastic Chips (Tons)
1-Aug-03	6,743.00	0.00	133.00	50.00	0.00	0.00	0.00	0.00
2-Aug-03	6,317.90	0.00	133.00	46.00	0.00	0.00	0.00	0.00
3-Aug-03	6,319.74	0.00	131.88	45.98	0.00	0.00	0.00	0.00
4-Aug-03	6,600.60	0.00	0.00	0.00	0.00	0.00	0.00	0.00
5-Aug-03	6,103.03	0.00	237.82	229.15	0.00	0.00	0.00	0.00
6-Aug-03	6,689.25	0.00	70.01	61.74	0.00	0.00	0.00	0.00
7-Aug-03	6,693.50	0.00	50.00	50.00	0.00	0.00	0.00	0.00
8-Aug-03	6,789.10	0.00	0.00	0.00	0.00	0.00	0.00	0.00
9-Aug-03	6,780.00	0.00	0.00	0.00	0.00	0.00	0.00	0.00
10-Aug-03	6,640.30	0.00	0.00	0.00	0.00	0.00	0.00	0.00
11-Aug-03	6,610.40	0.00	100.00	100.00	0.00	0.00	0.00	0.00
12-Aug-03	6,517.90	0.00	47.40	0.00	0.00	0.00	0.00	0.00
13-Aug-03	6,741.74	0.00	73.02	4.04	0.00	0.00	0.00	0.00
14-Aug-03	6,556.76	0.00	95.61	42.73	0.00	0.00	0.00	0.00
15-Aug-03	6,450.81	0.00	141.44	146.75	0.00	0.00	0.00	0.00
16-Aug-03	6,755.10	0.00	0.00	0.00	0.00	0.00	0.00	0.00
17-Aug-03	6,812.20	0.00	0.00	0.00	0.00	0.00	0.00	0.00
18-Aug-03	6,816.46	0.00	91.94	0.00	0.00	0.00	0.00	0.00
19-Aug-03	6,597.90	0.00	100.00	75.00	0.00	0.00	0.00	0.00
20-Aug-03	6,597.61	0.00	69.93	81.46	0.00	0.00	0.00	0.00
21-Aug-03	6,665.60	0.00	50.00	50.00	0.00	0.00	0.00	0.00
22-Aug-03	5,870.40	0.00	119.63	440.07	0.00	0.00	0.00	0.00
23-Aug-03	5,911.43	0.00	0.00	440.07	0.00	0.00	0.00	0.00
24-Aug-03	5,922.23	0.00	0.00	440.07	0.00	0.00	0.00	0.00
25-Aug-03	5,927.41	0.00	300.00	294.19	0.00	0.00	0.00	0.00
26-Aug-03	6,611.26	0.00	0.00	70.04	0.00	0.00	0.00	0.00
27-Aug-03	6,262.98	0.00	0.00	241.62	0.00	0.00	0.00	0.00
28-Aug-03	6,548.60	0.00	10.14	24.16	0.00	0.00	0.00	0.00
29-Aug-03	6,496.20	0.00	75.00	100.00	0.00	0.00	0.00	0.00
30-Aug-03	6,021.40	0.00	50.00	100.00	0.00	0.00	0.00	0.00
31-Aug-03	5,848.66	0.00	68.17	54.77	0.00	0.00	0.00	0.00
Adjustment	0.00							
Total Burned	200,219.47	0.00	2,147.99	3,187.84	0.00	0.00	0.00	0.00
Total Delivered	184,120.00	0.00	1,979.51	3,116.65	0.00	0.00	0.00	0.00
HHV	8575	0	15000	7187	0	0	0	0
% Ash	4.70%	0.00%	7.04%	1.10%	0.00%	0.00%	0.00%	0.00%
Tons Ash	9,417.23	0.00	151.22	35.07	0.00	0.00	0.00	0.00

BIG STONE PLANT
FUEL BURN RECORD - page 1
Sep-03

DATE	Coal (Tons)	P. Coke (Tons)	TDF (Tons)	Waste Seeds (Tons)	Toner (Tons)	Gran. Insul. (Tons)	Canvas Belting (Tons)	Plastic Chips (Tons)
1-Sep-03	6,062.70	0.00	0.00	0.00	0.00	0.00	0.00	0.00
2-Sep-03	6,086.80	0.00	0.00	0.00	0.00	0.00	0.00	0.00
3-Sep-03	5,671.17	0.00	210.82	68.41	0.00	0.00	0.00	0.00
4-Sep-03	5,901.99	0.00	72.78	46.73	0.00	0.00	0.00	0.00
5-Sep-03	6,225.60	0.00	100.00	50.00	0.00	0.00	0.00	0.00
6-Sep-03	6,367.08	0.00	121.38	45.94	0.00	0.00	0.00	0.00
7-Sep-03	6,247.40	0.00	0.00	0.00	0.00	0.00	0.00	0.00
8-Sep-03	6,102.54	0.00	118.94	45.62	0.00	0.00	0.00	0.00
9-Sep-03	6,146.21	0.00	93.05	23.64	0.00	0.00	0.00	0.00
10-Sep-03	6,064.33	0.00	73.44	22.13	0.00	0.00	0.00	0.00
11-Sep-03	6,289.50	0.00	50.00	25.00	0.00	0.00	0.00	0.00
12-Sep-03	6,321.90	0.00	120.00	75.00	0.00	0.00	0.00	0.00
13-Sep-03	6,091.00	0.00	120.00	75.00	0.00	0.00	0.00	0.00
14-Sep-03	5,974.33	0.00	122.40	61.67	0.00	0.00	0.00	0.00
15-Sep-03	6,299.81	0.00	46.85	76.14	0.00	0.00	0.00	0.00
16-Sep-03	5,977.12	0.00	50.40	97.98	0.00	0.00	0.00	0.00
17-Sep-03	5,232.80	0.00	50.00	100.00	0.00	0.00	0.00	0.00
18-Sep-03	5,167.98	0.00	72.67	23.15	0.00	0.00	0.00	0.00
19-Sep-03	5,666.01	0.00	42.13	57.86	0.00	0.00	0.00	0.00
20-Sep-03	6,506.90	0.00	0.00	0.00	0.00	0.00	0.00	0.00
21-Sep-03	6,583.80	0.00	0.00	0.00	0.00	0.00	0.00	0.00
22-Sep-03	6,181.04	0.00	94.33	274.73	0.00	0.00	0.00	0.00
23-Sep-03	5,796.03	0.00	72.63	25.94	0.00	0.00	0.00	0.00
24-Sep-03	6,275.00	0.00	25.47	13.83	0.00	0.00	0.00	0.00
25-Sep-03	6,363.60	0.00	25.00	25.00	0.00	0.00	0.00	0.00
26-Sep-03	6,267.41	0.00	66.80	107.39	0.00	0.00	0.00	0.00
27-Sep-03	5,787.30	0.00	0.00	100.00	0.00	0.00	0.00	0.00
28-Sep-03	6,336.90	0.00	0.00	100.00	0.00	0.00	0.00	0.00
29-Sep-03	6,446.52	0.00	95.13	46.25	0.00	0.00	0.00	0.00
30-Sep-03	6,170.55	0.00	125.33	23.02	0.00	0.00	0.00	0.00
Adjustment	3,000.00							
Total Burned	185,611.32	0.00	1,969.55	1,610.43	0.00	0.00	0.00	0.00
Total Delivered	194,770.48	0.00	1,969.55	1,610.43	0.00	0.00	0.00	0.00
HHV	8530	0	15000	7187	0	0	0	0
% Ash	4.59%	0.00	7.04%	1.10%	0.00%	0.00%	0.00%	0.00%
Tons Ash	8,526.64	0.00	51.48	12.52	0.00	0.00	0.00	0.00

B15 Fuel Analysis Record

BIG STONE PLANT	COAL ANALYSIS PER TRAIN
	Jul-03
	PAGE 1

DATE	TR #	MOIS %	% ASIHHV AR	HHV AR	S, % AR	% ASF DRY	HHV DRY	S, % DRY	NaO %	MAF HHV	COAL TONS	TONS OK
PREV. MC	ebm20	30.8	4.75	8357	0.43	6.86	12069	0.62	1.83	12958	14166.25	1296.77
PREV. MC	bam52	29.7	4.19	8605	0.23	5.96	12242	0.33	1.52	13018	14160.08	14160.08
1-Jul-03	0	0	0	0	0	0	0	0	0	0	0.00	
2-Jul-03	ebm21	31.2	4.85	8312	0.41	7.04	12075	0.6	1.76	12989	14166.88	14166.88
3-Jul-03	bam053	29.3	4.32	8606	0.25	6.12	12180	0.36	1.62	12974	14173.35	14173.35
4-Jul-03	0	0	0	0	0	0	0	0	0	0	0.00	
5-Jul-03	0	0	0	0	0	0	0	0	0	0	0.00	
6-Jul-03	0	0	0	0	0	0	0	0	0	0	0.00	
7-Jul-03	bam054	29.3	4.47	8595	0.28	6.32	12161	0.39	1.56	12981	12952.58	12952.58
8-Jul-03	0	0	0	0	0	0	0	0	0	0	0.00	
9-Jul-03	bam055	29.4	4.41	8585	0.26	6.24	12160	0.37	1.49	12969	14160.63	14160.63
10-Jul-03	0	0	0	0	0	0	0	0	0	0	0.00	
11-Jul-03	0	0	0	0	0	0	0	0	0	0	0.00	
12-Jul-03	0	0	0	0	0	0	0	0	0	0	0.00	
13-Jul-03	bam056	28.8	4.73	8623	0.3	6.65	12114	0.42	1.34	12977	14178.45	14178.45
14-Jul-03	0	0	0	0	0	0	0	0	0	0	0.00	
15-Jul-03	bam057	29.5	4.25	8610	0.26	6.03	12216	0.37	1.52	13000	14178.85	14178.85
16-Jul-03	0	0	0	0	0	0	0	0	0	0	0.00	
17-Jul-03	bam58	29	4.38	8706	0.29	6.17	12265	0.41	1.51	13072	14178.40	14178.40
18-Jul-03	0	0	0	0	0	0	0	0	0	0	0.00	
19-Jul-03	0	0	0	0	0	0	0	0	0	0	0.00	
20-Jul-03	0	0	0	0	0	0	0	0	0	0	0.00	
21-Jul-03	bam59	29.3	4.44	8634	0.31	6.28	12211	0.44	1.5	13029	14140.95	14140.95
22-Jul-03	ebm22	29.9	4.91	8472	0.49	7.01	12084	0.7	1.87	12995	14169.00	14169.00
23-Jul-03	0	0	0	0	0	0	0	0	0	0	0.00	
24-Jul-03	0	0	0	0	0	0	0	0	0	0	0.00	
25-Jul-03	0	0	0	0	0	0	0	0	0	0	0.00	
26-Jul-03	bam60	28.4	4.85	8630	0.26	6.78	12056	0.37	1.36	12933	14154.60	14154.60
27-Jul-03	bam61	28.8	4.18	8671	0.28	5.87	12179	0.4	1.55	12938	14182.30	14182.30
28-Jul-03	0	0	0	0	0	0	0	0	0	0	0.00	
29-Jul-03	0	0	0	0	0	0	0	0	0	0	0.00	
30-Jul-03	0	0	0	0	0	0	0	0	0	0	0.00	
31-Jul-03	0	0	0	0	0	0	0	0	0	0	0.00	
ADJ.												170092.84
Weighted Average		29.49	4.61	8561	0.30	6.55	12142	0.43	1.55			192005.80
											Tons. OK	192005.80
											Burn	192005.80

Monthly Mercury Analysis

Train #	Sample #	% Moist.	Mercury Chloride	
			ug/g dry basis	ug/g
	C1364	30.39	0.105	<0.01

BIG STONE PLANT COAL ANALYSIS PER TRAIN
Aug-03 PAGE 1

DATE	TR #	MOIS %	ASI %	HHV AR	S, % AR	% ASH DRY	HHV DRY	S, % DRY	NaO %	MAF HHV	COAL TONS	TONS OK										
PREV. MON.																						
PREV. MON.																						
1-Aug-03	ebm23	30.2	4.77	8449	0.43	6.84	12105	0.61	1.89	12994	14170.08	14170.08										
2-Aug-03	bam62	28.8	4.33	8708	0.3	6.08	12227	0.42	1.58	13019	14174.10	14174.10										
3-Aug-03	0	0	0	0	0	0	0	0	0	0	0.00											
4-Aug-03	0	0	0	0	0	0	0	0	0	0	0.00											
5-Aug-03	ebm24	30.3	5.12	8366	0.43	7.34	11997	0.62	1.78	12947	14185.32	14185.32										
6-Aug-03	0	0	0	0	0	0	0	0	0	0	0.00											
7-Aug-03	bam63	29	4.36	8721	0.28	6.14	12274	0.4	1.48	13077	14180.18	14180.18										
8-Aug-03	0	0	0	0	0	0	0	0	0	0	0.00											
9-Aug-03	0	0	0	0	0	0	0	0	0	0	0.00											
10-Aug-03	bam64	28.6	4.25	8714	0.29	5.95	12211	0.4	1.49	12984	14163.80	14163.80										
11-Aug-03	bam65	28.5	4.49	8712	0.31	6.28	12191	0.44	1.53	13008	14179.73	14179.73										
12-Aug-03	0	0	0	0	0	0	0	0	0	0	0.00											
13-Aug-03	0	0	0	0	0	0	0	0	0	0	0.00											
14-Aug-03	bam66	28.8	4.43	8645	0.29	6.23	12149	0.41	1.44	12956	14163.08	14163.08										
15-Aug-03	0	0	0	0	0	0	0	0	0	0	0.00											
16-Aug-03	bam67	28.7	4.71	8627	0.29	6.6	12099	0.41	1.46	12954	14179.60	14179.60										
17-Aug-03	0	0	0	0	0	0	0	0	0	0	0.00											
18-Aug-03	bam68	28.6	4.52	8663	0.29	6.33	12140	0.41	1.51	12960	14170.10	14170.10										
19-Aug-03	0	0	0	0	0	0	0	0	0	0	0.00											
20-Aug-03	0	0	0	0	0	0	0	0	0	0	0.00											
21-Aug-03	0	0	0	0	0	0	0	0	0	0	0.00											
22-Aug-03	bam69	29.3	4.79	8541	0.29	6.78	12083	0.41	1.63	12962	14042.45	14042.45										
23-Aug-03	bam70	29.4	4.67	8541	0.3	6.61	12099	0.43	1.54	12955	14179.40	14179.40										
24-Aug-03	0	0	0	0	0	0	0	0	0	0	0.00											
25-Aug-03	0	0	0	0	0	0	0	0	0	0	0.00											
26-Aug-03	0	0	0	0	0	0	0	0	0	0	0.00											
27-Aug-03	bam71	29.4	4.6	8591	0.3	6.52	12168	0.43	1.49	13017	14164.35	14164.35										
28-Aug-03	bam72	29.6	4.53	8590	0.27	6.43	12193	0.39	1.56	13031	14167.83	4375.44										
29-Aug-03	0	0	0	0	0	0	0	0	0	0	0.00											
30-Aug-03	0	0	0	0	0	0	0	0	0	0	0.00											
31-Aug-03	0	0	0	0	0	0	0	0	0	0	0.00											
											174327.63											
Weighted Average											29.29	4.70	8575	0.31	6.66	12127	0.45	1.56			Tons. OK	200219.47
																					Burn	200219.47

Monthly Mercury Analysis

Train Sample #	Sample #	% Moist.	Mercury Chlor.	
			ug/g dry basis	ug/g
	C1719	28.75	0.081	<0.01

BIG STONE PLANT

COAL ANALYSIS PER TRAIN

Sep-03

PAGE 1

DATE	TR #	MOIS. %	% ASI AR	HHV AR	S, % AR	% ASH DRY	HHV DRY	S, % DRY	NaO %	MAF HHV	COAL TONS	TONS OK								
PREV. MON.																				
PREV. MON.	bam72	29.55	4.53	8590	0.27	6.43	12193	0.39	1.6	13031	14167.83	9792.39								
1-Sep-03	bam74	29.19	4.33	8623	0.28	6.11	12178	0.4	1.6	12970	14175.15	14175.15								
2-Sep-03	0	0	0	0	0	0	0	0	0	0	0.00									
3-Sep-03	bam73	29	4.25	8640	0.26	5.99	12169	0.36	1.5	12944	13314.88	13314.88								
4-Sep-03	0	0	0	0	0	0	0	0	0	0	0.00									
5-Sep-03	0	30.35	4.7	8423	0.42	6.75	12093	0.61	1.9	12968	597.50	597.50								
6-Sep-03	ebm25	30.35	4.7	8423	0.42	6.75	12093	0.61	1.9	12968	14177.73	14177.73								
7-Sep-03	bam75	28.72	4.66	8667	0.3	6.54	12159	0.42	1.4	13010	14133.38	14133.38								
8-Sep-03	0	0	0	0	0	0	0	0	0	0	0.00									
9-Sep-03	0	0	0	0	0	0	0	0	0	0	0.00									
10-Sep-03	0	0	0	0	0	0	0	0	0	0	0.00									
11-Sep-03	ebm26	30.46	4.76	8404	0.42	6.84	12085	0.61	1.8	12972	14174.25	14174.25								
12-Sep-03	bam76	29.84	4.26	8573	0.25	6.07	12219	0.36	1.6	13009	12958.07	12958.07								
13-Sep-03	0	0	0	0	0	0	0	0	0	0	0.00									
14-Sep-03	0	0	0	0	0	0	0	0	0	0	0.00									
15-Sep-03	0	0	0	0	0	0	0	0	0	0	0.00									
16-Sep-03	bam77	29.81	4.23	8570	0.26	6.02	12210	0.37	1.6	12992	14189.58	14189.58								
17-Sep-03	ebm27	30.98	4.42	8364	0.34	6.4	12118	0.49	2	12947	13756.80	13756.80								
18-Sep-03	0	0	0	0	0	0	0	0	0	0	0.00									
19-Sep-03	0	0	0	0	0	0	0	0	0	0	0.00									
20-Sep-03	0	0	0	0	0	0	0	0	0	0	0.00									
21-Sep-03	ebm28	30.61	4.84	8385	0.43	6.98	12084	0.62	1.8	12991	13204.48	13204.48								
22-Sep-03	bam78	28.56	4.68	8662	0.29	6.55	12125	0.41	1.5	12975	14186.47	14186.47								
23-Sep-03	0	0	0	0	0	0	0	0	0	0	0.00									
24-Sep-03	0	0	0	0	0	0	0	0	0	0	0.00									
25-Sep-03	bam079	28.94	4.58	8635	0.29	6.45	12152	0.41	1.4	12990	14189.03	14189.03								
26-Sep-03	0	0	0	0	0	0	0	0	0	0	0.00									
27-Sep-03	0	0	0	0	0	0	0	0	0	0	0.00									
28-Sep-03	bam80	29.84	4.61	8515	0.26	6.57	12137	0.37	1.5	12990	13928.00	10046.71								
29-Sep-03	ebm29	30.12	4.87	8409	0.43	6.97	12034	0.61	1.7	12936	12972.78									
30-Sep-03	ebm30	30.4	4.91	8399	0.4	7.05	12068	0.58	1.8	12983	11613.50									
ADJ.												172896.42								
Weighted Average											29.71	4.59	8530	0.32	6.54	12136	0.45	1.62	Tons. OK	185611.32
																			Burn	185611.32

Monthly Mercury Analysis

Train #	Sample #	% Moist.	Mercury ug/g dry basis	Chlor. ug/g
	C2105	29.35	0.08	<0.01%

B16 Ash Analysis Record

None completed this quarter

B17 Ultimate Coal Analysis

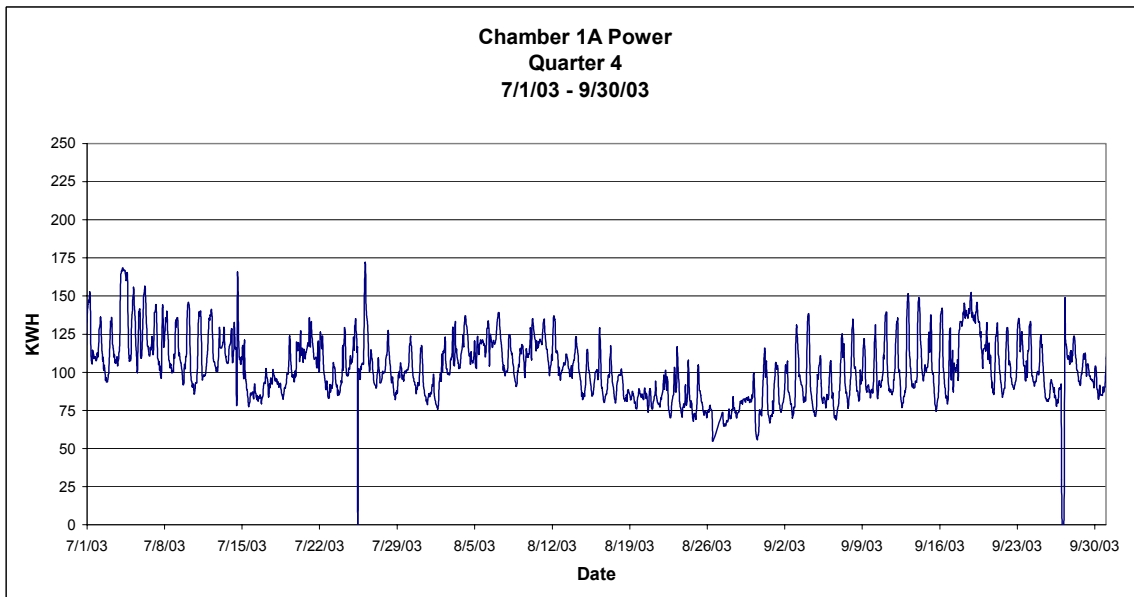
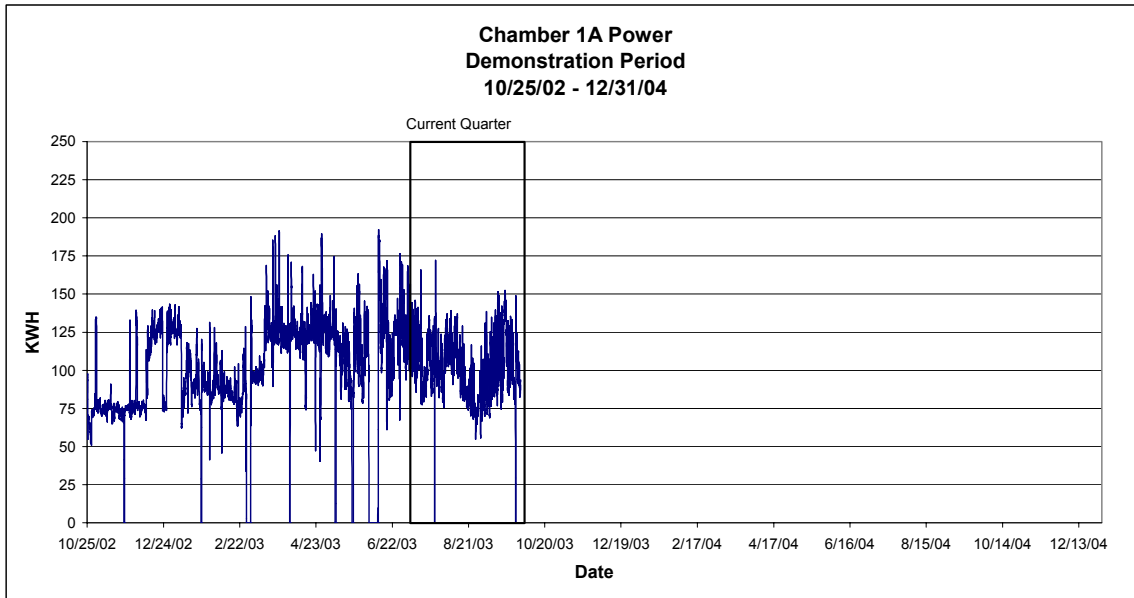
ULTIMATE ANALYSIS AS RECEIVED

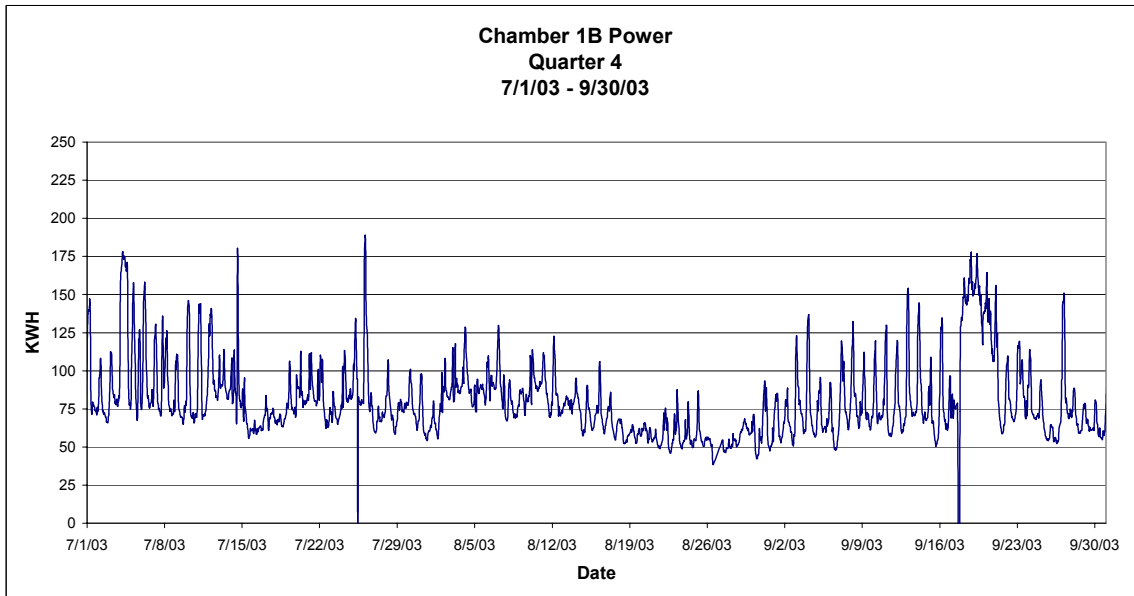
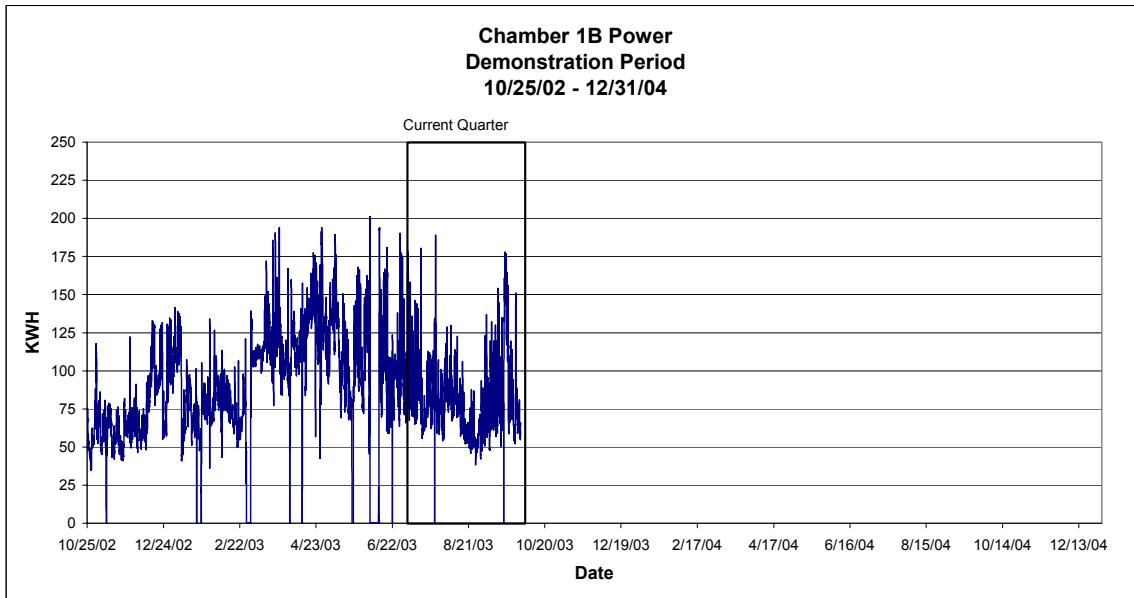
Sample Date	Moisture %	Ash %	Carbon %	Nitrogen %	Sulfur %	Hydrogen %	Oxygen %	HHV btu/lb	NaO %	Mercury ug/g Dry
05-Jan-03	30.31	4.60	48.51	0.65	0.50	3.43	12.00	8415	1.90	
06-Jan-03	29.75	4.79	48.86	0.64	0.39	3.43	12.14	8465	1.30	
07-Jan-03	29.82	4.74	48.39	0.67	0.39	3.03	12.96	8431	1.70	
08-Jan-03	28.79	4.86	49.34	0.68	0.40	3.05	12.88	8593	1.60	
12-Jan-03	28.85	4.19	50.03	0.69	0.24	3.04	12.96	8692	1.30	0.093
19-Jan-03	28.91	4.75	49.71	0.66	0.29	3.59	12.09	8696	1.40	
26-Jan-03	29.09	4.23	49.73	0.85	0.24	3.55	12.31	8624	1.30	
02-Feb-03	21.42	4.44	54.26	1.05	0.28	4.19	14.36	9477	2.00	
09-Feb-03	30.26	4.23	49.20	0.69	0.25	3.48	11.89	8487	1.40	0.103
16-Feb-03	27.91	4.37	50.12	1.08	0.28	3.79	12.45	8672	1.30	
23-Feb-03	26.60	5.10	48.81	1.36	0.31	4.14	13.68	8618	0.31	
02-Mar-03	NA	NA	NA	NA	NA	NA	NA	NA	NA	
09-Mar-03	29.99	4.48	49.46	0.63	0.26	4.21	10.97	8534	1.40	
16-Mar-03	29.23	4.53	49.32	0.66	0.26	3.74	12.26	8516	1.30	0.116
23-Mar-03	29.96	4.10	49.40	0.67	0.21	3.23	12.43	8581	1.10	
30-Mar-03	29.39	6.23	48.42	0.66	0.27	3.27	11.76	8402	1.80	
06-Apr-03	29.34	4.72	49.26	0.67	0.24	3.35	12.42	8514	1.20	
13-Apr-03	30.14	4.96	48.57	0.69	0.39	3.62	11.63	8474	1.60	0.116
20-Apr-03	30.16	4.87	48.65	0.68	0.49	3.70	11.45	8390	1.70	
27-Apr-03	30.74	4.33	48.77	0.67	0.35	3.54	11.60	8377	1.40	
04-May-03	30.57	4.81	48.95	0.66	0.30	3.59	11.12	8332	1.70	
11-May-03	29.97	4.56	50.35	0.68	0.35	3.73	10.36	8476	1.40	0.113
18-May-03	29.18	4.87	50.09	0.67	0.29	3.61	11.29	8572	1.10	
25-May-03	29.17	4.81	50.22	0.66	0.31	3.75	11.08	8557	1.40	
01-Jun-03	29.26	4.72	49.69	0.72	0.44	3.58	11.59	8501	1.80	
08-Jun-03	NA	NA	NA	NA	NA	NA	NA	NA	NA	
15-Jun-03	29.96	4.43	49.24	0.70	0.45	3.63	11.59	8476	1.70	0.013
22-Jun-03	29.52	4.42	49.74	0.65	0.32	3.42	11.93	8564	1.40	
29-Jun-03	30.43	4.74	48.83	0.71	0.36	3.40	11.53	8404	1.70	
06-Jul-03	29.10	4.56	50.03	0.67	0.30	3.42	11.92	8539	1.00	
13-Jul-03	30.39	4.90	48.72	0.67	0.42	3.10	11.80	8415	1.30	0.105
20-Jul-03	29.36	4.28	50.07	0.69	0.31	3.51	11.78	8663	1.20	
27-Jul-03	28.14	5.06	49.96	0.68	0.60	3.70	11.86	8633	0.90	
03-Aug-03	29.70	4.61	49.24	0.70	0.40	3.83	11.52	8474	1.40	
10-Aug-03	28.75	4.28	50.44	0.74	0.29	4.06	11.44	8663	1.10	0.081
17-Aug-03	29.04	5.44	49.38	0.76	0.33	3.88	11.17	8415	1.30	
24-Aug-03	28.98	4.84	49.89	0.65	0.29	3.54	11.81	8584	1.20	
31-Aug-03	28.92	4.85	49.86	0.69	0.27	3.51	11.90	8500	0.80	
07-Sep-03	29.69	4.23	50.77	0.70	0.27	3.69	10.65	8656	1.40	
14-Sep-03	29.35	4.52	49.83	0.68	0.32	3.28	12.02	8489	1.40	0.084
21-Sep-03	30.82	4.88	48.81	0.72	0.26	3.56	11.35	8275	1.10	
28-Sep-03	29.26	4.74	50.11	0.75	0.35	3.65	11.14	8590	1.10	
05-Oct-03										
12-Oct-03										
19-Oct-03										
26-Oct-03										
02-Nov-03										
09-Nov-03										
16-Nov-03										
23-Nov-03										
30-Nov-03										
07-Dec-03										
14-Dec-03										
21-Dec-03										
28-Dec-03										

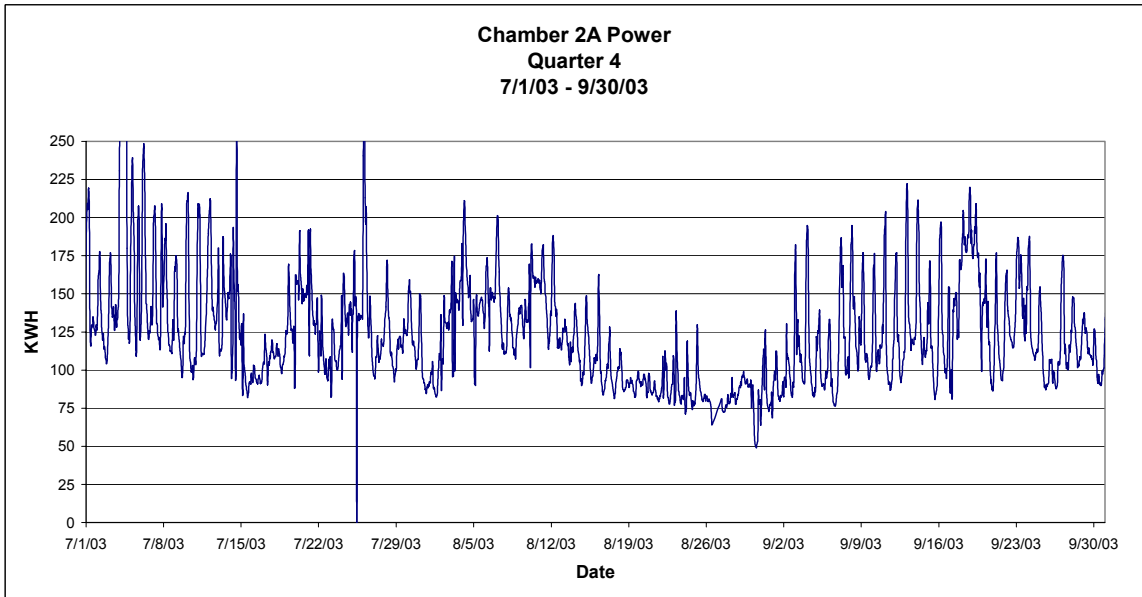
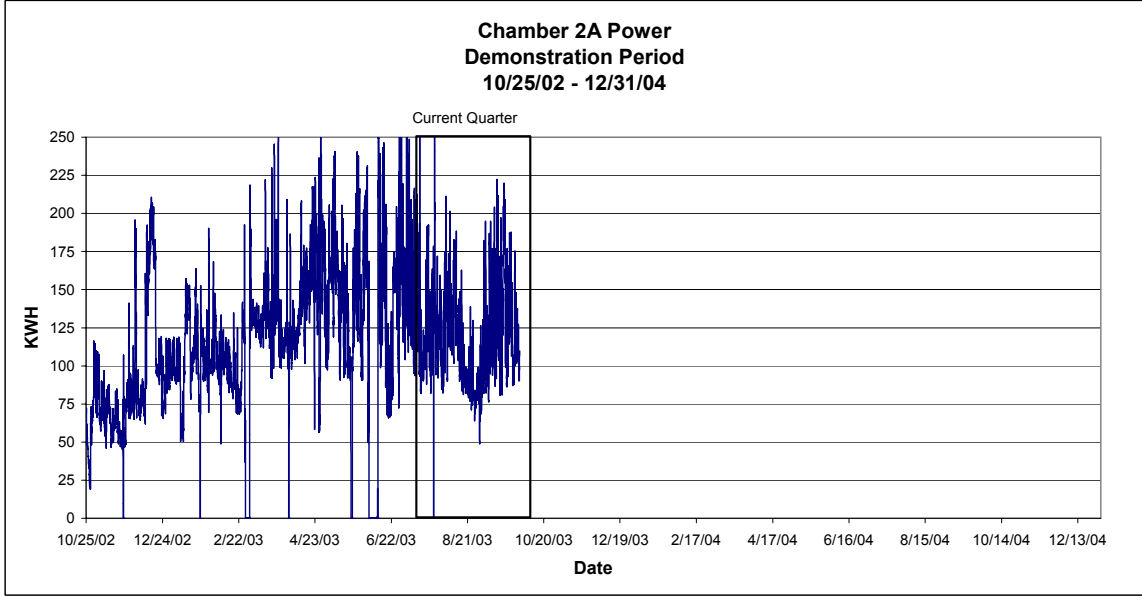
B18 Photographs

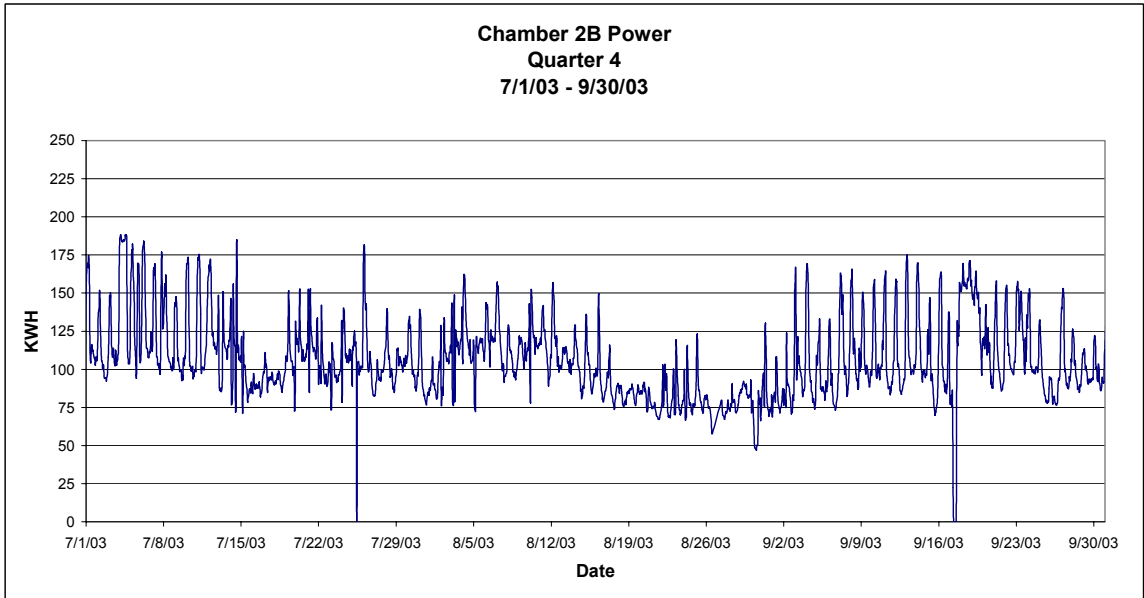
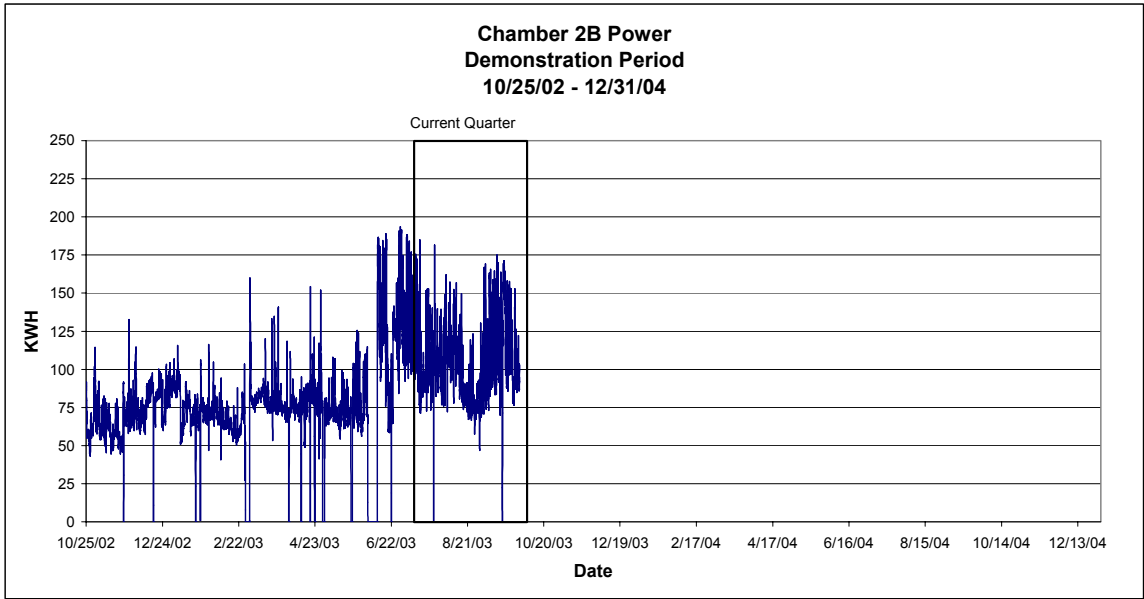
No photographs are included this quarter.

B19 ESP Power by Chamber









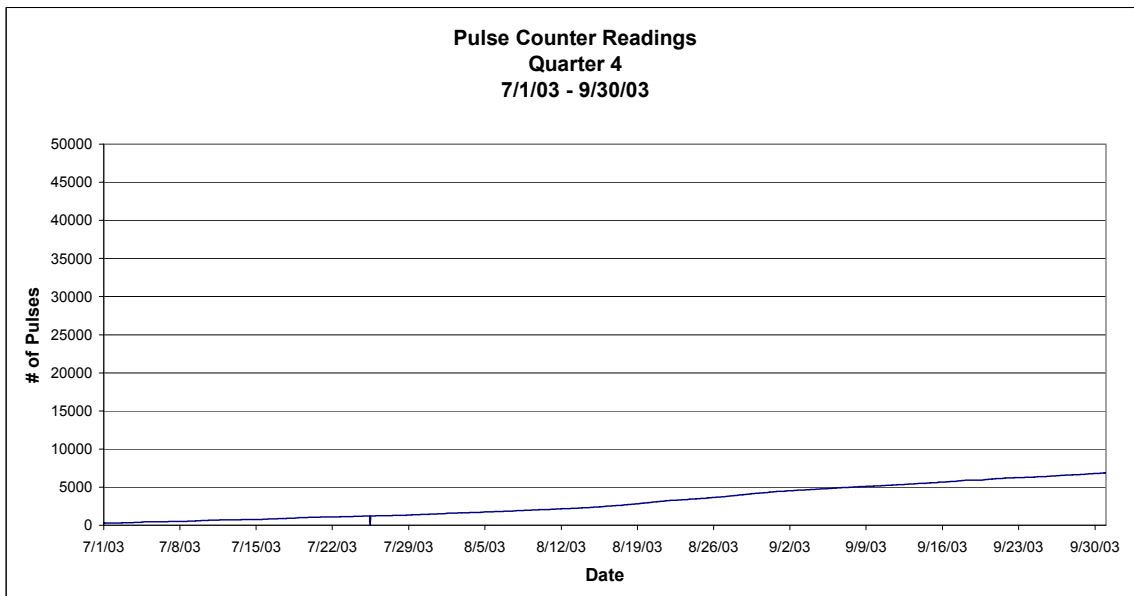
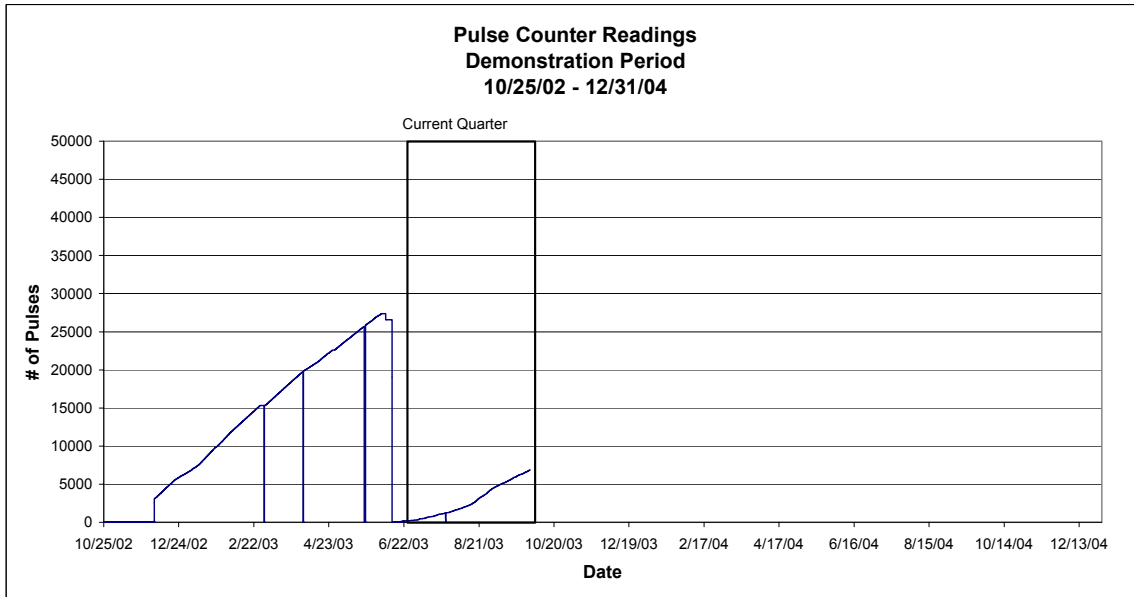
B20 ESP Tabular Data
Transformer/Rectifier Performance Readings

15-Jul-03 * Limiting factors highlighted												
Chamber	Field 1			Field 2			Field 3			Field 4		
	mA	kV	spm									
1A	68	63.7	47	370	45.2	19	751	47.7	19	770	52.6	19
1B	172	55.5	99	319	47	19	537	46.1	19	601	48.2	19
2A	260	57.8	99	492	49	19	498	49.1	19	653	48.5	19
2B	262	57.3	99	434	48.5	19	720	47.2	19	620	47.5	19

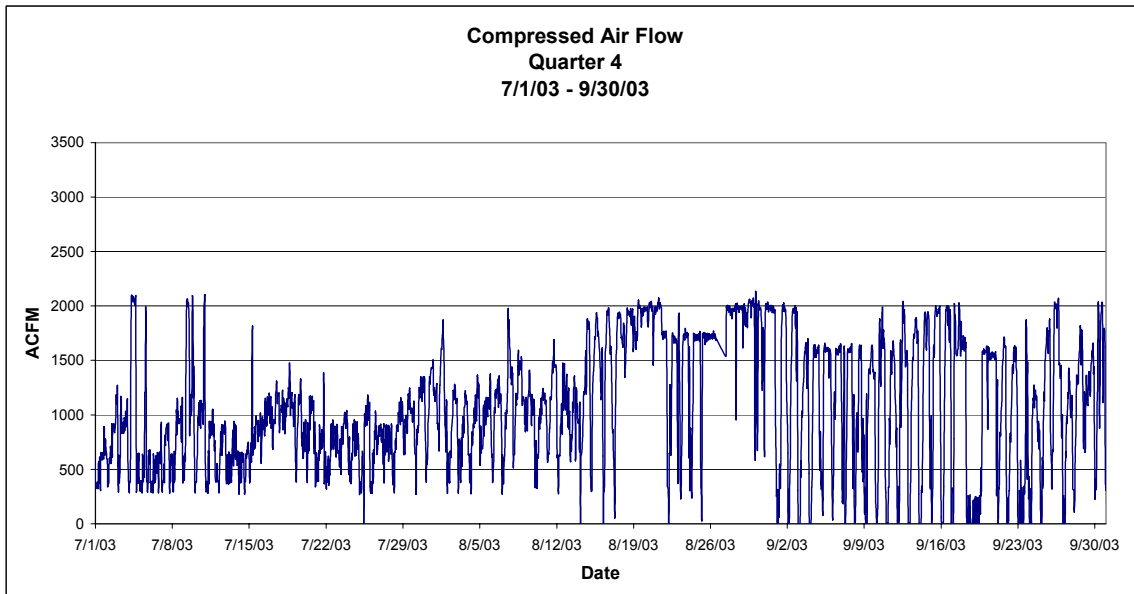
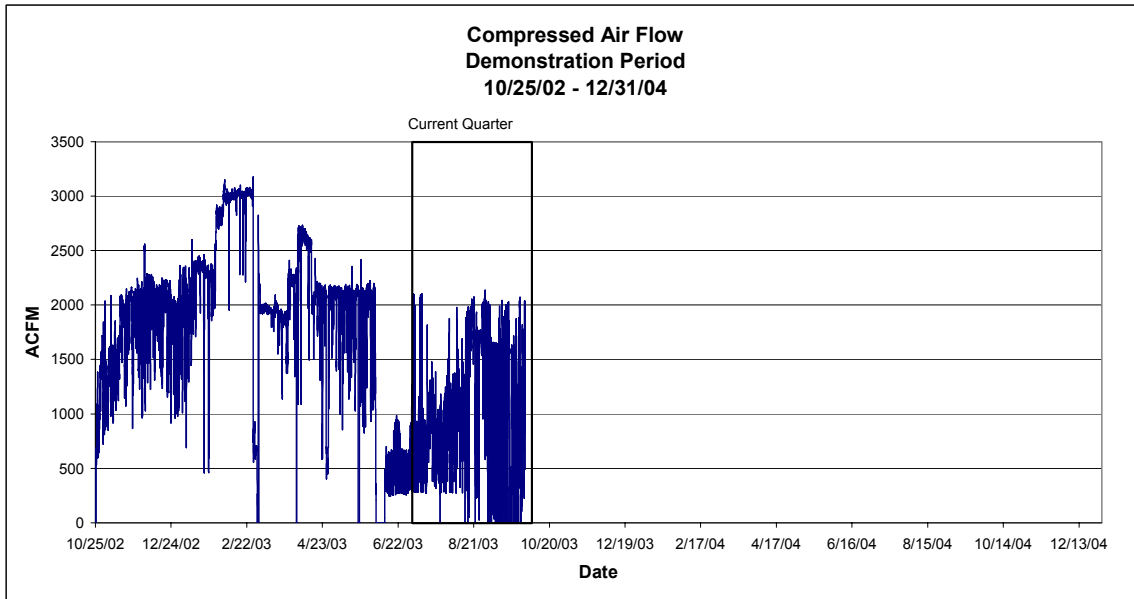
15-Aug-03 * Limiting factors highlighted												
Chamber	Field 1			Field 2			Field 3			Field 4		
	mA	kV	spm									
1A	116	62.3	87	413	44.9	19	758	47.2	19	806	52.1	19
1B	194	56.3	99	346	47.1	19	566	46.1	19	597	47.9	19
2A	324	59.3	99	541	49.6	19	546	49.5	19	665	48.2	19
2B	337	59	99	490	49.3	19	765	48	19	660	47.8	19

15-Sep-03 * Limiting factors highlighted												
Chamber	Field 1			Field 2			Field 3			Field 4		
	mA	kV	spm									
1A	95	64.4	33	456	46	19	848	49.1	19	882	54.1	19
1B	195	57.1	99	359	47.6	19	567	46.5	19	632	48.9	19
2A	336	60.4	98	552	51.5	19	541	50.6	19	706	49.8	19
2B	317	59.4	99	473	49.7	19	738	48.5	19	681	47.9	19

B21 Pulse Counter Readings

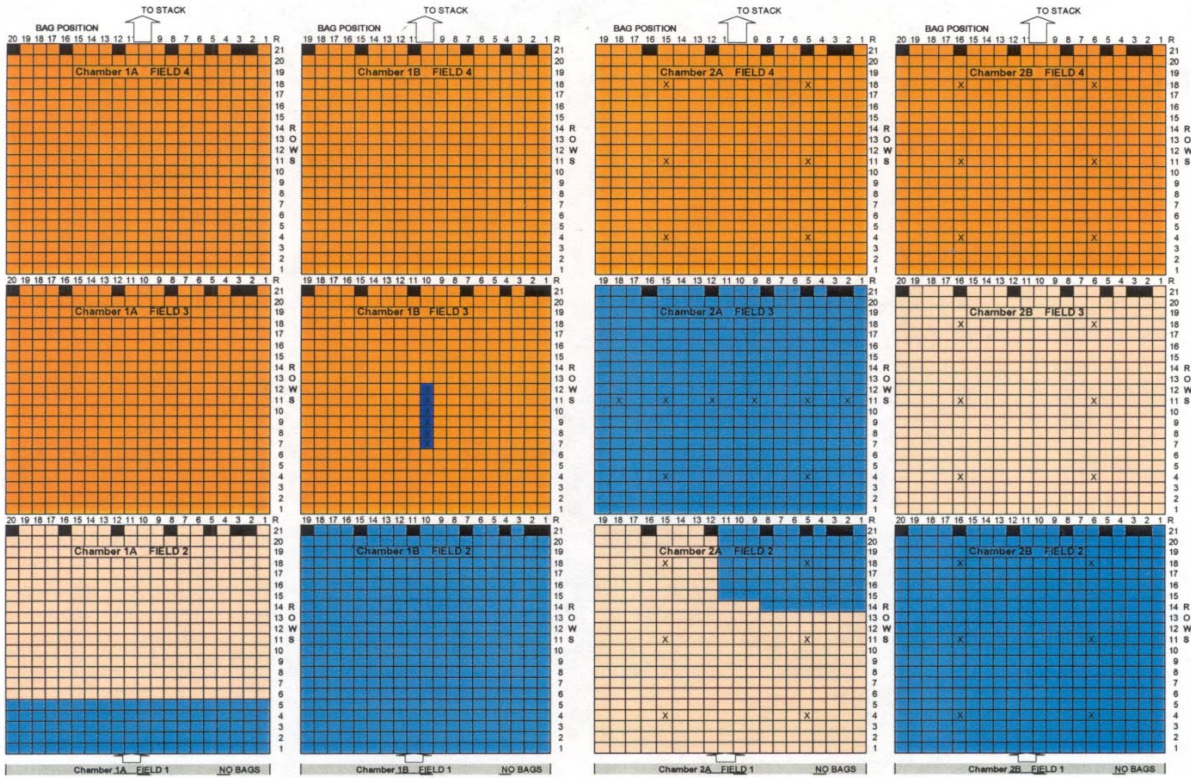


B22 Compressed Air Flow



B23 Bag Layout Diagram

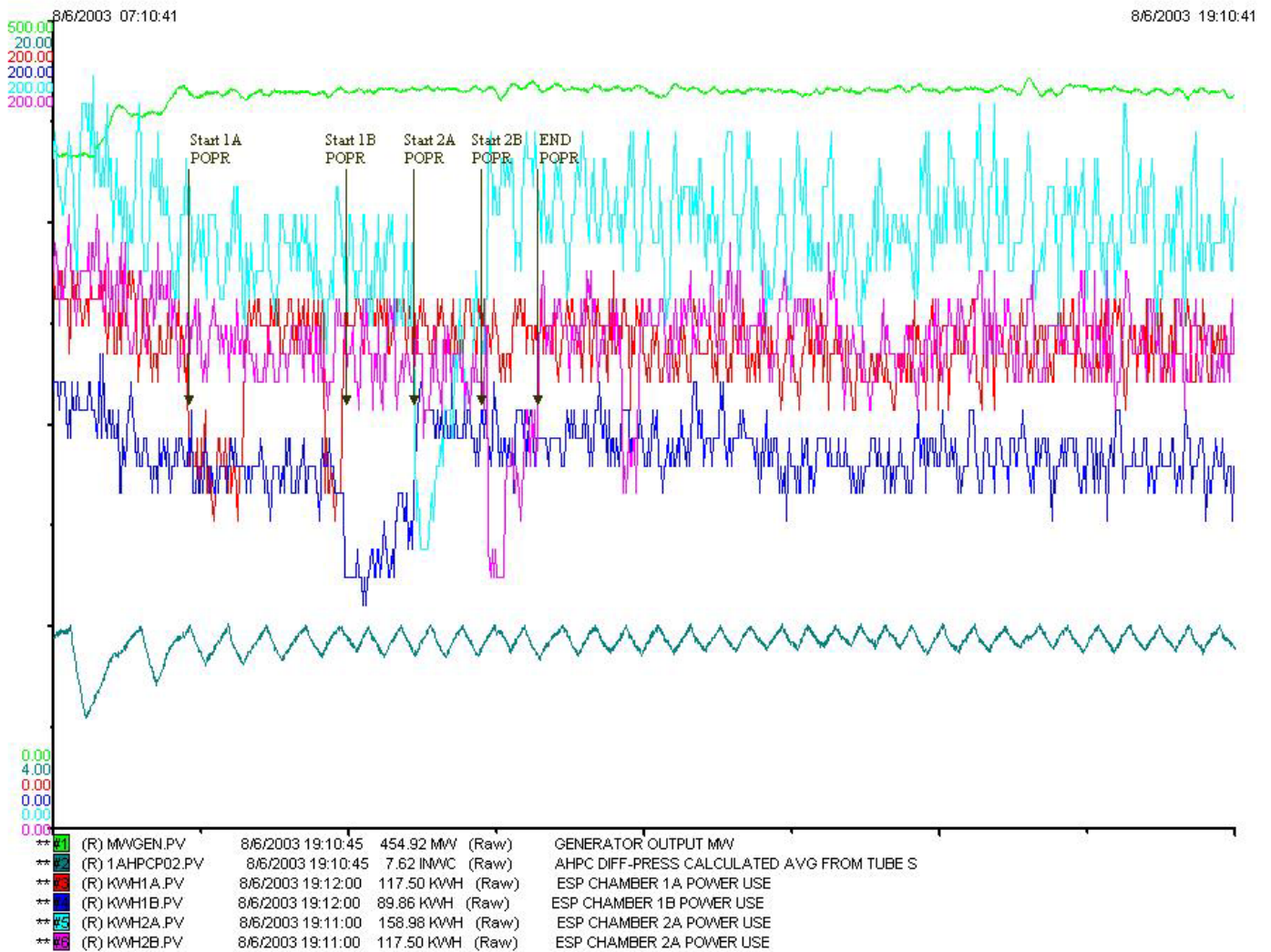
Advanced Hybrid Bag Map Big Stone Plant



- No Filter Bag
- Conductive Gore-Tex Membrane/Conductive Gore-Tex Felt (Installed 6/03)
- Conductive Gore-Tex Membrane/Conductive PPS Felt (Installed 6/03)
- Gore-Tex Membrane/PPS Felt (Installed 6/03)
- Test Bags (Installed 6/03)
- X Pitot Tube Location

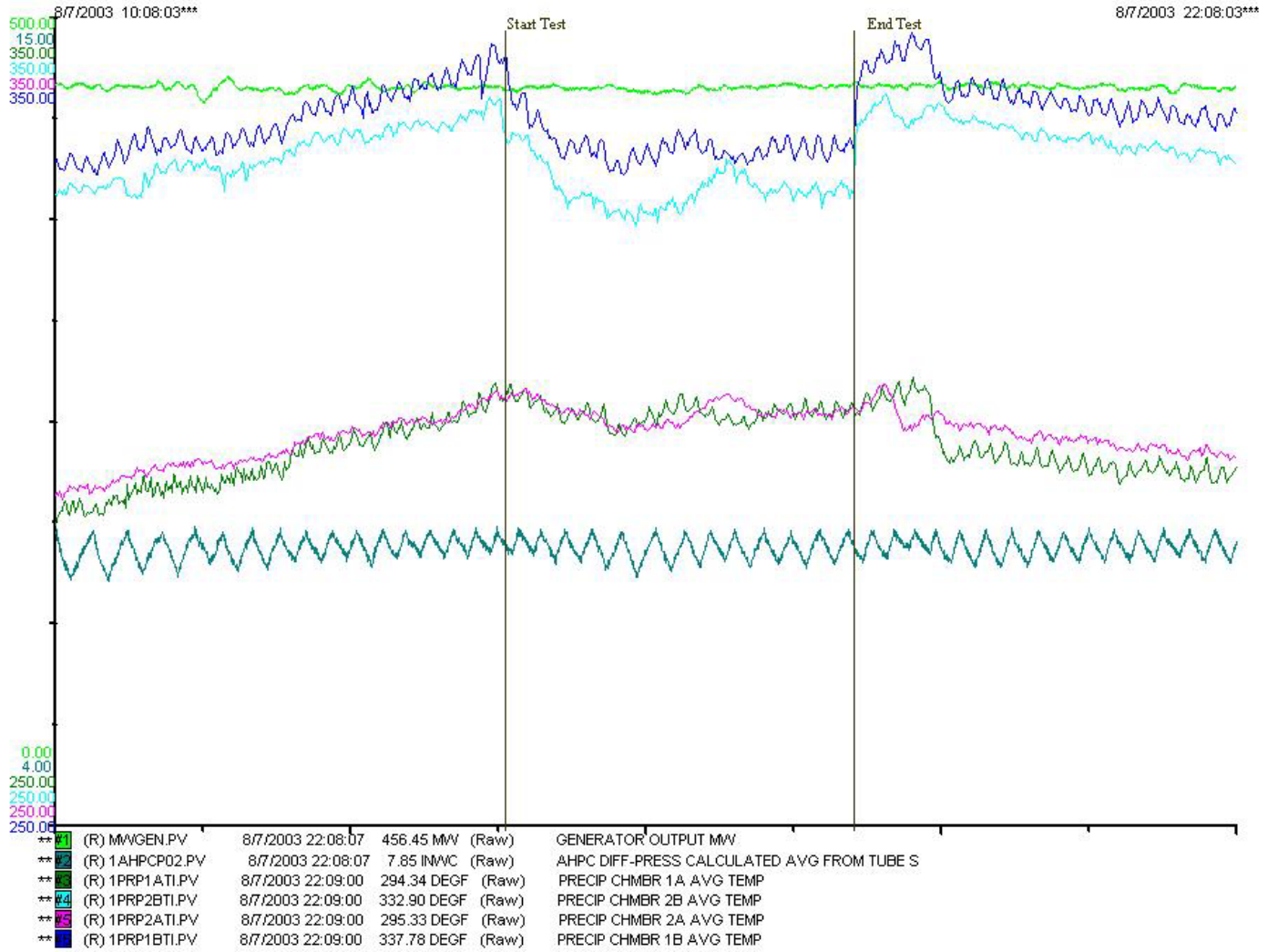
B24 POPR Test Results

POPR @ 12h 0m 0s



B25 Humidification Test Results

Humidification Test @ 12h 0m 0s



B26 Fluent Study

Background

The Advanced Hybrid Particulate Collector (AHPC) is a novel technology that combines the best features of electrostatic precipitators and fabric filters. Demonstration of a full-scale retro-fit of the AHPC technology is taking place at the $450MW_e$ coal-fired Big Stone power plant near Milbank, SD. The full-scale unit is demonstrating consistent high particulate collection efficiencies ($>99.99\%$) that far exceed that of a conventional electrostatic precipitator (ESP). However, the demonstration unit does experience problems with higher than expected pressure drops (Δp) and substantial variations in particle loading. These problems have lead to: (i) lowered power production due to limitations of the existing fan capacity and (ii) rapid cleaning frequency for the fabric filter bags.

The US Department of Energy (NETL), Otter Tail Power Company (who operates the Big Stone plant), and the parties involved in developing the AHPC technology are discussing several short and long term modifications to overcome the abovementioned problems. Since the uneven loading of fabric filter bags is believed to be largely a flow distribution problem, Fluent Inc. has been commissioned to propose a set of Computational Fluid Dynamics (CFD) studies to assist in the implementation of design modifications that ensure a better distribution of flow in the unit.

This technical memorandum is a project deliverable for this preliminary study. It presents a problem analysis and conclusions in the form of proposed CFD studies of the Big Stone AHPC unit.

Description of Big Stone AHPC Unit

The AHPC installation at Big stone consist of four parallel chambers retrofitted downstream of an existing ESP. Each chamber holds one existing ESP field and three AHPC filter compartments. Figure 1 gives a schematic representation of this arrangement. The AHPC compartments have 20 rows with 21 fabric filter bags each¹. Electrostatic charge electrodes are suspended between the rows of bags, with perforated collecting plates separating the fabric filter and ESP zones.

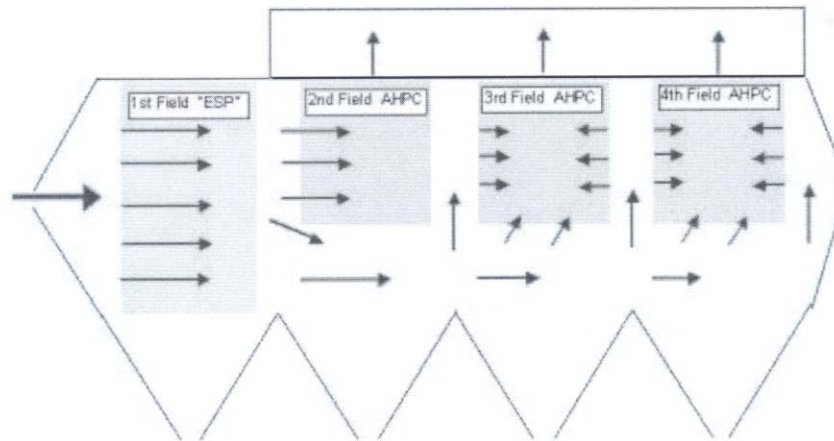


Figure 1: Big Stone AHPC unit. Arrows indicating assumed flow patterns.

¹ This translates to $3 \times 20 \times 21 = 1260$ bags per chamber.

As the old ESP unit is 40ft tall and the new AHPC compartments take up less height (24ft), flow may reach the compartments by way of the space below the retrofitted parts. From there, flow may either enter the ESP zones directly or via the spacing that separates the individual compartments. Thus, flow may enter the individual AHPC compartments from three directions: front, bottom, and back. To maximize the efficiency of the build-in ESP zones, it is desirable to have stratified flow (from one direction) with a reasonable residence time between the collecting plates. Furthermore, localized high velocities and turbulence levels should be avoided in order to prevent re-entrainment of fly ash.

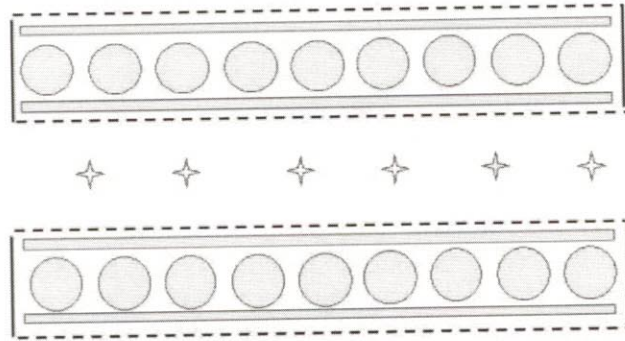


Figure 2: Schematic bottom-view of filter sections. Pictured is an ESP section bounded by two bag rows and their guide rails.

An additional flow-related problem is that of potential *gas sneakage*, i.e. flue gas bypassing the ESP zone and entering the filter bag sections directly. This is an undesired phenomenon, made possible by the lack of a physical separation at the bottom of the filter bag sections.² Gas sneakage will lead to higher particle loading of the filter bags, and so may be a contributing factor to the quick dustcake build-up being observed.

Proposed CFD studies

In the following, an overview of the proposed flow modeling of the Big Stone AHPC unit is presented. It is suggested to split this work into three distinct tasks:

1. Modeling of overall flow distribution in the *existing* unit
2. Modeling of overall flow distribution in the *modified* unit
3. Detailed modeling of simplified filter compartment

Tasks 1 and 2 will aim at respectively understanding and correcting the overall flow in an entire chamber, while Task 3 will address the abovementioned phenomenon of gas sneakage by means of a detailed CFD model for part of an advanced hybrid compartment. In the following, the technical approach for each of these tasks will be explained in more detail. Finally, Section 4 summarizes work effort, deliverables, and a time schedule for the proposed tasks.

² Metal disks block the bottom of filter bags and there is a set of two guide rails per bag row. A simple analysis shows that this leaves approximately half the surrounding face open to up-coming flow.

TASK 1: Simulation of existing AHPC design

This task aims at predicting overall flow patterns in the existing Big Stone AHPC unit. The CFD simulation will provide information on the directional partitioning of flow entering the individual AHPC compartments, and will help spot regions with localized high velocities that may have a detrimental effect on ESP performance. The insight into flow patterns gained from this task, may serve in the development and refinement of flow correcting design modifications. The impact of these design modifications will subsequently be evaluated in Task 2.

While designing the AHPC retrofit for the Big Stone power plant, Elex AG conducted CFD simulations of a full chamber, similar to what is proposed as Task 1 here. At that time, the model size was severely limited by the available computer resources.³ However, the Computer Aided Design (CAD) model developed in that context will serve as a good starting point for the current effort. Section 1.1 outlines the CFD modeling approach, and explains the improvements over the Elex model that we intend to implement.

1.1 Modeling approach

The advanced hybrid filter is a complex system both in terms of geometry and involved physics, for which reason certain simplifications are necessary. As regards physical modeling, simulations will consider isothermal single-phase gas flow. That means, no attempt will be made to model the entrainment of fly ash particles in the flue gas. At the same time this relieves any need to include models for the electro-magnetic field and charge-carrying ability of ash particles. Most coal-derived flue gases are sufficiently dilute to warrant the assumption that the presence of particles does not influence the gas flow.

The pressure drop across the thin fabric filter membranes is modeled using a porous jump condition in the Fluent CFD code. The thin porous medium has a finite thickness over which the pressure change is defined by a combination of Darcy's Law and an additional inertial loss term.

$$\Delta p = - \left(\frac{\mu}{\alpha} v + C_2 \frac{1}{2} \rho v^2 \right) \Delta m \quad (1)$$

where μ is the molecular fluid viscosity, α is the medium permeability, C_2 is the pressure-jump coefficient, v is the velocity normal to the porous face, and Δm is the medium thickness. Parameters for the porous jump model will be assigned values based on existing measurements of filter bag pressure drops. For the purpose of overall flow modeling (Tasks 1 and 2), the pressure drop across the perforated collecting plates and the fabric filters are lumped. This means that a simple rectangular box represents one row of filter bags and the plates bounding it.⁴

1.1.1 Geometric modeling and meshing

The first step will consist in modifying the existing CAD-model so that it corresponds more accurately to the actual retrofit geometry. Here is a commented list of the geometry changes that will be implemented:

³ Simulations were carried out using Fluent 5.5 on a 500 MHz Pentium III processor with 1 Gb memory.

⁴ The slender rectangular boxes have porous sides (exception being the outermost bag rows in each compartment that have one solid side), a porous bottom, a solid front and back, and an open top face leading to the clean gas plenums.

- Add collecting plates for old ESP field

The original ESP remains in operation, but its collecting plates were not contained in the existing CFD model. However, these solid plates (spaced 1ft apart), are poised to efficiently stratify the gas flow in its approach to the AHPC compartments. The plates will be modeled as solid walls of infinitesimal thickness.

- Remove girdles from two rear AHPC compartments

In the CFD model created by Elex, there is a 400mm high rectangular plate placed perpendicular to the direction of the incoming flow just below the front of each AHPC field. This component (referred to as a girdle) is related to the rapping system that cleans dust of the collecting plates. However, in the actual Big Stone retrofit there is only one such girdle placed in connection with the first AHPC compartment.

- Include catwalk floor in model.

A further assesment is necessary to determine whether the model should be augmented with porous faces representing the floor of catwalks. There is one long grated walkway in the space behind each AHPC compartment. The actual flow blockage from these catwalks is most likely fairly modest, but they are placed in potentially critical spots and their presence may have localized effects in the corners of filter compartments.

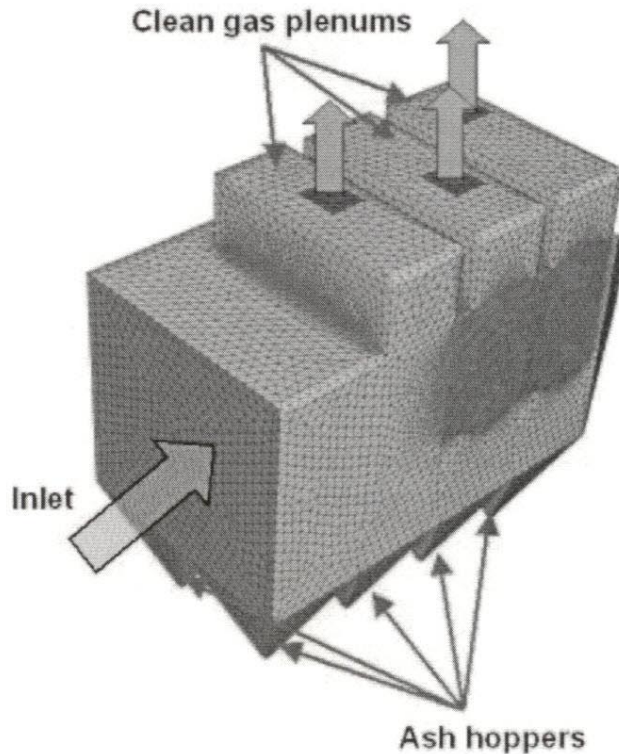


Figure 3: Computational mesh from existing CFD model.

The Elex CFD model used a mesh discretization with approximately 1.5 million computational cells, see Figure 3. Approximately 2/3 of these cells were used to describe the three AHPC compartments. The computer resources available to Elex made it infeasible to further increase mesh resolution, although it remained relatively coarse inside the compartments.⁵ For the proposed work, use of parallel processing on the extensive computing clusters at NETL in Morgantown will enable an expansion of the model size by a factor of 2-3. Our preliminary investigations indicate that this would be sufficient to resolve the actual geometry of the individual filter bags, but it is our recommendation not to do so but rather to maintain the porous box approach with a finer mesh. The filter bag geometry will be considered in the proposed Task 3.

In contrast to the Elex mesh that consisted of 100% tetrahedral cells, we will be employing hexahedral meshing in as far as possible. Because of the spatial interpolation schemes involved in CFD this will achieve a higher solution accuracy. Moreover, a hexahedral mesh typically has significantly lower cell count than a comparable tetrahedral one.

1.1.2 Boundary conditions

Current theories on gas flow patterns inside a hybrid filter chamber, see Figure 1, were developed based on Pitôt tube data collected inside a chamber at the Big Stone power plant. These measurements, which may be correlated to the flue gas dust loading, were performed at three locations in each AHPC compartment: front, middle, and back. It is our intent to incorporate this measured data by implementing variations in the Δp characteristics (porous jump conditions) that model the pressure drop over filter bags.

All boundary conditions will be re-visited in cooperation with the power plant and technology developers to ensure consistency with the real operating conditions at Big Stone. In comparison with the Elex CFD model, the following changes in the handling of porous jump faces will be implemented.

- Lengthwise splitting of porous jump faces

Each of the large porous faces that separate the ESP zones from the filter bag zones will be sub-divided into three zones. Since a variation in Δp over one porous jump face cannot be assigned in Fluent, this sub-division is necessary to allow for variation. The resulting three zones may subsequently be assigned individual jump conditions based on the abovementioned Pitôt data from the front, middle, and back of that compartment. Other subdivisions are possible, but only make sense whenever matched by data.

- Define porous bottom of filter bag zones

Change the bottom of filter sections from a solid to a porous face. Notice the conditions for this face must also contain the (dominant) pressure drop across the fabric filters.

- Catwalk floor porosity

If it is chosen to include the grated walkways in the CFD model, empirical expressions for the induced pressure drop must be taken from literature and implemented.

⁵The ESP sections were described using only one cell across the width, while two cells were used inside the porous box that represents a row of bags.

1.1.3 Simulations

We propose to initially perform two different simulations: (a) with a uniform pressure drop across all filter bag sections (this corresponds to the Elex model with geometric modifications only), and (b) with a variation in pressure drop that reflects the measured data better. A comparison between these two simulations will reveal how sensitive the overall flow distribution is to perturbations in the prescribed pressure drop conditions. The filter membranes are by far the biggest source of frictional resistance in the entire unit, so logically one would expect these particular boundary conditions to have a significant impact on the distribution of flue gas flow.

After completing these initial CFD simulations, a comparison will be made between predicted and measured flow rates through the individual clean gas plenums. If the split of flow between compartments is predicted with reasonable accuracy, this helps build confidence in the simulations. Another option for model validation is to do additional velocity measurements, preferably by traversing the chamber-width at a position below or in between hybrid compartments. The recorded velocity profile may then be compared with simulation results.

A third simulation (c) will investigate the importance of the inlet velocity profile. In this simulation, an artificially skewed velocity profile will be assigned at the model inlet. This is in contrast to the uniform inlet profile applied in cases (a) and (b). Quite possibly the narrowly spaced collecting plates of the old ESP field may annul this perturbation in inlet velocities. However, should a significant change in flow distribution result there is reason to consider building a separate CFD model that considers the flow manifolding from the air preheater to the four AHPC chambers.⁶

1.1.4 Post-processing

Postprocessing of simulation data will produce a collection of plots that describe the chamber flow pattern. Moreover, the directional partitioning of flow *into* each AHPC compartment (from the front, back, and bottom respectively) will be quantified. This data will help confirm or modify the current hypothesis on flow distribution, which will briefly be outlined under Task 2. Due to the geometric simplifications in representing the filter bag rows, care should be exhibited in interpreting flow patterns *within* the AHPC compartments. The detailed model, proposed as Task 3 of this effort, will provide a much better basis for such interpretations.

⁶ Incidentally, such a study might help explain some of the variation that exists between the performance of the four parallel filter chambers. It is currently thought that this variation results from variations in chamber temperatures that impact the ESP performance.

1.2 Estimated work effort for Task 1

Table 1 gives an estimate of the work hours involved in Task 1. Sub-tasks correspond more or less to the previous sections.

TASK 1 : Modeling of *existing* unit

Sub-task	Task description	Work effort [h]	Comments
1.1	Geometric modeling and meshing	80	
1.2	Boundary condition setup	40	
1.3	Simulations	90	Simulations <i>(a)</i> , <i>(b)</i> , and <i>(c)</i>
1.4	Post-processing	30	
TOTAL		240 h	

Table 1: Estimated man-hours for carrying out the proposed Task 1

TASK 2: Simulation of design modifications

This task will determine the effect of two simple design modifications that both aim at improving the flow patterns in the Big Stone AHPC. Based on the already mentioned Pitôt tube measurements, the AHPC technology developers have formed a theory on the gas flow dynamics of this unit, see Figure 1. For the first AHPC compartment, it is believed that gas enters mostly from the front and flows towards the back while gradually effusing via the collecting plate perforations. In the two rear compartments, flow seems to enter the ESP zones from multiple directions (front, back, and bottom). The flow simulations of the existing unit will help confirm or refine this understanding, so that it is advisable to revisit the suggested design modifications after completion of the Task 1.

2.1 Suggested design modifications

As mentioned earlier, electrostatic precipitation will generally benefit from a uni-directional gas flow in the electro magnetic field between the collecting plates. For this reason, design modifications should first and foremost attempt to alter flow in the two rear compartments, where cross- and counter-flow is believed to be most prevalent. After consulting with the AHPC developers, it is proposed to investigate the following two design modifications:

A Installation of steel plates on the end of all AHPC compartments

The gas flow in this configuration can enter the ESP zone from the front or bottom of fields. This measure reduces the possible routes that the gas may travel. A simulation will reveal whether this results in a more uniform gas distribution or not.

B Installation of steel plates on both ends of the two rear AHPC compartments

In this configuration the first AHPC field remains unchanged, while gas flow can only enter the rear fields from the bottom. This should ensure similar pat-

terns in the two affected fields, but may increase problems with gas sneakage and may also cause significant lengthwise variations in the loading of the individual bags.

These two design modifications may have to be implemented in conjunction with a deflector system to limit gas sneakage from the bottom. This will be addressed by the detailed study of a compartment in Task 3. From a CFD perspective, the abovementioned design changes can be easily implemented in the model from Task 1; accomplished by a change in boundary conditions rather than geometry. In both cases it is also possible to investigate the use of perforated rather than solid plates. For both design studies, we will determine the directional re-partitioning of flow and also report any regions of high velocity or turbulence intensity.

2.2 Estimated work effort for Task 2

As this Task makes use of the CFD model developed under Task 1, a faster turn-around time can be expected for this second task. Estimates are given in Table 2.

TASK 2 : Modeling of *modified* unit

Sub-task	Task description	Work effort [h]	Comments
2.1	Model modification	25	Design studies A and B
2.2	Simulations	60	
2.3	Post-processing	20	
TOTAL		105 h	

Table 2: Estimated man-hours for carrying out the proposed Task 2

TASK 3: Detailed Modeling of Filter Compartment

With this task it is proposed to build a separate CFD model, which consider a portion of a filter compartment with a more refined geometry representation. This model is intended to predict flow details that cannot reasonably be described by the overall CFD model (Task 1). Most importantly, it will shed light on the sneakage ratio, i.e. the fraction of flow that bypasses the ESP section and instead enters the filter bag sections vertically. The model can also be used to assess deflector arrangements to reduce sneakage.

3.1 Modeling approach

The model will comprise a layer-wise arrangement of three full bag rows and four ESP zones, see Figure 4. Symmetry boundary conditions will be prescribed at the two model boundaries that cut through the center of an ESP zone. This configuration emulates a sub-domain inside a larger compartment, where the inclusion of several bag rows aims at limiting boundary effects. Flow will exit the model via an artificially defined plenum that receives gas from the bags.

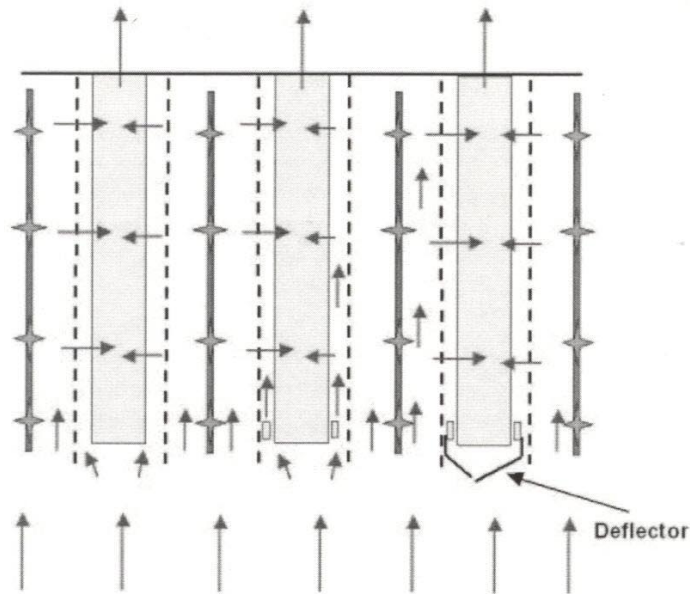


Figure 4: Detailed model of hybrid compartment. Shown discharge electrodes not modeled.

The inlet flow condition will be prescribed in terms of a uniform velocity from the bottom, which may be either vertical or at an angle. The exact velocity magnitude and direction will be estimated based on the flow simulations for the overall chamber (Task 1 and 2). Variations in the approaching flow will exist depending on what part of a compartment you consider. The sensitivity in modeling results can be assessed by computing the sneackage ratio for a series of detailed model simulations with changes in the inlet velocity direction and/or magnitude.

The perforated collecting plates and the individual bags (3×21 in the model) will be modeled using different porous jump conditions, see section 1.1. The flow resistance of the perforated plates will be derived from an empirical relation, and should be significantly lower than the flow resistance of the bags.

3.2 Design studies

The second part of Task 3 will be a design study, considering the impact of equipping bag rows with a deflector arrangement to limit gas sneackage. An example of such a bag deflector can be seen for the right bag row in Figure 4. The exact deflector design will be provided later by the AHPC technology developers. Simulations will be performed for the same set of inlet conditions that was used in subtask 3.1. While it will be difficult to experimentally verify the predicted sneackage ratios, it is believed that the outlined CFD models (with and without deflectors) will predict trends with confidence.

3.3 Estimated work effort for Task 3

TASK 3 : Detailed Flow Simulation

Sub-task	Task description	Work effort [h]	Comments
3.1	Geometric modeling and meshing	60	From scratch
3.2	Boundary condition setup	20	
3.3	Simulations	50	Varying inlet conditions
3.4	Post-processing	20	
3.5	Design variation studies	60	Bottom deflector plate
TOTAL		210 h	

Table 3: Estimated man-hours for carrying out the proposed Task 3

4 Deliverables and Schedule

A strategy for the deployment of CFD modeling to assist in trouble-shooting of the AHPC unit at Big Stone power plant has been outlined. This section will summarize deliverables, estimated work effort, and present a time schedule for completion of the proposed tasks.

4.1 Project Deliverables

Project progress will be reported on a monthly basis in a short written status report. After successful completion of the project, **Fluent Inc.** will deliver the following items:

- Report summarizing CFD results from modeling of overall chamber flow (Tasks 1+2).
- Report summarizing results from detailed modeling of a filter compartment (Task 3).
- Fluent case/data files for all completed simulations.

4.2 Project time schedule

The specific breakdown into tasks and an estimate of the engineering hours have been compiled in Table 4.

Task	Task description	Work effort [h]
1	Modeling of overall flow distribution in the <i>existing</i> unit	240
2	Modeling of overall flow distribution in the <i>modified</i> unit	105
3	Detailed modeling of simplified filter compartment	210
TOTAL		555 h

Table 4: Summary of estimated man-hours for all tasks

Figure 5 shows the time schedule for completion of the specific subtasks. This chart has been based on work commencing October 1st 2003. As it appears, the total elapsed time

to complete the project is expected to be six months. While Tasks 1 and 2 are essentially sequential activities, the schedule for completion has been accelerated by working on Tasks 1 and 3 in parallel.

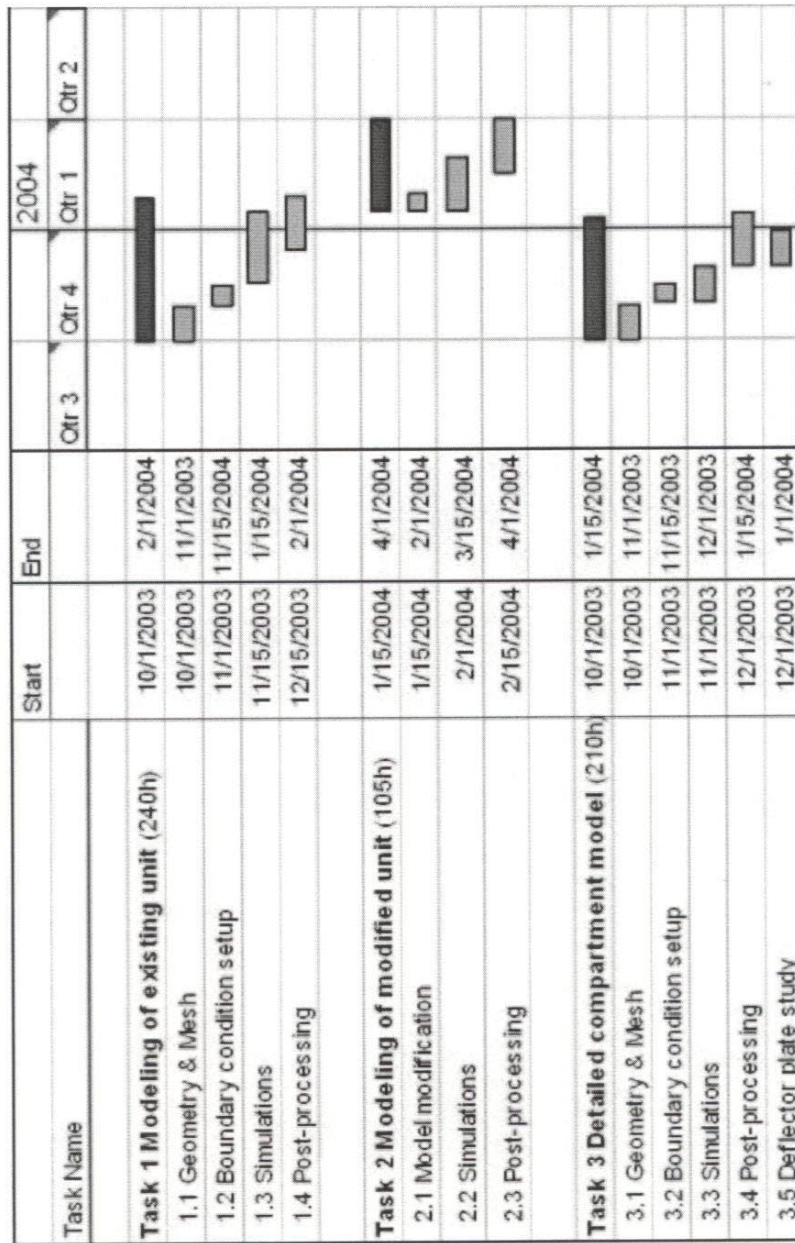


Figure 5: Projected timeline for completion of proposed tasks.

Advanced Hybrid™ Filter

Proposed Filter Bag Bottom Flow Restriction Baffle Design

To:

John Caine SEI

Ulrich Leibacher ELEX

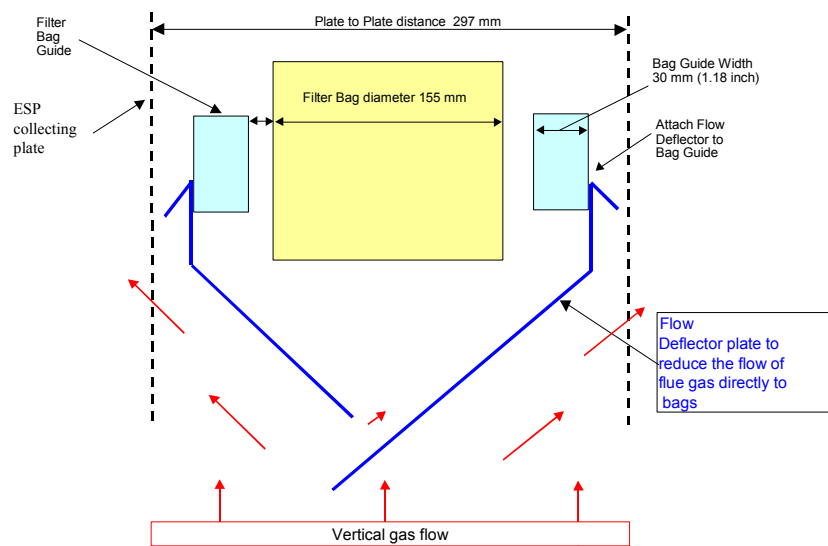
Peter Studer ELEX

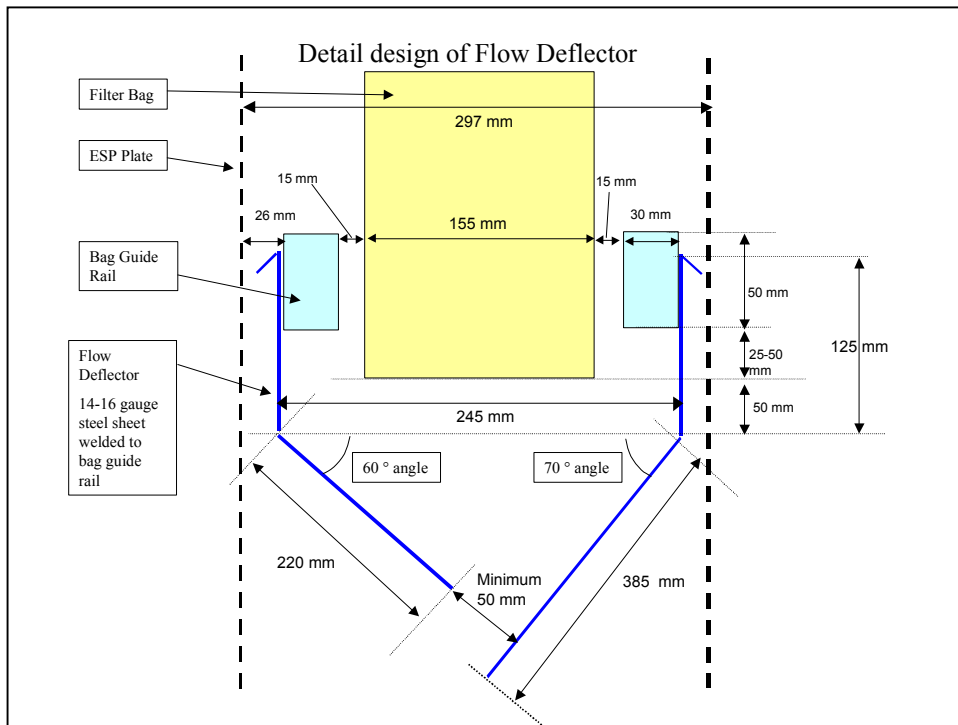
From:

Rich Gebert W.L. Gore

September 30, 2003

Expanded end view of the bottom of the filter bag and the proposed flow deflector





Dimensions

- The drawings and information contained in this proposal are to be used as a guide for the design of the flow deflector plates.
- The bag guides or rectangular tubing dimensions based on the ELEX drawings are: 30 mm wide by 50 mm high by 4570 mm in length and are placed 15 mm from the bags and 26 mm from the collecting plates.
- The bag diameter is 155 mm and they are spaced 200 mm on center down the row with 21 bags per row creating a 4.2 meter length of bags.
- The proposed steel sheet deflector plates are designed to reduce the amount of gas flow that passes between the filter bags in the bag row and between the ESP collecting plates.
- The steel sheet 14 - 16 gauge can be spot welded, stick or mig welded to the bag guide rail.
- The downward angle is 60-70 degrees to allow the collected dust to fall into the hopper and the minimum clearance between the two plates must be 50 mm.
- Plate #1 at 60 degrees comprises 125mm of vertical section and a 220mm length at 60 degrees. The overall area is 1.4 sqmeter (51 sqft).
- Plate #2 at 70 degrees has 125 mm vertical section and 385 mm of sheet at 70 degrees at length of 4.2 meters. The overall area is 2.14 m2 (75 sqft).
- The area and weight of these plates for 16 gauge steel is 127 lbs and 187 lbs which may be in excess for the structural design limits.